The background features a complex, abstract composition. On the left, a dark, textured structure resembling a protein or molecular assembly is visible. A bright, glowing lightning bolt strikes downwards from the top center. The right side is dominated by a green, translucent, crystalline or geometric structure. The overall color palette transitions from dark reds and oranges on the left to bright greens and blues on the right.

Investigation of Different Parameters Important for the Secretion of Active Indolicidin in *P.* *pastoris*

Master's Thesis in Nanobiotechnology

by Christian Skjødt Hansen
June 2012



AALBORG UNIVERSITY

Department of Physics and Nanotechnology

Skjernvej 4A

DK-9220 Aalborg

Phone 9940 9215

Fax 9815 6502

<http://www.nano.aau.dk/>

Title: Investigation of Different Parameters Important for the Secretion of Active Indolicidin in *P. pastoris*

Project Period: September 2011 – June 2012

Author: _____
Christian Skjødt Hansen

Supervisors: Eva Maria Petersen, Associate Professor, Department of Physics and Nanotechnology, Aalborg University
Niels Thomas Eriksen, Associate Professor, Department of Biotechnology, Chemistry and Environmental Engineering, Aalborg University

Copies: 5

Number of pages: 77

Number of appendices: 2

Project finished: June, 2012

Abstract

The antimicrobial peptides indolicidin and its single-tryptophan derivative indolicidin-4 can only be expressed in *E. coli* by the use of fusion proteins to disable toxicity towards the host organism. However purification of active recombinant peptides is difficult and the yield is generally low. In the present study, IL and IL4 were produced in the active form by secreted expression in *P. pastoris*. The productions were made in shake-flasks and fed-batch fermentations. However, the presence of recombinant peptides could not be detected in the supernatant from these productions. It was suggested that the expression was blocked by intracellular interactions or by digestion from proteolytic activity. Synthetic non-amidated IL and IL4 was found to be highly susceptible to proteases found in the supernatant. A number of attempts were made to control proteolysis, such as lowering temperature and pH and utilizing protease-deficient host organisms but without success. The importance in minimising the methanol-induced cell stress has been reported. This could be done by the controlled environment of a bioreactor equipped with a methanol substrate detector.

The antimicrobial activity of compounds produced natively by *P. pastoris* during methanol inductions at pH 3 has been reported in the current study. The compounds very effectively inhibited the growth of *E. coli*, *B. subtilis* and *M. luteus*. Supernatant containing antimicrobial activity was analysed in tricine SDS-PAGE and RP-HPLC but the compounds could not be identified.

Resumé

Udtrykkelsen af to antimikrobielle peptider, indolicidin og indolicidin-4, kan kun ske i *E. coli* ved hjælp af fusionsproteiner, for at deaktivere toksicitet mod værtsorganismen. Oprensning af aktivt rekombinant peptid er imidlertid vanskelig, og udbyttet generelt lavt. I denne rapport blev IL og IL4 produceret i deres aktive form, ved hjælp af sekretet udtrykkelse i *P. pastoris*. Produktionen blev foretaget i rystekolber og fed-batch fermenteringer. Tilstedeværelsen af rekombinante peptider kunne dog ikke detekteres i det overskydende væske fra disse produktioner. Det blev foreslået at udtrykkelsen kunne være blokeret af intracellulære interaktioner eller af nedbrydelse p.g.a. proteolytisk aktivitet. Syntetiseret ikke-amideret IL og IL4 blev målt til at være stærkt modtagelige overfor proteaser fundet i det overskydende væske. Adskillige forsøg blev gjort for at kontrollere proteolyse, som f.eks. sænkning af temperatur og pH, samt anvendelse af protease-fattig værtsorganismen, men uden succes. Betydningen af minimisering af methanol-induceret cellestress blev også anmeldt. Dette kunne blive gjort i kontrollerede omgivelser som en bioreaktor udstyret med en methanolsensor tilbyder.

Den antimikrobielle aktivitet af stoffer produceret nativt i *P. pastoris*, under methanol inducering ved pH 3, blev rapporteret i dette projekt. Stofferne udviste meget effektiv inhibering af væksten af *E. coli*, *B. subtilis* og *M. luteus*. Overskydende væske indeholdende denne antimikrobielle aktivitet blev analyseret med tricine SDS-PAGE samt RP-HPLC, men stofferne kunne ikke identificeres.

Preface

This master's thesis is composed by Christian Skjødt Hansen and is based on experimental work conducted from September 1st 2011 until May 30th 2012. The experimental work was carried out at the Department of Physics and Nanotechnology as well as Department of Biotechnology, Chemistry and Environmental Engineering at Aalborg University.

The master's thesis considers the recombinant expression of the antimicrobial peptides indolicidin and indolicidin-4 in *P. pastoris* by shake-flask and fed-batch fermentation. The report is divided into five chapters, starting with two chapters of introduction. The first chapter is intended as an overview of cationic antimicrobial peptides and their potential for clinical applications. The second chapter focus on recombinant production of cationic antimicrobial peptides both in general and specialized in *Pichia pastoris* expression systems. The third chapter is the materials and methods used to produce the results mentioned in chapter four. Finally chapter five is a discussion on the results made in the project and ends in a conclusion.

Figures, tables and equations are numbered in accordance to the section and order of appearance. All figures in this report are made by the author, unless sources are specified in the caption. Citations are done using the numbering method, where a bracket contains a number connected to the source position in the reference section. The sources are placed in the order in which they appear in the project, listed with surname and initials of the authors, title, journal, volume, number, year and page of the book/article. Abbreviations are listed after the table of content.

Abbreviations

ACN	Acetonitrile
AMP	Antimicrobial peptide
AOX	Alcohol oxidase
AOX1	Alcohol oxidase gene
BMGY	Buffered Glycerol-complex Medium
BMMY	Buffered Methanol-complex Medium
EtBr	Ethidium Bromide
HBTU	2-(1H-benzotriazole-1yl)-1,1,3,3-tetramethyluronium hexafluorophosphate
HOBt	1-Hydroxybenzotriazole hydrate
IL	Indolicidin
IL4	Indolicidin-4
LB	Lysogeny Broth
Mut ⁺	Methanol utilization plus
Mut ^s	Methanol utilization slow
NAD ⁺	Nicotinamide adenine dinucleotide
NADH	Nicotinamide adenine dinucleotide
p _{AOX1}	AOX1 promoter
pO ₂	Percentage oxygen dissolved
PCR	Polymerase chain reaction
RP-HPLC	Reverse Phase-High Performance Liquid Chromatography
SDS-PAGE	Sodiumdodecylsulphate polyacrylamide gel electrophoresis
SPPS	Solid Phase Peptide Synthesis
TFA	Trifluoroacetic acid
YPD	Yeast Extract Peptone Dextrose Medium
YPDS	Yeast Extract Peptone Dextrose Medium Sorbitol

Organisms

<i>E. coli</i>	<i>Escherichia coli</i>
<i>M. luteus</i>	<i>Micrococcus luteus</i>
<i>P. putida</i>	<i>Pseudomonas putida</i>
<i>B. subtilis</i>	<i>Bacillus subtilis</i>
<i>P. pastoris</i>	<i>Pichia pastoris</i>
<i>S. cerevisia</i>	<i>Saccharomyces cerevisia</i>

Contents

1	Cationic Peptides: A Source of Antibiotics	1
1.1	Introduction	1
1.2	The Cationic Antimicrobial Peptide Indolicidin	2
1.2.1	Mechanisms of Antimicrobial Activity	2
1.3	Limitations of Antimicrobial Peptides as Therapeutic Agents	3
2	Recombinant Expression of Cationic Peptides	5
2.1	Heterologous Expression in <i>Pichia pastoris</i>	6
2.1.1	Methanol metabolism	6
2.1.2	The <i>AOX1</i> and <i>GAP</i> Promoters	7
2.1.3	<i>P. pastoris</i> Expression Strains and Vectors	8
2.1.4	Homologous Recombination	9
2.2	Challenges in Secretory Expression of Heterologous Proteins	9
2.2.1	The Proteolytic System of <i>P. pastoris</i>	10
2.2.2	Glycosylation	12
2.3	Fermentation Technology	13
2.3.1	Methanol-Limited Fed-Batch Technique	13
2.4	Experimental Strategy	14
3	Materials and Methods	15
3.1	Chemicals and Biologicals	15
3.2	Construction of Expression Vector	17
3.2.1	Chemical Transformation of pPICZ α A into <i>E. coli</i> DH5 α	17
3.2.2	Plasmid DNA Purification	17
3.2.3	Ethanol Precipitation	17
3.2.4	Digestion of pPICZ α A Plasmid Vector	17
3.2.5	Annealing and Phosphorylation of Oligonucleotides	18
3.2.6	Ligation of Insert into Digested pPICZ α A Vector	18
3.2.7	Chemical Transformation of pPICZ α A-IL/pPICZ α A-IL4 into <i>E. coli</i> DH5 α	18
3.3	DNA Electrophoresis	18
3.4	Transformation Screening	18
3.4.1	PCR Screening for Correct Insert	18
3.4.2	Screening for Correct Insert by <i>NcoI</i> Digestion	19
3.4.3	PCR Screening of Multiple Integrated Copies of Foreign Genes	19
3.5	Transformation of pPICZ α A-IL/pPICZ α A-IL4 into <i>P. pastoris</i>	19
3.6	Extraction of Genomic DNA from <i>P. pastoris</i>	20

3.7	DNA Sequencing	20
3.8	Small-scale expression study	20
3.9	Tricine Sodium Dodecyl Sulfate Polyacrylamide Gel Electrophoresis	21
3.10	Fermentation Strategy	21
3.11	Zone Inhibition Assay	23
3.12	RP-HPLC analysis	23
3.13	MALDI-TOF Mass Spectrometry	24
3.14	Chemical Synthesis of IL and IL4	24
3.14.1	Purification of Synthetic Peptides	24
4	Results	27
4.1	Construction of Expression Vector	27
4.2	Transformation of <i>P. pastoris</i>	29
4.3	Sequencing of Construct	32
4.4	Expression Study of Recombinant IL and IL4	33
4.4.1	Zone Inhibition Assay on Culture Supernatant	35
4.4.2	Size-Analysis on Culture Supernatant by Tricine SDS-PAGE	38
4.4.3	RP-HPLC Analysis of Culture Supernatant	39
4.5	Fermentation of recombinant <i>P. pastoris</i>	40
4.5.1	Zone Inhibition Assay of Fermentation Supernatant	43
4.5.2	RP-HPLC Analysis of Fermentation Supernatant	45
5	Discussion	47
5.1	Expression of IL and IL4	47
5.1.1	Intracellular Processing of IL and IL4	47
5.1.2	Proteolytic Digestion of IL and IL4	48
5.2	Causes of Bacterial Inhibition	50
6	Conclusion	53
A	Shuttle vectors	61
B	Sequencing of Insert	63

Cationic Peptides: A Source of Antibiotics

1

1.1 Introduction

The discovery of antibiotics more than 80 years ago unquestionably changed the course of human history by curing previously deadly diseases. Recently, however, the wide-spread use of antibiotics has prompted the emergence of a number of multi-resistant bacteria, such as Methicillin-resistant *Staphylococcus aureus* (MRSA), vancomycin-resistant *Enterococci*, *Acinetobacter baumannii* and *Escherichia coli*. Most traditional antibiotics targets specific bacterial enzymes that has been genomically modified in resistant bacteria. Numerous attempts has been made to identify new bacterial targets, using high-throughput screening and combinatorial chemical libraries, but most targets vital for the cell are inaccessible for the drugs^[1]. Additionally the chemical libraries are not large enough to mirror the complexity of naturally produced antibiotics. Most antibiotics currently under development are new and improved versions of old natural products, because the chemical modification of existing molecules remains the most cost-efficient way to develop novel drugs active against resistant strains. However, the development of resistance is inherent to the mode of action of traditional antibiotics and is indeed the greatest threat to successful antibiotic coverage, and hence the driving force behind the search for new therapeutic agents.

Short cationic amphiphilic peptides are evolutionary ancient antibiotics found in virtually every life form and are proposed as a basis of a new class of therapeutic antibiotics. The wide-spread distribution in host organisms suggest that they provide significant activity against the adaptive microbes. Species that lack the adaptive immune system rely solely on these type of defence mechanisms. Although these host defense peptides show rather low antimicrobial activity under physiological conditions (*in vitro*) they offer broad-spectra activity and weak selection of bacterial resistance due to multiple mechanisms of actions that does not involve receptor-based targets^[1]. While the term 'host defense peptides' are often used to classify peptides involved in the modulation of the innate immune system, the term 'antimicrobial peptide' are often used only when studying the capabilities of inhibiting microbial growth by direct killing. Since other characteristics have since been identified, the term 'antimicrobial peptide' will in this thesis be used to describe both properties of these peptides.

Antimicrobial peptides shows similar 'rapid evolution' to several proteins involved in host defense and immunity^[2,3]. The diversity of sequence is so enormous that the same peptide sequence is rarely recovered from two closely related species^[4]. However, certain features are common. They are generally short (10-50 amino acids) peptides with an net positive charge and with a significant hydrophobic region. These properties permits folding into three dimensional amphiphathic structures upon interaction with membranes. Generally four structural classifications exists: α -helix (for example, LL-37, cecropins or magainins), β -sheet (for example, human α - and β -defensins, plectasin or protegrins), extended structure rich in certain amino acids (for example, indolicidin) and loop peptides with one disulfide bridge (for example, bactenecin). Most antimicrobial peptides are derived from larger precursors that are then activated by proteolytic cleavage or in some case glycosylation, carboxy-terminal amidation and isomerisation^[4]. In plants defensins often undergo splicing and cyclization to form θ -defensins, a highly stable antimicrobial peptide that compensates for the lack of adaptive immune system^[5].

1.2 The Cationic Antimicrobial Peptide Indolicidin

Indolicidin (IL) is a 13-residue antimicrobial peptide first isolated and characterised from the cytoplasmic granules of bovine neutrophils^[6]. Indolicidin belongs to a group of peptides denoted cathelicidin, which are host defence peptides, that, together with defensins, are responsible for the innate immune system of all mammalian cells. Indolicidin is an extended peptide, having a stretched structure with neither α -helices nor β -sheets^[7]. Usually, extended peptides have one or two predominant amino acids. This is also the case for indolicidin, which consists of 38% tryptophan and 23% proline.

Indolicidin shows activity against fungi^[8,9], Gram-negative and Gram-positive bacteria^[10] as well as HIV-1^[11]. The possibility of using indolicidin as a therapeutic agent is however limited since it is highly haemolytic, showing activity against rat erythrocytes^[10,12] and human erythrocytes^[8]. On the contrary, some indolicidin derivatives have shown great potential for use in medicine. For example, indolicidin-F (ILF), where all tryptophans have been substituted with phenylalanine, retains its antimicrobial activity, but have a haemolytic activity of only 20% compared to indolicidin^[10]. The activities of ILF brought attention to the many tryptophans of indolicidin, and the influence of this amino acid on the haemolytic activities was further confirmed by the studies on the single tryptophan derivatives indolicidin-4 (IL4), indolicidin-8 (IL8) and indolicidin-11 (IL11), where all tryptophans except Trp4, Trp8 or Trp11, respectively, have been substituted with leucine. IL4, IL8 and IL11 show only slightly decreased antibacterial activity, but no activity against rat erythrocytes^[10].

1.2.1 Mechanisms of Antimicrobial Activity

The cationic and amphiphilic nature of indolicidin is associated with the antimicrobial activity. Conventionally the antimicrobial peptide was thought to adopt its antimicrobial activity by direct killing of microbes through membrane lysis or interactions with intracellular targets^[13]. More recent it has been demonstrated that indolicidin (as well as other antimicrobial peptides) also posses immunomodulatory functions (Figure 1.1)^[14,15].

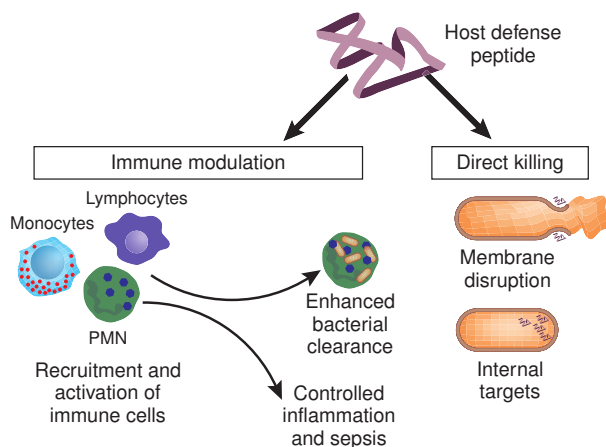


Figure 1.1: Biological mechanisms of antimicrobial peptides includes direct killing and immune modulation.^[14]

The attractive electrostatic forces between the cationic peptide and the negatively charged bacterial surface is the first step in the antimicrobial peptide-mediated cell killing^[16]. Once close to the microbial surface, indolicidin must traverse the capsular polysaccharides before gaining access to the cytoplasmic membrane (gram positive) or outer membrane (gram negative). Since indolicidin-membrane association is greatly influenced by specific electrostatic interactions, lipid fluidity and the peptide concentration, it is not clear by which mechanism

indolicidin permeabilizes the membrane *in vivo*^[17]. However, it has been reported that the permeabilization of the outer membrane of *E. coli*, at peptide concentrations three times higher than MIC, does not perturb the membrane significantly, leaving the cell potential intact. This suggests other mechanisms important for the cell lysis such as the disruption of intracellular mechanisms, and that the membrane binding properties of indolicidin are only important to enter the cell^[18]. Subbalakshmi *et al* found that indolicidin induces filamentation of *E. coli* due to inhibition of DNA synthesis^[13]. Inhibition of RNA synthesis was also observed in *E. coli* to lesser extent^[13].

Because the activity of antimicrobial peptides in mammals are rather weak, their ability to modulate the immune response is suggested to be more important^[14]. Lipopolysaccharide (or endotoxin) are major components of the outer surface of gram negative bacteria and are powerful stimulants of the immune system^[19]. Endotoxins binds to TLR4 receptors of macrophages, monocytes, and neutrophils and stimulates the secretion of a variety of inflammatory products that result in septic shock and other immune diseases^[19,20]. It has been shown that indolicidin has the potential to inhibit endotoxin-induced proinflammatory responses by binding directly to the lipopolysaccharides, serving as antagonists to such receptors^[15]. They were also shown to promote chemotaxis by inducing the chemokine production in certain cells, enhancing the innate immune response^[15].

Indolicidin may exhibit other immunomodulating functions, such as recruitment and activation of immune cells and promotion of wound healing that all play a major role in the fight against bacterial infections^[21]. The indolicidin variant CP-226, for instance, is currently in stage 2 clinical trials as a potential drug against catheter-associated inflammation^[14].

1.3 Limitations of Antimicrobial Peptides as Therapeutic Agents

Despite nature's favour of enormous structural diversity of antimicrobial peptides as well as decades of design efforts, providing an impressive array of clinically potent agents, there has been limited success in the clinical-efficacy trials^[22]. Before antimicrobial peptides can be considered as viable alternatives for conventional antibiotics a number of obstacle needs to be addressed. The antimicrobial spectrum of the antimicrobial peptides must be confirmed, synergistic effects must be determined, toxicity towards host must be studied and the activity under physiological conditions (salt, pH, serum proteins and proteases) must be determined^[23]. For example, small antimicrobial peptides are easily susceptible to proteases upregulated in inflammatory or infectious sites^[21].

In contrast to the mechanisms of conventional antibiotics, nature appear to favour different concepts for the evolution of innate antimicrobial peptides. Instead of blocking a specific high-affinity target such as cell-wall synthesis precursors, peptides often disturb many biological functions^[5,14]. This way peptide antibiotics may extend the clinical half-life beyond the 1–2 decades appreciated by most conventional antibiotics. However, there is no question that these peptides will also (eventually) induce resistance^[24]. Countermeasures towards antimicrobial peptides have been discovered within bacteria themselves^[5,16,24]. Gram negative bacteria may hinder peptide attachments by lowering the net negative surface charge by altering the lipopolysaccharides^[16]. In *S. typhimurium*^[5] and *P. aeruginosa*^[16] mechanisms has been identified that directly control a two-component regulator (PmrA-PmrB) whose downstream genes are involved in covalent modifications of lipopolysaccharides as well as genes involved in the expression of membrane proteases. Also, in *S. aureus*, genes have been identified to include covalent modifications of lipopolysaccharides as well as membrane phosphatidylglycerol consequently lowering the negative charge of the cell wall and membrane respectively^[5]. Apart from changing the net negative charge of the cell envelope, many of these mechanisms also change the fluidity of the outer membrane^[16].

Antimicrobial resistance is also associated with the ability to transport antimicrobial peptides out of the cell^[16]. For example, *N. meningitidis* include active extrusion of cationic antimicrobial peptides from the bacterial membrane which limits the antimicrobial effect from especially intracellular mechanisms of actions^[24]. The immunomodulatory properties of antimicrobial peptides will of course not be affected by these mechanisms of bacterial resistance.

The major issue in the field of antimicrobial peptides as anti-infectious agents is arguably the high cost of production^[14]. Solid-Phase chemical synthesis of peptides are in the range of \$100 – \$600 per gram^[14,21], which is prohibitive when considering therapeutic applications. This means that all efforts in development of peptide drugs must take this into account. As such, there is a growing need to develop cost-effective production methods. This issues could be overcome if antimicrobial peptides could be produced recombinantly and by large scale fermentations and purification means.

Recombinant Expression of Cationic Peptides

2

Heterologous expression of antimicrobial peptides has been reported in various expression systems. The choice of expression system and success of production depends on the class of antimicrobial peptide. The most simple antimicrobial peptides to produce by heterologous expression are unmodified bacteriocins because they offer restricted antimicrobial activity and are relatively simple in structure and require no further modifications^[23]. These peptides can be readily produced in active forms using simple bacterial expression systems. Most antimicrobial peptides, however, shows significant antimicrobial activity against favoured bacterial expression systems which limits the strategies of heterologous expression in active form.

Table 2.1 lists examples of antimicrobial peptides produced heterologous in various expression systems. The expression level (purified peptide) varies immensely with the various strategies and peptides expressed. Over the past three decades *E. coli* has been extensively used as cellular host for heterologous protein expression, and is one of the most well studied expression systems. However, antimicrobial peptides active against gram negative bacteria needs to be inactivated during expression. Therefore most smaller cationic antimicrobial peptides expressed in bacteria are fused to larger proteins, either as single peptides or as tandem repeats, to disable toxicity^[25,26,27]. Only few small antimicrobial peptides have been reported to be expressed in active form by *E. coli*. Many fusion strategies are limited in applications since they require exposures to cleavage reagents such as CNBr or site specific proteases such as SUMO-proteases or TEV proteases. CNBr is a very toxic chemical and may cause side chain modifications rendering it unsuitable for clinical applications^[28].

The intracellular expression of foreign peptides in *E. coli* may facilitate aggregation of denatured peptides leading to the formation of inclusion bodies^[29]. This often complicates the purification process because the peptides need to be solubilized. Additionally, small peptides are highly susceptible to proteolytic digestion, which is reinforced in intracellular expressions by the presence of many proteases. Protease deficient *E. coli* strains are therefore a necessity when working with peptides, reducing the proteolytic activity^[27].

Bacillus subtilis offers secreted expression of the heterologous peptides overcoming the inclusion problems from its bacterial counterpart. Like *E. coli*, it serves as an efficient expression host offering theoretically high yields and inexpensive production. *B. subtilis* also requires inactivation of peptides that shows antimicrobial activity towards the host^[29].

Secretory expression of active antimicrobial peptides in *Pichia pastoris* and *S. Cerevisia* has been reported several times. The yeasts are popular expression hosts since they offer high cell densities and secretion of many recombinant proteins as well as easy manipulation. Although the specific productivity of most proteins is relatively low in *P. pastoris*, it is compensated by a relatively constant productivity over many days even in high cell densities^[46,47]. The secretory expression also serves as a first step of purification since *P. pastoris* and *S. Cerevisia* secretes only few homologous proteins^[48,49]. This permits expression without purification tags that may affect the antimicrobial activity. Another reason that yeast is attractive is the capability of performing a large variety of post-translational modifications such as disulphide bond formation required when expressing cysteine rich antimicrobial peptides such as defensins.

Table 2.1: Expression system for recombinant antimicrobial peptide production.

Expression System	Technology	Peptide	Size (a.a.)	Affinity Tag	Yield (mg/L) ^a	Reference
<i>Escherichia coli</i>	Fusion	Halocidin 18	18 (+33.6 kDa) ^b	His ₆	0.26	[26]
		CA-MA	22 (+13 kDa) ^b	His ₆	6.8	[30]
		Indolicidin	13 (3) ^c	His ₆ +S-Tag	0.15	[27]
		MBI 11B7 HSL	12 (15) ^c	Untagged	0.1	[31]
		Buforin II	21 (3) ^c	Untagged	107	[32]
	Direct	Scygonadin	102	His ₆	65.9	[33]
		MiAMP1	76	Untagged	2.5	[34]
		CrustinPm1	128	His ₆	53	[35]
		BmK AS	66	His ₆	4.2	[36]
		Hepcidin	26	His ₆	16-20	[37]
<i>Bacillus subtilis</i> , (secreted)	Direct	Tachyplestin	17	Untagged	5	[38]
	Fusion	Tachyplestin	17 (2) ^c	Untagged	10	[38]
		Cecropin AD	37 (+12 kDa) ^b	Untagged	30.6	[29]
<i>Pichia pastoris</i> , (secreted)	Direct	Sp-AMP	79	His ₆	0.4	[39]
		Ch-penaeidin	71	Untagged	100 (crude)	[40]
		ABP-CM4	35	Untagged	15	[41]
		CA-MA	22	Untagged	22	[42]
		Scygonadin	102	His ₆	70	[43]
		hPAB-β	39	Untagged	241	[44]
		GLP-1	30	Untagged	59	[45]
<i>Saccharomyces cerevisiae</i>	Direct	GLP-2	33	Untagged	28.2	[45]
		Glycagon	29	Untagged	18.2	[45]

^a Yield of purified (>95%) activated peptide.

^b The number in parantheses indicate mass of fusion partner.

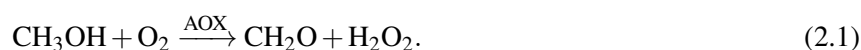
^c The number in parentheses indicate peptide is expressed as (number) tandem multimers fused by linker peptides.

2.1 Heterologous Expression in *Pichia pastoris*

P. pastoris is a methylotropic yeast capable of metabolising methanol. This feature is commonly exploited in expression strategies where methanol is being used as the sole carbon source to control *P. pastoris* growth and (as described later) to control the expression of the heterologous protein.

2.1.1 Methanol metabolism

The methanol metabolic pathway of *P. pastoris* is similar to most yeast capable of growth on methanol. First, methanol is oxidised to form formaldehyde by the enzyme alcohol oxidase (AOX):



A by-product of this reaction is hydrogen peroxide, which is subsequently reduced to form water and molecular oxygen^[50]. To avoid toxicity, the reaction takes place in the peroxisome organelle. The formaldehyde is then utilised in two pathways: dissimilation and assimilation. Some formaldehyde diffuses to the cytosol and is oxidised to formate and further to carbon dioxide by the NAD⁺-dependent dehydrogenases formaldehyde

dehydrogenase (DH1) and formate dehydrogenase (DH2), as presented in Figure 2.1. The formaldehyde dehydrogenase does not catalyse the oxidation of free formaldehyde but rather S-formylglutathione¹. The product is initially hydrolysed to form formate and glutathione. In these oxidation steps NAD^+ is regenerated to NADH, a source of energy for the cell. Note that the formation of NADH in the cytoplasm is unique for the metabolism of methanol as the only carbon source^[51]. The consequence of NADH being formed in the cytoplasm is a reduction in ATP production from 2.5 (in mitochondria) to 1.5 from the electron pair of a single NADH^[52,53].^[51,54]

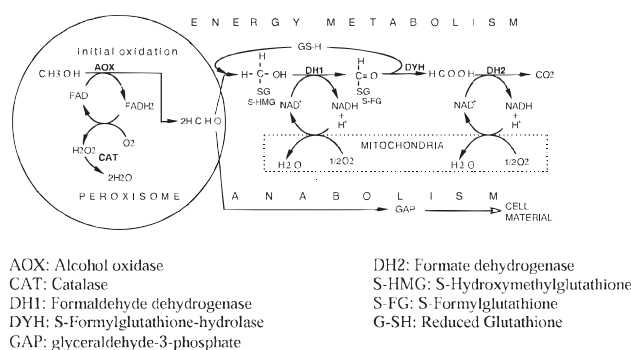


Figure 2.1: Methanol metabolism of *P. pastoris*. The figure was adopted and modified from Gellissen, G.^[54]

The remaining formaldehyde enters the assimilatory pathway, involving the formation of dihydroxyacetone and the C_3 compound glyceraldehyde-3-phosphate (GAP) from a transketolase reaction between formaldehyde and xylulose-5-phosphate (Xu5P). The aldehyde derivative is further assimilated in the cytosol for the formation of biomass. Xu5P is regenerated from dihydroxyacetone by subsequent enzymatic reactions ending the cycle.^[51,54]

2.1.2 The *AOX1* and *GAP* Promoters

Because AOX has a low affinity to O_2 in the initial oxidation steps, the genes coding for this enzyme, *AOX1* and *AOX2*, have very strong promoters. This compensates for the deficiency of AOX by enabling the production of large amount of the enzyme^[55]. The majority of AOX is produced from the *AOX1* gene, making this promoter ideal for heterologous protein expression^[56,57]. The promoter is repressed when certain other carbon sources are available, such as glycerol or dextrose. Additionally, this provides another advantage of this promoter; the ability to switch it off during growth with other carbon sources than methanol, which minimizes selection of non-expressing mutants during biomass accumulation^[55]. This also provides the possibility of expressing proteins that may be toxic for the yeast when biomass has been well established. This is indeed a benefit when expressing antimicrobial peptides without knowledge about disruptive activity when introduced to the intracellular environment, that would otherwise not show up under standard extracellular inhibition assays.

The glyceraldehyde-3-phosphate dehydrogenase enzyme (GAPDH) involved in the assimilatory pathway, described above, also has a strong promoter (P_{GAP}) that has recently been used in heterologous expression^[55]. This promoter is induced by other carbon sources than methanol and generates high expression levels without the need for methanol, making it attractive for industrial scale fermentations^[57]. Comparing induction by methanol, glycerol and glucose, the latter has been reported to produce the highest expression levels and in some studies the *GAP* promoter has been shown to generate higher expression levels than the *AOX1* promoter^[55]. This promoter, however, is ill advised for expression of products that may be toxic to the cell^[58].

¹A spontaneous linkage of formaldehyde and reduced glutathione (GS-H)

2.1.3 *P. pastoris* Expression Strains and Vectors

Various *P. pastoris* expression strains are commercially available, that offers a wide range of genotypes. The genotype and phenotype of the most common *P. pastoris* strains are summarized in Table 2.2. While X33 wild type *P. pastoris* can be used in many cases, higher expression levels may be achieved with other strains^[57]. GS115 and KM71 is lacking *his4* genes responsible for Histidine biosynthesis and can be used for selection of transformants based on their ability to grow on non-histidine medium. In KM71 the *AOX1* gene has been deleted and replaced with *S. cerevisiae ARG4* gene, coding for argininosuccinate lyase, which catalyses the final step in the arginine biosynthesis pathway^[57,55]. *AOX1* is responsible for approximately 85% of the metabolism of methanol, so these strains utilizes methanol in much slower rates than wild type strains. *P. pastoris* wild-type with regard to *AOX1* are termed Methanol Utilization Plus (Mut⁺) for their ability to utilize both *AOX1* and *AOX2* genes while those with disrupted *AOX1* genes are appropriately termed Methanol Utilization Slow (Mut^s).

Protease deficient strains such as SMD1165H and SMD1168H lacks Protease B1 and peptidase A-encoding genes respectively, making them suitable when proteolytic digestion decreases expression levels. However, peptidase A is required for the activation of Protease B1 and carboxypeptidase Y rendering SMD1168H effectively deficient in both proteases^[59].

Table 2.2: Genotype and phenotype of the most common *P. pastoris* expression strains.

Expression Strain	Genotype	Phenotype
X33 ^a	Wild type	Mut ⁺
Auxotrophic strains		
GS115	<i>his4</i>	Mut ⁺ , His ⁻
KM71	<i>his4, aox1:ARG4</i>	Mut ^s , His ⁻
Protease deficient strains		
SMD1168H ^a	<i>pep4</i>	Mut ⁺ , Pep4 ⁻
SMD1165H	<i>prb1</i>	Mut ⁺ , Prb1 ⁻

^a Strain used in this study.

Table 2.3: Features of common *P. pastoris* expression vectors.

Expression Vector	Selection marker	Features
Intracellular		
pPICZ	R _{zeo}	<i>AOX1</i> promoter; Zeocin selection
Secretion		
pPICZα ^b	Zeo ^R	<i>AOX1</i> promoter; α-MF; Zeocin selection
pPIC9K	<i>HIS4; kan^R</i>	<i>AOX1</i> promoter; α-MF; HIS4 selection; Geneticin selection (<i>kan</i>)
pGAPZα	Zeo ^R	<i>GAP</i> promoter; α-MF; Zeocin selection

^b Vector used in this study.

Several plasmid vectors designed for heterologous protein expression in *P. pastoris* are commercially available (Table 2.3). They have several common features, such as they are all shuttle type, i.e. they include features necessary to grow and maintain selectivity in both *E. coli* and *P. pastoris*. Additionally they all offer stable integration into the *P. pastoris* chromosome. The two most popular expression vectors that utilises the *AOX1* promoter are pPICZ and pPICZα. pPICZ is used for intracellular expression while pPICZα allows cloning in frame with the *S. cerevisiae* α-mating pre-pro leader sequence (α-MF) used for targeting the secretory pathway. They both contain the Zeocin selection gene for positive selection, while the pPIC9K expression vector offer positive selection under Geneticin antibiotic pressure as well as HIS⁺ selection for transformation into *his4* mutant strains. Additionally, pPICZ vectors include c-myc epitope and polyhistidine purification tag downstream the multiple cloning site, allowing a broader range of purification methods^[56,57]. These tags may however lower the antimicrobial activity of the peptides expressed. pGAPZα is an example of a more recent expression vector that utilises the *GAP* promoter for expression, where other carbon sources can be utilized for induction.

2.1.4 Homologous Recombination

Several transformation vectors offer chromosomal integration in *P. pastoris*. The advantages of chromosomal integration are high expression cassette stability, generation of multicopy integrants, the ability to engineer site-specific integration and utilization of chromosomal promoters, such as P_{AOX1} or P_{GAP} . Linearising pPICZ or pPICZ α vectors with *SacI* generates a vector whose ends are homologous to the 5' and 3' regions of the *AOX1* locus of *P. pastoris*. Transformation with such vector result in a single crossover event leaving the *AOX1* gene intact or, in rare cases, a double crossover event of the *AOX1* 5' and 3' region that replaces the *AOX1* gene (Figure 2.2)^[55]. However, since the Zeocin™ resistance marker is not integrated into the chromosome during double crossover events, it is fair to assume that only the Mut⁺ phenotypes will colonise under Zeocin selection pressure.

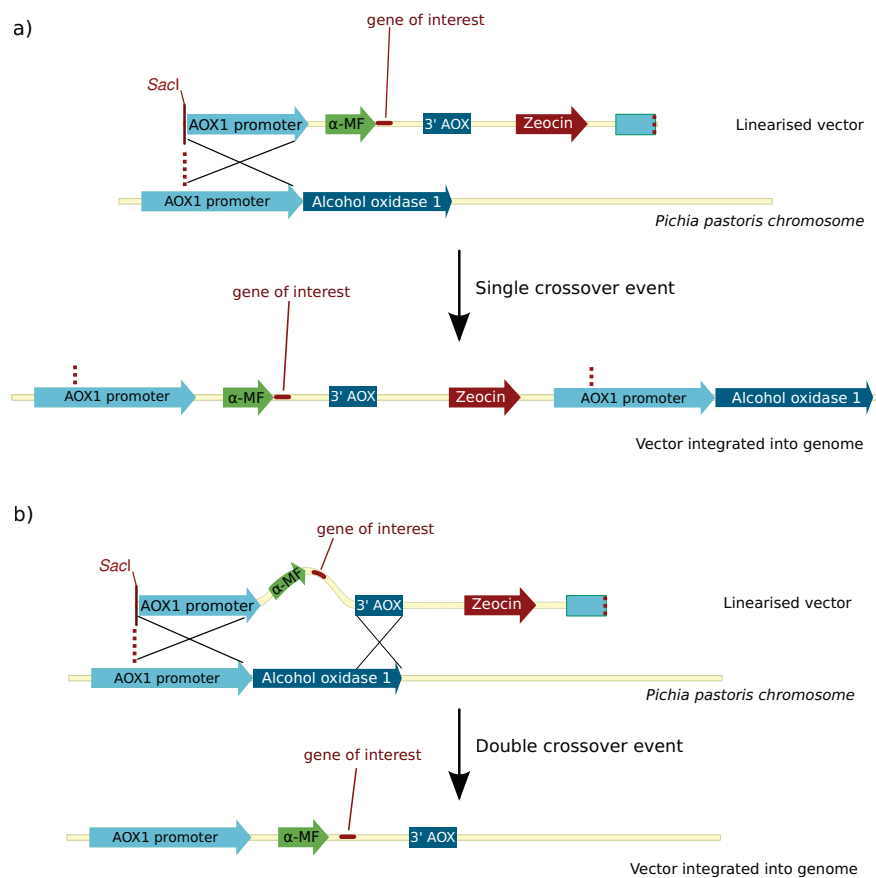


Figure 2.2: Chromosomal integration occur as a single crossover event of the *AOX1* promoter (a), resulting in a full vector integrated into the genome of *P. pastoris* with in intact *AOX1* gene. b) In rare cases a double crossover event may occur where the *AOX1* gene is replaced by part of the vector. In this case though, the Zeocin resistance marker is not integrated into the chromosome and such strain will not survive Zeocin selection pressure.

2.2 Challenges in Secretory Expression of Heterologous Proteins

Because *Pichia pastoris* only secretes low level of endogeneous proteins, secretion of heterologous proteins serves as the first step of purification. However, a number of challenges exist for optimising protein expression. Increasing expression level by optimisation of the secretory pathway includes three main topics: (1) protein

folding and quality control system in ER^[60], (2) protein trafficking pathway^[61] and (3) post-secretory proteolytic degradation^[50,56]. These challenges often include strain engineering and can be highly specific for the protein to be expressed. Another challenge when expressing proteins for pharmaceutical use is glycosylation, leading to high antigenic interactions and degradation in the liver when introduced intravenously^[62].

Misfolded proteins are recognized by the quality control (QC) system and transported to the cytosol for ER-associated protein degradation^[63]. As a result of the QC system, the folding system may become the rate-limiting bottle-neck of protein secretion. Over expression of chaperone BiP by strain engineering, for instance, could lead to a 26-fold increase in bovine prochymosin secretion in *S. cerevisiae* as it reduced the number of misfolded proteins^[64]. However, this result is not trivial and opposite effects (a 10-fold decrease in secretion) have been observed in other expression hosts^[60].

Other studies demonstrate the effects of traffic modification in the strain. These approaches are highly complex since they require knowledge of what causes mis-sorting and ineffective trafficking and because they often have an impact on cell viability^[63]. Instead of strain engineering, Ahn *et al.* reported a 7-fold increase in secretion of *Bacillus stearothermophilus* L1 lipase in *S. cerevisiae* by fusion with cellulose-binding domain (CBD)^[61]. A KEX2 cleavage site was introduced in the junction between the fused proteins. Since the fusion protein is cleaved in the Golgi apparatus, these results suggest that the CBD-linker probably plays a role in the ER-to-Golgi trafficking^[63].

Several protein features may play a role in the expression levels in *P. pastoris*. An extensive study of 79 human genes expressed intracellularly in *P. pastoris* were made by Boettner *et al.*, linking various protein properties to the expression levels obtained^[65]. A significant association was found between relatively high isoelectric points (above 7.8) and zero expression levels. This decrease in expression levels with increased pI, are important factors to consider when working with cationic antimicrobial peptides. No associations were found between hydrophobicity or length and low expression levels although the study only included proteins of relatively large size (<5% of the proteins had lengths below 100 amino acids), so this should be taken lightly when studying peptides, where a significant effect on hydrophobicity and lengths are expected^[65].

2.2.1 The Proteolytic System of *P. pastoris*

One of the major challenges in heterologous protein secretion is post-secretory degradation. Proteolytic degradation is a problem for a large variety of heterologous proteins expressed in *P. pastoris* since their functions are often reduced or missing upon digestion. Some proteins are more susceptible to proteases than others. The activity of proteases depends on the motifs of the target proteins and the availability of cleavage sites. Intracellular proteases in yeast has been well studied, most of which in regards to *S. cerevisiae*. The proteolytic system is however similar to the one present in *P. pastoris*, consisting of mainly three classes of proteases; cytosolic proteasomes, vacuolar proteases and proteases linked to the secretory pathway^[66].

Cytosolic proteasome

The proteases found in the cytosol are very asimilar to the other classes. These proteases are multicatalytic and high in molecular weight (≈ 700 kDa) with a complex multi-subunit structure that enables functions central to the intracellular proteolytic pathway, such as the degradation of ubiquitinated proteins^[67]. These so-called proteasomes are responsible for rapid degradation of proteins detrimental to the cell growth and are upregulated as a response to environmental stress^[68,66]. These upregulations may also happen under adaption of a new carbon sources, such as the transition from glycerol to methanol nutrients during fermentations (as described later). These events require the synthesis of new proteins needed for the methanol metabolism and rapid degradation of those no longer needed by glycerol metabolism (or vice versa)^[68].

Vacuolar proteases

Vacuolar proteases are responsible for the majority of the proteolytic digestion in *P. pastoris*. The peroxisomes (where the AOX enzymes resides) are degraded in the vacuole when alcohol is no longer available^[68]. There has been found a total of 7 vacuolar proteases, whereas 3 is well described.

Peptidase A (or sometimes called proteinase A) is an aspartyl protease encoded by the *pep4* chromosomal gene and is capable of self-activation as well as subsequent activation of other vacuolar proteases such as protease B1, carboxypeptidase-Y and -S^[58]. Although *P. pastoris* expresses no known extracellular proteases, it has been observed that when peptidase A is overexpressed in yeast, a part of the protease is secreted^[69]. Both vacuolar and secretory proteins are trafficking through ER and Golgi during process of synthesis, but since this is an atypical elevated expression it is unknown whether this effect may be detected in standard cultivations of *P. pastoris*.

Protease B1 (PrB) is, as earlier mentioned, encoded by the *prb1* gene. Firstly a 69 kDa precursor is translocated into ER where it is activated by peptidase A. The mature enzyme has a molecular mass of 31–33 kDa^[66]. Prior to activation by peptidase A the precursor is already approximately 50% bioactive^[58]. This means that strains deficient in peptidase A, will also lack the serine proteases (carboxypeptidase-Y and -S) and be only partially deficient in protease B1. Several aminopeptidases has been found recently, such as dipeptidyl aminopeptidase, aminopeptidase-Y, -I and -Co but only few informations has been reported about these proteases^[66].

Proteases in the secretory pathway

The main function of the proteases found in the secretory pathway is to process or activate precursor-proteins according to their signal peptides. The α -MF is often used as secretion signal in heterologous expression. This sequence comprises of a 19 amino acid signal peptide (pre-sequence), followed by a 60 amino acid pro-region^[55]. After translation, the pre-sequence is cleaved by signal peptidase and the pro-region is recognized by Kex2 protease. Specifically, kex2 protease is a serine protease that cleaves the carboxyl end of Lys-Arg or Arg-Arg paired amino acids. The cleavage efficiency of Kex2 proteases can be influenced by steric hindrance or close proximity of proline residues^[57]. Kex1 carboxypeptidase is a serine protease showing high homology to the carboxypeptidase-Y found in the vacuole^[70]. Kex1 can cleave the carboxy-terminal arginine or lysine of target proteins^[71].

During high-density fermentation, *P. pastoris* is exposed to significant environmental stress, such as starvation, substitution of carbon source and previously described oxidative stress caused by molecular oxygen^[50]. The proteolytic activity is significantly upregulated during this environmental stress^[66,72]. It has been reported that *P. pastoris* grown to the same density by methanol or glycerol contained higher cellular levels of vacuolar proteases when grown on methanol presumably due to the oxidative stress caused by the methanol metabolism^[73]. It was also observed that protease activities found in *P. pastoris* culture supernatant increased from near-detection-limit levels to significant levels after a period of 60-72 hours of a specific growth rate, μ_s , of 0.025 h^{-1} ^[73]. This correspond to an average level of 10-40 times lower than the levels inside the cell. Xiao *et al.* reported that 25% of *P. pastoris* cells were membrane damaged at the end of a 96 hour methanol fed-batch fermentation due to oxidative stress^[50]. Such damage and environmental stress may cause the leakage of vacuolar proteases into the culture broth or a cell response by secretion of proteases for defensive degradation^[63].

Controlling proteolysis

To overcome proteolysis, a number of approaches exists, including changing the growth conditions (temperature, pH etc.), adding antioxidants or using protease-deficient yeast strains. Success with changing the pH during induction has been reported with various heterologous proteins. Optimal expression of a hookworm anticoagulant peptide (75 amino acids) occurred at pH 7 and at 28°C^[74] while optimal conditions for the expression of recombinant cytokine growth-blocking peptide (25 amino acids) was at pH 3 at 30°C^[75]. *P. pastoris* tolerates a pH range of the medium between 2.8 and 6.5 without affecting growth rate^[48,56], and offers considerable freedom of optimising pH to one that is optimal for protease inactivation.

The temperature has also been reported to increase the expression levels, presumably by decreasing the activity of key proteases. Although temperature does effect growth rate below 20°C, induction temperatures between 15-32°C should be tested for optimal expression. The lower temperatures may also cause stabilisation effects on the cellular membrane and reduce the protease leakage to the supernatant^[76].

The effects of cell medium composition on heterologous protein expression levels is also a valid area of optimisation^[56]. Complex medium containing yeast extract and peptone as amino acid supplements may improve the inactivation of proteolysis immensely. The excess level of small peptides serves as competing targets of the proteases and may repress protease expression induced by starvation^[66]. The downside of these complex medium is the level of noise peptides introduced in the downstream purification processes when working with small antimicrobial peptides^[77]. Using simple basal salt medium is preferred with regards to purification. Another way to reduce proteolysis is by the supplementation with casamino acids^[55,66]. L-arginine, L-arginine-hydrochloride or ammonium ions have also been reported to inhibit extracellular proteases^[55,66]. Adding antioxidants such as ascorbic acid to prevent accumulation of molecular oxygen also reduces protease secretion by enhancing cell viability but is rather expensive in industrial scale production^[50,63].

Since the leakage of vacuolar proteases to the fermentation medium is delayed during induction, as described earlier, the length of induction may also help to overcome proteolysis. This techniques however limits the advantage of *P. pastoris* being able to grow to high cell densities and renders the recombinant production labour intensive, and so other approaches to decrease proteolysis should be tested first.

2.2.2 Glycosylation

Protein glycosylation is one of the most common post-translational modifications that are carried out in yeast. It is important to take into account when working with expression in yeast since the addition of oligosaccharides may effectively terminate the desired function of the recombinant protein. *P. pastoris* is capable of N-linked glycosylation on the amide nitrogen of Asn-X-Thr/Ser recognition sequons^[78,55]. N-linked glycosylation starts in the ER where pre-assembled Glc₃Man₉GlcNAc₂ oligosaccharides are transferred to the amide group of asparagine residues. Subsequently three glucose residues and one mannose residue are removed, giving the protein an N-linked Man₈GlcNAc₂ core. The glycoprotein is then transferred to *cis*-Golgi for further processing where further mannose units are linked to the inner core. Unlike the hyper-glycosylation happening in *S. cerevisiae*, the majority of the N-linked glycosylation occurring in *P. pastoris* produces chains of Man₈₋₁₄GlcNAc sizes^[78]. Additionally the use of strong promoters such as P_{AOX1} is suggested to limit the degree of glycosylation of newly synthesised proteins in the secretory pathway^[78].

Also, O-linked glycosylation of threonine and serine residues occur in the Golgi apparatus of *P. pastoris*, although less frequently than N-linked glycosylation^[78]. There is no recognition sequons for O-linked glycosylation^[55], but the probability of glycosylation is enhanced when proline residues are in close proximity to the threonine/serine residues^[79].

2.3 Fermentation Technology

When expressing recombinant proteins in *P. pastoris* various techniques exist for cultivating cells and inducing protein production. Cultivation of *P. pastoris* in controlled environments of bioreactors facilitates growth to very high densities ($\geq 150 \text{ g L}^{-1}$ dry cell weight). Batch cultivations involve exponential consumption of nutrients and oxygen and thus provide rapid accumulation of cells. As a result the dissolved oxygen (DO) will eventually become the growth limiting factor as long as nutrients are available in excess. This renders batch systems unfit for high density cultivations over longer periods of time but suitable for rapid cell mass accumulation before turning to fed-batch cultivations.

2.3.1 Methanol-Limited Fed-Batch Technique

The cultivation is typically initiated by glycerol for a number of reasons. Firstly, the cells grow faster on glycerol over methanol and methanol toxicity is avoided. Secondly, the high oxygen demand by alcohol oxidase during induction may also become a growth-limiting factor. Thirdly, the presence of glycerol also represses the AOX promoters and as such disables any selection for mutations defective in heterologous gene expression, which is most critical during the low cell density growth stage. As such the fermentation is commonly divided into four stages, illustrated in Figure 2.3

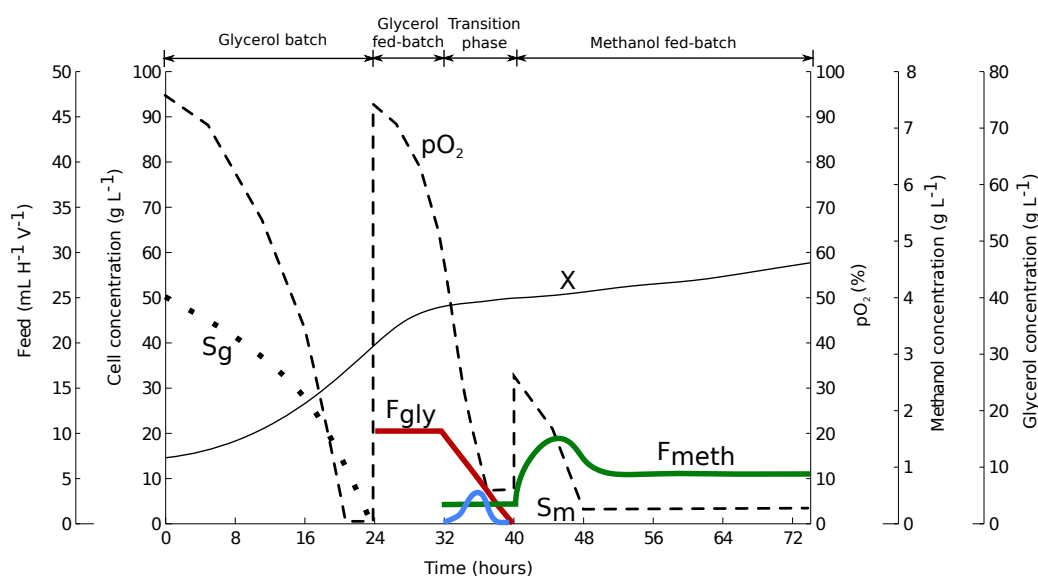


Figure 2.3: Four common phases of a fed-batch fermentation: Glycerol batch (0-24 hours), Glycerol Fed-batch (24-32 hours), Transition phase (32-40 hours) and Methanol fed-batch induction phase (from 40 hours). After the glycerol batch phase, glycerol is fed under limited conditions (red line). In the transition phase the glycerol feed is ramped down while a small methanol feed (green line) is initiated to promote AOX enzyme production. Low amounts of methanol (blue line) accumulates during the first period of methanol feed. After a while enough AOX enzymes are produced (not shown) and methanol feed is increased. **Please note that all data are fictive!**

Glycerol Batch. In the initial batch, the fermentation medium contains high amount of glycerol (maximum 40 g L^{-1} due to toxicity when overexposed to glycerol), providing rapid accumulation of biomass. The end of the batch phase is typically marked by a spike in pO_2 when all glycerol is consumed.

Glycerol Fed-Batch. Once all glycerol is consumed the accumulation of biomass continues under glycerol limited conditions. This way the cells are exposed to a controlled amount of glycerol until a desired density is reached (typically 200 g L^{-1} wet cells). The glycerol batch phase can also be used to adjust the pH needed for the induction phase to lower proteolytic activity.

Transition Phase. Since the cells produce no AOX during the previous phases, a very low initial methanol feed should be applied to avoid intoxication when the methanol fed-batch induction is initiated. Jahic *et al.* (2002) reported a decline in cell concentration by 3 gL^{-1} over 12 hours when abruptly shifting from unlimited growth on glycerol to a methanol feed^[46]. The adaption can be done during limited glycerol feed when glycerol concentrations are not sufficiently high to provide a complete repression of the AOX promoter. Afterwards, glycerol is ramped down and the cells are fully adapted to methanol as the sole carbon source.

Methanol Fed-Batch Induction Phase. Methanol concentration should be carefully controlled during induction either by monitoring the methanol levels directly using methanol sensors or indirectly using dissolved oxygen sensors. In the latter case a temporary pause in methanol feed should immediately cause a response in the oxygen consumption, visible by an increase in $p\text{O}_2$, if methanol is growth limiting. Although this technique offers high sensitivity, it only applies to Mut^+ cultures fully adapted to methanol, where AOX activity is not growth rate limiting^[48,51].

2.4 Experimental Strategy

The aim of this project is to recombinantly produce the antimicrobial peptide indolicidin (IL) and its single-tryptophan derivative indolicidin-4 (IL4) in the *P. pastoris* expression system. The expression will be made using wild-type and protease deficient *P. pastoris* strain to investigate the difference in expression levels. The pPICZ α A expression vector will be utilized to facilitate secretion of the antimicrobial peptides. The strategy of expression is based on homologous recombination of the *AOX1* gene, utilizing the strong AOX1 promoter inducible by methanol.

The effect of expression conditions, such as pH and temperature, on the expression levels will be analysed by shake-flask expressions. Detection of IL and IL4 in the supernatant will be made using SDS-PAGE, Reverse Phase-HPLC and MALDI-TOF Mass Spectrometry. Additionally, Zone Inhibition Assays will be used to indicate the presence of antimicrobial peptides in the supernatant. Scale-up expressions will be performed in a bioreactor using a four-phase fermentation strategy similar to the one previously mentioned. Also, fermentation will be performed in defined minimal growth medium to simplify downstream purification.

Materials and Methods

3

3.1 Chemicals and Biologicals

Table 3.1: Chemicals

Chemicals	Description	Manufacturer	Source/Reference
Acetic Acid	CH ₃ COOH	Merck	Lot: K39595863-903
Acetonitrile	HPLC-grade	Hiperpur Panreac	Lot: 0000184378
Acrylamide	Bis solution 30%	Bio-Rad	Cat. no: 161-0156
Agar		Sigma-Aldrich	Lot: BCBC2317
Agarose		Sigma-Aldrich	CAS: 9012-36-6
Ammonium Hydroxide	NH ₄ OH 28-30%	Sigma-Aldrich	Lot: SZBB1390V
Ammonium Sulphate	(NH ₄) ₂ SO ₄	Sigma-Aldrich	Lot: SZBB0180V
Boric Acid	H ₃ BO ₃ , ≥99%	Sigma-Aldrich	CAS: 100043-35-3
Calcium Chloride	CaCl ₂ , ≥99.5% ACS reagent	Merck	Cat. No: 1.02382
Citric acid monohydrate	99%	Sigma-Aldrich	Lot: 5949-29-1
Copper Sulphate	CuSO ₄ ·5H ₂ O, ≥98% ACS reagent	Sigma-Aldrich	CAS: 7758-99-8
d-Biotin	≥99%	Sigma-Aldrich	CAS: 58-85-5
D-(+)-Dextrose		Sigma-Aldrich	CAS: 50-99-7
D-Sorbitol		Sigma-Aldrich	Lot: BCBD5878V
dATP		Fermentas	Lot: 100-846
dCTP		Fermentas	Lot: 9701
dGTP		Fermentas	Lot: 8603
dTTP		Fermentas	Lot: 00020452
DNA loading dye	6X	Fermentas	Lot: 00034551
DreamTaq™ Buffer	10X	Fermentas	Lot: 00058293
Ethidium Bromide (EtBr)	10 mg/mL	Roche Diagnostics	
Formaldehyde	CH ₂ O 36.5–38%	Sigma-Aldrich	Lot: SZBB2800V
Generuler™ 1 kb DNA ladder		Fermentas	Lot: 00032587
Generuler™ 50 bp DNA ladder		Fermentas	Lot: 00028112
Glycerol	≥99%	Sigma-Aldrich	CAS: 56-81-5
H ₂ O	MB grade	Sigma-Aldrich	Lot: 50K8414
Iron(II) Sulphate	FeSO ₄ ·7H ₂ O, ≥99.5%	Fluka	CAS: 7782-63-0
Isopropanol	2-propanol, HPLC-grade	Sigma-Aldrich	Lot: 81955
Laemmli Sample Buffer	2X concentrate	Sigma-Aldrich	Cat. no: S3401
Lithium Acetate dihydrate	LiOAc	Sigma-Aldrich	Lot: 011M00051V
PageRuler	Unstained Low Range Protein	Fermentas	Lot: 00063008
Magnesium Sulphate	MgSO ₄ ·7H ₂ O, ≥99% ACS reagent	Fluka	CAS: 10034-99-8
Methanol	99.6%	Sigma-Aldrich	Lot: 58844-469
Peptone enzymatic digest from Casein		Fluka Analytical	Lot: BCBD0141V
Coomassie Brilliant Blue	PhastGel Blue-R350	Amersham Pharmacia	Lot: 0289363
Phosphoric Acid	85%	Sigma-Aldrich	CAS: 7664-38-2
Potassium Iodide	KI, ≥99.5%	Merck	Cat. No: 1.05043
Potassium Phosphate dibasic	ACS reagent, 98%	Sigma-Aldrich	CAS: 7758-11-4
Potassium Phosphate monobasic	KH ₂ PO ₄ , ACS reagent, 98%	Sigma-Aldrich	CAS: 7778-77-0

3.1 Chemicals and Biologicals

Table 3.1: Chemicals (continued)

Chemicals	Description	Manufacturer	Source/Reference
Potassium Sulphate	K ₂ SO ₄ , ≥99%	Sigma-Aldrich	7778-80-5
Select Agar	Ultra Pure	Sigma-Aldrich	CAS: 9002-18-0
Silver Nitrate	AgNO ₃ ≥99%	Sigma-Aldrich	CAS: 7761-88-8
Sodium Acetate		Sigma-Aldrich	Lot: 112K1373
Sodium Dodecyl Sulphate	99%	Sigma-Aldrich	CAS: 151-21-3
Sodium Molybdate dihydrate	MoNa ₂ O ₄ ·2H ₂ O, ≥99%	Sigma-Aldrich	CAS: 10102-40-6
Sulphuric Acid	H ₂ SO ₄ , 95–98%	Sigma-Aldrich	CAS: 7664-93-9
Trifluoroacetic acid	TFA, peptide-grade	Iris Biotech GmbH	CAS: 76-05-1
Tris/Tricine/SDS Buffer	10X	Bio-Rad	Cat. no.: 161-0744
Trizma base		Sigma-Aldrich	CAS: 77-81-1
Tryptone		AppliChem	Lot: 0F007962
Yeast Extract		Fluka Analytical	Lot: BCBD0078V
Yeast Nitrogen Base	Without amino acids	Sigma-Aldrich	Cat. No: Y0626
Zeocin™		Invitrogen	Lot: 849072

Table 3.2: Biologicals

Biologicals	Description/Genotype	Manufacturer	Source/Reference
Microbial Strains			
<i>Bacillus subtilis</i>			DSMZ 2109
<i>Escherichia coli</i> DH5α	F ⁻ φ80dlacZΔM15, Δ(<i>lacZYA-argF</i>)U169, <i>deoR</i> , <i>recA1</i> , <i>endA1</i> , <i>hsdR17</i> (<i>rK</i> ⁻ 1 <i>mK</i> ⁺) <i>phoA</i> , <i>supE44λ</i> ⁻ , <i>thi</i> – 1, <i>gyrA96</i> , <i>relA1</i> .		NEB
<i>Micrococcus luteus</i>			ATCC 4698
<i>Pichia pastoris</i> X33	Wild-type	Invitrogen	
<i>Pichia pastoris</i> SMD1168H	<i>pep4</i>	Invitrogen	
<i>Pseudomonas putida</i>			DSM291
Plasmids			
pPICZαA		Invitrogen	
pPICZαA-IL	pPICZαA containing <i>IL</i> gene within polylinker.		
pPICZαA-IL4	pPICZαA containing <i>IL4</i> gene within polylinker.		
pPICZαA-IL4 _{new}	pPICZαA containing a new <i>IL4</i> gene within polylinker (remade).		
Enzymes			
DreamTaq™ DNA Polymerase		Fermentas	Lot: 00061554
<i>Xba</i> I	5′-T [†] CTAGA-3′	NEB	Lot: 0401101
<i>Xho</i> I	5′-C [†] TCGAG-3′	NEB	Lot: 0581008
<i>Sac</i> I	5′-GAGCT [†] C-3′	NEB	Cat. No: R0156S
<i>Nco</i> I	5′-C [†] CATGG-3′	NEB	Cat. No: R0193T
T4 DNA Ligase		NEB	Cat. No: M0202T
Primers			
3′ AOX1	(all from DNA technology A/S) 5′-TGTCAGAATGCCATTTGC-3′		
α-factor	5′-TATTGCCAGCATTGCTGCT-3′		
<i>pre</i> AOX	5′-AGGTTTCATGAGTCGCAACC-3′		
Oligonucleotides			
IL ⁺	(all from DNA technology A/S) 5′-TCGAGAAAAGAATCTTGCCATGGAAGTGGCCATGGTGGCCATGGAGAAGATAATGAT-3′		
IL ⁻	3′-CTTTTCTTAGAACGGTACCTTCACCGGTACCACCGGTACCTCTTCTATTACTAGATC-5′		
IL4 ⁺	5′-TCGAGAAAAGAATCTTGCCATGGAAGTTGCCATTGTTGCCATTGAGAAGATAATGAT-3′		
IL4 ⁻	3′-CTTTTCTTAGAACGGTACCTTCACCGGTAACAACGGTAACTCTTCTATTACTAGATC-5′		

3.2 Construction of Expression Vector

3.2.1 Chemical Transformation of pPICZ α A into *E. coli* DH5 α

Competent DH5 α *E. coli* cells was thawed on ice for 10 minutes. 2 μ L of pPICZ α A vector was added and the mixture was finger flicked 5 times and placed on ice for 30 minutes before heat shocked at 42°C for exactly 10 seconds followed by 5 minutes of incubation on ice. 950 mL low-salt LB medium (room temperature) was added and the cells were incubated at 37°C and 250 rpm shaking for 60 minutes. The mixture was inoculated on Zeocin (25 μ g/ml) plates and incubated overnight at 37°C.

3.2.2 Plasmid DNA Purification

The *Sigma Aldrich GenElute™ Miniprep Kit* was used for purification of plasmid DNA from 5 mL *E. coli* cultures incubated overnight in low-salt LB Zeocin (25 μ g/ml) medium at 37°C with shaking at 225 rpm. The plasmid was purified according to the protocol supplied with the kit and suspended in 10 mM Tris-HCl buffer or MB grade H₂O.

The *QIAGEN Plasmid Midi Kit* was used for purification of 100 mL *E. coli* main cultures incubated overnight in low-salt LB Zeocin (25 μ g/ml) medium at 37°C with shaking at 225 rpm, inoculated from a 2 mL overnight preculture in similar conditions. The method is based on anion-exchange column purification and was made according to the protocol supplied.

The *MILLIPORE Ultrafree® -DA Kit* was used for purification of DNA from preparative agarose gel electrophoresis. The agarose gel was analyzed with low-intensity UV light and the bands of interest was cut out and frozen (-20°C) for 2 hours. The frozen fragments was then loaded to the supplied column and DNA was purified according the the protocol supplied. The extracted DNA was then precipitated with ethanol (see below).

3.2.3 Ethanol Precipitation

DNA was precipitated by addition of 2 \times sample volume of 96% EtOH and $\frac{1}{10}\times$ sample volume of 3M NaOAc. The solution was mixed and incubated at -20°C for 30 minutes followed by 30 minutes of centrifugation at 20,000 g at 4°C. The pellet was resuspended in 200 μ L 70% ethanol and centrifuged again for 10 minutes under same conditions. Finally the pellet was air dried and resuspended in 50 μ L MB grade H₂O and stored at -20°C.

3.2.4 Digestion of pPICZ α A Plasmid Vector

Plasmid DNA from two 100 mL main cultures of selected pPICZ α A transformed *E. coli* colonies were purified and dissolved in 50 μ L MB grade H₂O. The pPICZ α A vector was digested with *Xba*I and *Xho*I restriction enzymes to facilitate gene insertion. First, 10 μ L plasmid DNA was digested with 100 units of *Xba*I enzyme, supplemented with 10 μ L 10X NEBuffer 2, 1 μ L 100X BSA, and 69 μ L MB grade H₂O, in a total volume of 95 μ L. The reaction mixture was incubated at 37°C for 2 hours followed by heat inactivation at 64°C for 20 minutes. The second digestion was made with similar conditions by addition of 100 units of *Xho*I enzyme to a final volume of 100 μ L. The digestion was verified by analytical agarose gel electrophoresis (described below) before the second digestion. A preparative agarose gel electrophoresis were made on the final digestion product and the correctly sized DNA was extracted as described previously. The final product was dissolved in 30 μ L MB grade H₂O and the concentration was crudely determined by gel electrophoresis.

3.2.5 Annealing and Phosphorylation of Oligonucleotides

The forward and reverse oligonucleotides (TAG Copenhagen A/S) encoding IL and IL4 were dissolved in 10 mM Tris-HCl buffer (pH 6) to a concentration of 100 μ M. 5 μ L of complementary oligonucleotides (IL⁺/IL⁻ and IL4⁺/IL4⁻) were added to 20 μ L of 10 mM Tris-HCl buffer (pH 6) and annealed at 95°C for 5 minutes and slowly cooled to room temperature and finally stored at 4°C. Phosphorylation of the DNA was done using T4 Polynucleotide Kinase (Fermentas). The annealed DNA was added to the following reaction mixture: 37 μ L MB grade H₂O, 8 μ L 10X Reaction Buffer A, 1 μ L 10 mM ATP, 4 μ L 10u/ μ L T4 Polynucleotide Kinase, to a total volume of 80 μ L. The reaction solution was mixed thoroughly and incubated at 37°C for 30 minutes followed by heat inactivation at 75°C for 10 minutes.

3.2.6 Ligation of Insert into Digested pPICZ α A Vector

5 pmol prepared insert was ligated into 1.66 pmol digested pPICZ α A (3:1 molar ratio) using 20 units of T4 DNA Ligase in a total reaction volume of 10 μ L. The reaction was buffered with T4 DNA Ligase Reaction Buffer assisted with 1 mM extra ATP and incubated overnight at 16°C followed by heat inactivation at 65°C for 10 minutes. This yielded pPICZ α A-IL and pPICZ α A-IL4 shuttle vectors. A small fragment of the resulting DNA sequences of the circular vector is presented in Figure A.1 and A.2 in Appendix A, highlighting important primer sites and restriction sites utilized in this project.

3.2.7 Chemical Transformation of pPICZ α A-IL/pPICZ α A-IL4 into *E. coli* DH5 α

Competent DH5 α *E. coli* cells was thawed on ice for 10 minutes. 10 μ L of ligation mixture (pPICZ α A-IL or pPICZ α A-IL4) was added and the mixture was finger flicked 5 times and placed on ice for 30 minutes before heat shocked at 42°C for exactly 10 seconds followed by 5 minutes of incubation on ice. 500 μ L low-salt LB medium (room temperature) was added and the cells were incubated at 37°C and 250 rpm shaking for 60 minutes. The mixture was inoculated on Zeocin (25 μ g/ml) plates and incubated overnight at 37°C.

3.3 DNA Electrophoresis

Size analysis of DNA from PCR, enzyme digestions or plasmid purifications were made using agarose gel electrophoresis. 1% agarose in 1X TAE buffer and 0.5 μ L EtBr were used for DNA fragments/plasmid above 1,000 bp against a GeneRulerTM 1 kb DNA Ladder (Fermentas, Helsingborg, Sweden). 2% agarose in 1X TAE buffer and 0.5 μ L EtBr were used for smaller fragments against a GeneRulerTM 50 bp DNA Ladder (Fermentas, Helsingborg, Sweden). Samples were mixed with 6X DNA Loading Dye (Fermentas, Helsingborg, Sweden) in 5:1 ratios. The electrophoresis was run for 70 minutes at 70 V (DC) and analyzed in high intensity UV-light (analytical) or low intensity UV-light (preparative).

3.4 Transformation Screening

3.4.1 PCR Screening for Correct Insert

Screening for successful insertion of plasmid DNA isolated from transformed *E. coli* or chromosomal DNA isolated from transformed *P. pastoris* was done using α -factor(5'-TATTGCCAGCATTTGCTGCT-3') and 3'AOX1(5'-TGTCAGAATGCCATTTGC-3') primers. The PCR was performed in a total volume of 100 μ L with 1X

DreamTaqTM Buffer, 25 mM MgCl₂, 0.2 mM dNTP each, 1 μ M forward sequence primer, 1 μ M reverse sequence primer, 2-3 units of DreamTaqTM DNA Polymerase and template DNA. The thermal cycling conditions of the PCR is shown in table 3.3. The PCR product was analyzed by agarose gel electrophoresis against a GeneRulerTM 50 bp DNA Ladder.

Table 3.3: PCR Thermal Cycling Conditions

Step	Temperature	Time	Cycle
Heat Soak	94 °C	2 minutes	1X
Denaturation	94 °C	1 minutes	
Annealing	54 °C ^a	1 minutes	25X
Extension	72 °C	1 minutes	
Final Extension	72 °C	10 minutes	1X

^a Found as the lowest melting temperature (T_M) minus 5°C.

Table 3.4: *Nco*I Restriction Analysis on pPICZ α A-IL and pPICZ α A-IL4

Plasmid Isolate	Position	Length (bp)
pPICZ α A-IL (3564) ^a	2132-1202	2634 ^b
	1224-2131	908
	1203-1214	12
pPICZ α A-IL4 (3564) ^a	1215-1223	9
	2132-1202	2634 ^b
	1203-2131	929
pPICZ α A (3593) ^a	0	3593

^a Number in parentheses are plasmid size (bp).

^b DNA fragment screened for by agarose gel electrophoresis.

3.4.2 Screening for Correct Insert by *Nco*I Digestion

Enzymatic digestion was used to support PCR screening of successful insertion. A suitable restriction enzyme (*Nco*I), that digests inside the IL/IL4 gene of the two vector constructs (pPICZ α A-IL and pPICZ α A-IL4), was found using the enzyme restriction site library of New England Biolabs^[80]. Table 3.4 summarizes the restriction analysis of the two vector constructs using *Nco*I. The enzymatic digestion of 5 μ L isolated vector was performed using 5 units of enzymes in a total volume of 20 μ L assisted with 1X Buffer TangoTM. The mixture was incubated at 37°C for 4 hours followed by heat inactivation at 65°C for 10 minutes. The digested product was analysed by agarose gel electrophoresis against a GeneRulerTM 1 kb DNA Ladder.

3.4.3 PCR Screening of Multiple Integrated Copies of Foreign Genes

When transforming *P. pastoris* with pPICZ α A vectors it is possible to isolate strains containing tandem copies of the entire expression cassette. To screen for multiple integrated copies of genes the 3' AOX1(5'-TGTCAGAA-TGCCATTTGC-3') were used with the *pre*AOX(5'-AGGTTTCATGAGTCGCAACC-3') primer complementary to a chromosomal DNA fragment positioned upstream the 5' AOX crossover site and thus outside the pPICZ α A vector. A single-copy isolate results in a 1.6 kbp PCR product while multiple copies result in ≥ 4.7 kbp products. Chromosomal DNA was isolated from transformed *P. pastoris* colonies, as described later, and the PCR was performed under the same¹ reaction conditions and thermal cycling conditions as above. The PCR product was analyzed by agarose gel electrophoresis against a GeneRulerTM 1 kb DNA Ladder.

3.5 Transformation of pPICZ α A-IL/pPICZ α A-IL4 into *P. pastoris*

Preparation of vector were done by incubating 100 mL main cultures of *E. coli* cells transformed with pPICZ α A-IL and pPICZ α A-IL4 in low-salt LB medium containing Zeocin (25 μ g/ml) at 37°C overnight. The plasmid DNA was purified as described and 50-100 μ g was linearized by 40 units of *Sac*I restriction enzyme in a total volume of 150 μ L containing NEBuffer1 and BSA (1X). The digestion was proceeded at 37°C incubation

¹ Although 20 μ L of chromosomal DNA isolate was used as template DNA.

for 4 hours followed by heat inactivation at 65°C for 20 minutes. 5 µL of digested samples were run on gel electrophoresis to verify successful digestion. The linearized DNA was precipitated by ethanol and the samples were stored at -20°C.

Preparation of P. pastoris were made by incubating electrocompetent strains (X-33 and SMD1168H) in 2 mL YPD medium at 30°C and 250 rpm overnight. The cells were inoculated on fresh YPD plates and grown overnight at 30°C. A single colony was grown overnight in 5 mL YPD medium in a 50 mL conical at 30°C with shaking (225 rpm). 500 µL of the overnight culture was inoculated in 300 mL fresh medium in a 2 liter flask and incubated overnight at 30°C, 225 rpm. The cells were centrifuged at 1,500×g for 5 minutes at 4°C. The pellet was washed in 300 mL ice cold sterile water and centrifuged again (repeated 3 times). After the last centrifugation the pellet was resuspended in 20 mL ice cold 1M sorbitol and centrifuged again. Finally the pellet was resuspended in 1 mL 1M sorbitol and kept on ice. 80 µL of the high concentrated cells were mixed with approximately 15 µg of linearized vector (pPICZαA-IL and pPICZαA-IL4) and transferred to an ice cold electroporation cuvette and incubated on ice for 5 minutes. The cells were pulsed using MicroPulser™ Electroporator (Bio-Rad Laboratories) with settings for *Pichia pastoris* (5 ms at 2 kV) and 1 mL of ice cold 1M sorbitol was immediately added to the cuvette and the content was transferred to a 12 mL sterile test tube and incubated at 30°C without shaking for 2 hours. 25, 50, 100 and 200 µL of cells were spread on YPDS-Zeocin plates (100 µg/ml) and incubated at 30°C for several days until colonies were formed. 10 Colonies were selected and grown in 2 mL YPD-Zeocin medium for 4 hours and streaked onto YPD-Zeocin plates and incubated overnight at 30°C. The colonies were labeled X33-ILA-J, X33-IL4A-J, SMD-ILA-J and SMDIL4A-J for the appropriate strain and insert used.

3.6 Extraction of Genomic DNA from *P. pastoris*

In order to isolate chromosomal DNA from *P. pastoris* for PCR-based screenings, cells were picked from the YPD-Zeocin plates and suspended in 100 µL 200 mM LiOAc solution containing 1% SDS and incubated at 70°C for 15 minutes. 300 µL 96% ethanol was added and the samples were mixed and incubated at 4°C for 20 minutes and the DNA was extracted by centrifugation at 15,000×g for 5 minutes at 4°C. Precipitated DNA was dissolved in 100 µL MB grade H₂O and centrifuged again. The pellet was discarded and 70µL supernatant was stored at 4°C, and later used to verify integrations by PCR analysis.

3.7 DNA Sequencing

Purified pPICZαA-IL and pPICZαA-IL4 plasmid DNA was sequenced using the 3'AOX(5'-TGTCAGAATGC-CATTTGC-3') primer. No reverse primer was used for sequencing. Additionally, the PCR products from the chromosomal DNA screening using *pre*AOX(5'-AGGTTTCATGAGTCGCAACC-3') together with 3'AOX(5'-TGTCAGAATGCCATTTGC-3') were also sequenced to test for successful transformation. The sequencing was performed by DNA Technology A/S (Risskov, Denmark), using a 3130 XL Genetic Analyzer (Applied Biosystems).

3.8 Small-scale expression study

Multiple shake-flask expressions were made on recombinant *P. pastoris* in order to investigate the optimal temperature and pH during induction. Three different pH (3, 4.5 and 6) and two different temperatures (20°C and 30°C) were studied for highest expression levels. Colonies of X33-IL, X33-IL4, SMD-IL and SMD-IL4

were selected and incubated in 25 mL BMGY medium (10 g/L yeast extract, 20 g/L peptone, 10 g/L glycerol and 100 mM potassium phosphate adjusted to pH 6) in 6×250 mL shaking flasks at 30°C, 250 rpm overnight (12-16 hours). The cells were harvested by centrifugation at 1,500×g for 5 minutes and resuspended in 150 mL pH adjusted BMMY (10 g/L yeast extract, 20 g/L peptone, 0.5% methanol and 100 mM potassium phosphate adjusted to pH 3, 4.5 and 6, respectively) to an OD₆₀₀ of roughly 0.9. The cells were incubated at 20°C and 30°C with shaking at 250 rpm for 96 hours in 2L baffled flasks covered with 3 layers of cheese cloth to enhance aeration during the induction. Every 24 hours 5 mL samples were collected and the OD₆₀₀ was measured in duplicates. The samples were centrifuged at 1,500×g for 5 minutes and the supernatant was collected and frozen with liquid nitrogen and stored at -20°C. The pH of the running batch was adjusted using 2M ortho-phosphoric acid and 2M KOH and methanol was added to a final concentration of 0.5% to maintain induction.

3.9 Tricine Sodium Dodecyl Sulfate Polyacrylamide Gel Electrophoresis

Samples collected from shake-flask expressions of recombinant X33IL-A and SMDIL-E after 48 hours and 96 hours respectively were analysed by tricine SDS-PAGE using 10-20% Mini-Protean® Tris-Tricine Precast Gels (Bio-Rad, Copenhagen, Denmark). 100 µM and 10 µM synthesized IL was used as reference. The electrophoresis cell was assembled with the precast gel and added Tris-Tricine SDS running buffer (Bio-Rad, Copenhagen, Denmark). Samples were prepared by mixing 30 µL sample with with 25 µL 2X Laemmli Sample Buffer (Sigma, Copenhagen, Denmark) and was incubated at 100°C for 3 minutes. The samples were then spinned briefly at 2000×g and placed on ice. The wells were loaded with 35 µL prepared sample or PageRuler™ Unstained Low Range Protein Ladder (Fermentas, Helsingborg, Sweden) as standard. The electrophoresis cell were finally topped with running buffer and a 200 V potential was applied until the dye front had reached the bottom.

Coomassie Blue R staining: After the electrophoresis, the gel was fixed using fixing solution (40% ethanol, 10% acetic acid) for 30 minutes and rinsed with water. The gel was suspended in 200 mL staining solution (0.1% (w/v) Coomassie blue R350, 30% (v/v) ethanol, and 10% (v/v) acetic acid) for 3 hours at room temperature with gentle agitation. The staining solution was replaced with 200 mL destain solution (10% acetic acid, 30% ethanol) and destained until the desired result was achieved.

Silver staining: After the electrophoresis, the gel was fixed using fixing solution (40% ethanol, 10% acetic acid) for 30 minutes and rinsed with water. The gel was then suspended in 7% acetic acid for 10 minutes and rinsed with water. The water was then replaced with 200 mL 50% methanol and the gel was stirred for 20 minutes. The gel was fixed twice to prevent sample loss from diffusion. Meanwhile, the silver staining solution was prepared by adding solution A (0.8 g AgNO₃ in 4 mL H₂O) drop-wise to solution B (6.18% (v/v) NH₄OH, 0.36% (w/v) NaOH). The gel was then suspended in the stain for 15 minutes and rinsed twice in 200 mL H₂O for 5 minutes. Subsequently the gel was soaked into 200 mL development solution (1 mL citric acid, 100 µL 37% formaldehyde in 198.9 mL H₂O) until bands were visible (5-15 minutes). The development was stopped by rinsing three times with 200 mL H₂O.

3.10 Fermentation Strategy

Scale-up expressions of IL were performed on a BIOSTAT® A plus bioreactor from Sartorius with a capacity of 2 L. The fermentor was equipped with a sterilisable OXYFERM™ O₂ sensor and pH electrode (Hamilton, Bonaduz, Switzerland) that were both calibrated before autoclavation. Agitation was done using two turbines and a standard air-pump was used for oxygen-supply. The fermentor was equipped with a cooled condenser to avoid evaporation from the medium. The integrated feeding pump did not provide satisfying sensitivity,

so an external ISMATEC® REGLO analog tubing pump was used instead, allowing feeding rates down to 25 $\mu\text{L}/\text{min}$ with the capacity for multiple tubes. The pump was controlled by a MCCDAQ USB-1208 digital-to-analog converter and software was written in C# to control the feeding pump. The fermentor sensors were also integrated in the software to allow feedback from the oxygen levels to be used to control the pump speed. This was used to automatically monitor oxygen spikes, for immediate activation of the feeding pump.

The pO_2 electrode was calibrated in terms of percentage oxygen saturation. Zero reference calibration was made before sterilisation by replacing air inflow with nitrogen gas while 100% pO_2 reference was made after the fermentation medium had cooled down from autoclavation using air-pump and 1000 rpm stirring. The pH was calibrated by two-point calibration (pH 4 and pH 7 buffers) before sterilisation and re-calibrated after sterilisation using external pH meter.

Inoculum preparations: The culture was made by inoculating 100 μL *P. pastoris* expression colonies in 100 mL BMGY medium in a 2 L baffled flask. The culture was grown for 24 hours at 30°C and 250 rpm agitation. Cells were harvested by centrifugation at 1500 \times g in 50 mL sterile conical tubes and resuspended in 100 mL sterile basal salt medium (13 g/L KH_2PO_4 , 2.7 g/L K_2HPO_4 , 0.1 g/L NaCl, 2 g/L $\text{MgSO}_4\cdot 7\text{H}_2\text{O}$, 15 g/L $(\text{NH}_4)_2\text{SO}_4$, 2 g/L K_2SO_4 and 0.2 g/L CaCl_2) containing 20 g glycerol.

Glycerol batch: The fermentor was loaded with 1 L basal salt medium and sterilized by autoclavation. The temperature was set to 25°C and pH was maintained at 5 by automatic addition of 2 M ortho-phosphoric acid and 28% NH_4OH . Agitation was set to 1000 rpm and constant air was supplied using external air pump during the entire fermentation. After the temperature was settled, cell suspension were loaded to the fermentor and 2 mL of trace elements solution (6 g/L $\text{CuSO}_4\cdot 5\text{H}_2\text{O}$, 0.09 g/L KI, 3 g/L $\text{MnSO}_4\cdot \text{H}_2\text{O}$, 0.02 g/L H_3BO_3 , 0.24 g/L $\text{MoNa}_2\text{O}_4\cdot 2\text{H}_2\text{O}$, 0.5 g/L CoCl_2 , 10 g/L ZnCl_2 , 20 g/L $\text{FeSO}_4\cdot 7\text{H}_2\text{O}$, 0.2 g/L biotin and 5 mL/L H_2SO_4) was added. The batch was started immediately and since the substrate concentrations (methanol and glycerol) were not monitored, the pO_2 was monitored for a sudden spike, indicating depletion in glycerol substrate.

Glycerol fed-batch: As soon as a spike in pO_2 was recorded a feed of 50% (v/v) glycerol at 36.6 $\mu\text{L}/\text{min}$ was initiated and subsequently regulated according to the oxygen level. Glycerol was fed at growth limiting conditions for 5-10 hours.

Transition: At the end of the glycerol fed-batch the temperature and pH was changed to induction conditions (pH 3 and 20°C). In one of the fermentations a methanol feed (99.9% methanol added 12 mL/L trace elements solution) was applied simultaneously with the glycerol feed, to enable the production of AOX enzymes. The feeding rate was 36.6 $\mu\text{L}/\text{min}$ for both substrates and after three hours the glycerol feed was stopped. 0.5 mL antifoam was added to the reactor during transition to methanol. 5 mL of magnesium and ammonium supplementation (50 g/L $(\text{NH}_4)_2\text{SO}_4$ and 12.5 g/L $\text{MgSO}_4\cdot 7\text{H}_2\text{O}$) was added prior to induction by methanol to avoid depletion according to Maghsoudi *et al*^[81].

Methanol fed-batch: During induction, methanol was fed in growth-limiting feeding rates controlled manually according to the oxygen levels. The pO_2 level was attempted to be kept at 15-25% during this phase. Methanol feed was stopped briefly during induction and the oxygen feedback was observed. This was done to ensure that methanol was kept at growth-limiting conditions and avoid accumulation of methanol indicated by a delayed response in pO_2 .

Samples were collected each day and the cells were separated from the supernatant by centrifugation at 5000 \times g for 5 minutes. The cell pellet was heated at 110°C for 24 hours and the dry cell weight was measured (this was done in duplicates). The supernatant from 5 mL sample was frozen in liquid nitrogen and freeze-dried for two days and stored at -80°C for future analysis.

3.11 Zone Inhibition Assay

Measurements of antimicrobial activity of culture supernatant from recombinant expressions were performed by growth inhibition of *B. subtilis*. The bacteria was replated onto a fresh peptone-yeast extract agar plate and incubated overnight at 37°C. Cell material was scraped off the plate and suspended in 500 µL H₂O. Fresh peptone medium (5% peptone, 5% yeast extract, 5% agarose) was prepared and heated to boiling temperature using a microwave oven. 20 mL medium was added to 50 mL tubes and left to cool to 45-50°C before the bacterial suspension was added and the mixture was poured out on sterile petri dishes and left to solidify at room temperature. 5 mm wells were punched in the agarose medium by 10-200 µL pipette tips and 20µL samples were loaded. References used include 100 µg/mL ampicillin, 100 µM synthesized IL (non-amidated), 100 µM synthesized IL (amidated) and 165 µM synthesized IL4 (non-amidated). After loading samples, the plates were incubated at 37°C for 24 hours. Additional controls were evaluated by zone inhibition assays including 10X concentrated BMGY medium at pH 3, 4.5 and 6 as well as 10X concentrated basal salt medium at pH 3, 4.5 and 6. All samples were sonicated for 5 minutes and vortexed prior to loading.

Prior to the measurements of antimicrobial activity of culture supernatant, zone inhibition assays were made on synthesized IL (non-amidated) and IL (amidated) on *M. luteus*, *P. putida*, *E. coli* and *B. subtilis* to find the bacteria with highest susceptibility to the antimicrobial activity of IL. The protocol was the same as above, except *M. luteus* and *P. putida* were suspended in LB medium (10% tryptone, 5% yeast extract, 5% NaCl and 5% agarose) and incubated at 28°C while *E. coli* was suspended in LB medium and incubated at 37°C overnight. *B. subtilis* was chosen as bacteria for the zone inhibition assays and used for the rest of the project.

3.12 RP-HPLC analysis

The medium fractions were analysed by Reverse Phase-HPLC using UltiMate® 3000 Basic Manual LC System (Dionex, Sunnyvale, CA, USA) with an UltiMate® 3000 Quaternary Analytical Pump LPG-3400SD (Dionex) and a DAD-3000RS Rapid Separation Diode Array Detector (Dionex) and equipped with a 4.6×150 mm Acclaim® 300 C18 Protein and Peptide Column (Dionex). The column was equilibrated with 2% acetonitrile (ACN) and 0.1% trifluoroacetic acid (TFA). Two columns were used in the project. A new column was acquired during the project, and the flow-rate was increased from 0.5 mL/min to 1 mL/min with the new column. The ACN elution gradient was optimized according to synthesized IL (non-amidated), to ensure most optimal separation from the complex supernatant. The elution gradient is shown in Figure 3.1. Some samples were, however, analysed by a full gradient as shown in Figure 3.2.

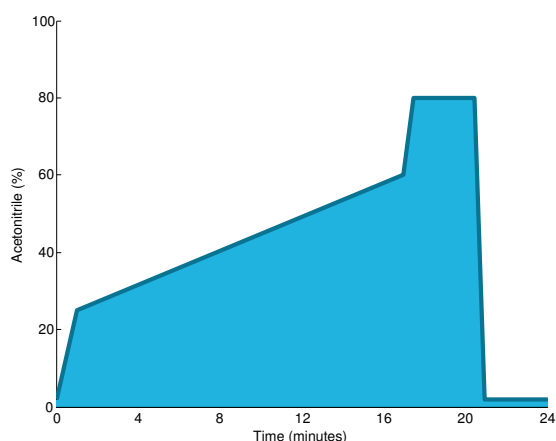


Figure 3.1: Acetonitrile gradient used in analytical RP-HPLC.

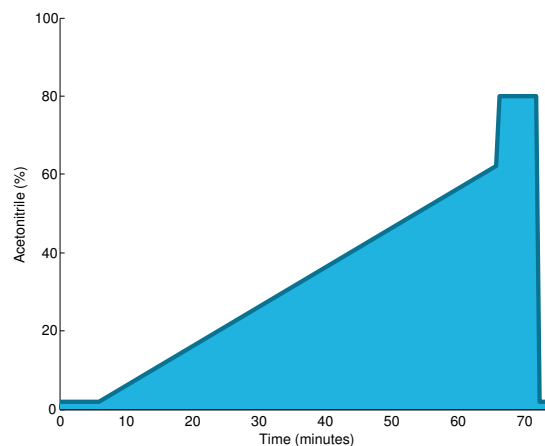


Figure 3.2: Acetonitrile gradient used in analytical RP-HPLC.

Freeze-dried supernatant (5 mL) from recombinant expressions was resuspended in 500 μ L 10 mM Tris-HCl (pH 6) and sonicated for 10 minutes. The samples were further diluted 1:10 and filtered by 450 nm syringe filters before being loaded to the 150 μ L injection loop yielding a final concentration of 1:1 from the original supernatant concentration. As reference, synthesized IL and IL4 (both non-amidated) were used.

To test for degradation of IL in the supernatant by proteolytic activity, synthesized IL (non-amidated) was mixed with culture supernatant and 10 mM Tris-HCl (pH 6) to a final dilution of supernatant of 1:2 and a final concentration of IL at 11.3 μ M. The mixture was filtered and incubated overnight at room temperature and loaded to the HPLC for analysis.

3.13 MALDI-TOF Mass Spectrometry

The intention was to analyse the supernatant samples collected from shake-flask and fermentation studies using MALDI-TOF MS. Unfortunately the apparatus was broken down at the time of writing. Instead samples from culture and fermentation supernatant were prepared for Liquid-Chromatography Mass Spectrometry. However, the result from these experiments were not obtained prior to the deadline for this project.

3.14 Chemical Synthesis of IL and IL4

IL² and IL4³ was chemically synthesized using Fmoc based solid phase peptide synthesis (SPPS) on an Activo-P11 Automatic Peptide Synthesizer (Activotec, Cambridge, USA). The reactor vessel was loaded with 200 mg Fmoc-L-Arg(Pbf)-Wang resin with a theoretical yield of 0.1 mmol. The synthesis was made using the protocol summarized in Table 3.5. The initial swelling was done by the synthesizer, using DMF as solvent for the rest of the process.

The synthesized IL and IL4 were cleaved from the resin by addition of 2 mL of cleavage solution (95% TFA, 2.5% TIS, 2.5% Milli-Q water) followed by 90 minutes shaking. This was done on an Activotec ActivoP12 Cleavage Machine. The cleaved peptides were drained through the filter of the reactor vessel and collected in a 50 mL conical tube. 2 mL 100% TFA was added to the reactor vessel that was then shaken for 2 minutes before being drained into the conical tube. To precipitate the peptides 30 mL of -20°C diethyl ether was added and the solution was centrifuged at $5,000\times g$ for 5 minutes and the supernatant was decanted. This step was repeated and the pellet was dried in vacuum overnight.

3.14.1 Purification of Synthetic Peptides

The synthesized peptides were purified by Reverse-Phase HPLC on the same setup as above including a AFC-3000 fraction collector (Dionex, Sunnyvale, CA, USA). The HPLC was equipped with a 10×250 mm Gemini-NX 5μ C18 110A column (Phenomenex, Værløse, Denmark). The dried peptides were resuspended in 20 mL equilibration buffer (0.1% TFA 2% ACN) and was loaded to the pre-equilibrated HPLC in 2 mL injection volumes and separated against an acetonitrile gradient shown in Figure 3.2 at a flow rate of 5 mL/min. The absorbance was measured at wavelengths of 213 nm and 280 nm and the automated fraction collection was set to monitor wavelength of 280 nm. The collected fractions were freeze-dried for 4 days and stored at -80°C .

²ILPWKWPWWPWRR

³ILPWKLPLLPLRR

Table 3.5: SPPS Synthesis Cycle for chemical production of IL and IL4

Procedure	Adding	Time	# Cycles
Swelling	2.0 mL DMF	15 min	1
	2.0 mL DMF	60 min	
Deprotection	2.0 mL Piperidine 25%	3 min	13
Washing	2.0 mL Piperidine 25%	12 min	
	2.0 mL DMF	1 min	
	2.0 mL DMF	1 min	
	2.0 mL DMF	1 min	
	2.0 mL DMF	1 min	
Dissolving amino acid	1.0 mL 0.48 M HB-TU/HOBt	12 min	
Activation of amino acid	0.5 mL DIPEA	1 min	
Coupling	Activated amino acid ^a	40 min	
	2.0 mL DMF	1 min	
Washing	2.0 mL DMF	1 min	
	2.0 mL DMF	1 min	
	2.0 mL DMF	1 min	
Washing	2.0 mL DMF	1 min	5
Washing	2.0 mL DCM	1 min	3

^a Arg12 was double coupled to ensure high coupling rate.

Results

4

4.1 Construction of Expression Vector

To construct the expression vector for *P. pastoris*, pPICZ α A plasmid was first transformed into *E. coli* and a single colony was selected for the following cloning process. Two purified samples of pPICZ α A plasmid from this colony was digested with *Xho*I and *Xba*I restriction enzymes. To verify that the plasmid had been digested correctly, the samples was digested separately with one of the two restriction enzymes. The result of a single digestion was analysed by gel electrophoresis and shown in Figure 4.1. The DNA samples are both linear (defined band) with a size matching the plasmid (3593 nucleotides). The second digestion was made using opposite restriction enzyme and the digested product was loaded on a gel and collected by preparative gel electrophoresis and purified by ethanol precipitation. This sample was then analysed by gel electrophoresis (Figure 4.2), confirming correct digestion by the formation of a fragment around 3500 bp in size, corresponding to the expected 3506 bp fragment.

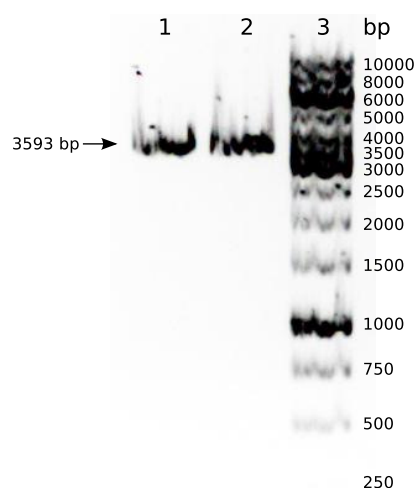


Figure 4.1: Two samples of pPICZ α A plasmid analysed in 1% agarose gel. The plasmid was digested with 1) *Xba*I and 2) *Xho*I restriction enzymes. 3) is a 1 kb standard (Fermentas, Helsingborg, Sweden).

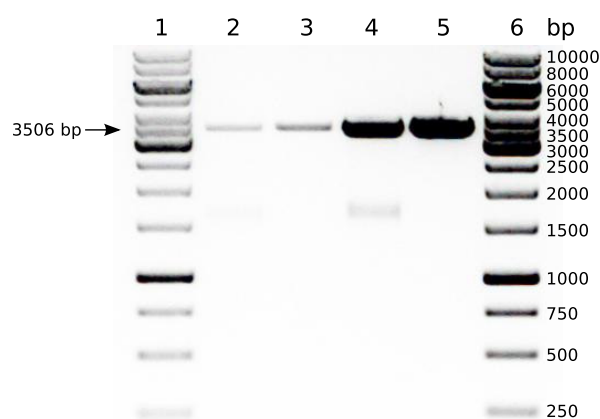


Figure 4.2: pPICZ α A plasmid digested with *Xba*I and *Xho*I restriction enzymes and analysed by 1% agarose gel in dilutions of 2+3) 1:6 and 4+5) 4:6. Content of 1) and 6) is a 1 kb standard (Fermentas, Helsingborg, Sweden)

Inserts of the IL and IL4 genes, made by annealing complementary oligonucleotides containing *Xho*I and *Xba*I restriction sites, were ligated into each of the digested pPICZ α A plasmid samples (without confirmation) and transformed into *E. coli* yielding colonies labelled pPICZ α A-IL-A through H and pPICZ α A-IL4-A through H. The insertion was verified by PCR analysis on purified plasmid DNA using α -factor and 3'AOX primers. A gel electrophoresis analysis of colonies pPICZ α A-IL-A and -B and pPICZ α A-IL4-A and -B are shown in Figure 4.3. Expected fragments size of both PCR products were 268 bp. However, the PCR screening suggest differences in the plasmid sizes of pPICZ α -IL and pPICZ α -IL4, which should not be the case. To investigate this, a digestion was prepared using *Nco*I restriction enzyme, which should produce a fragment of 2634 bp on both plasmids and another fragment of 908 bp by pPICZ α -IL and 929 bp by pPICZ α -IL4. A 1% agarose gel electrophoresis of the digested products are shown in Figure 4.4. Only pPICZ α -IL4-A showed fragments

4.1 Construction of Expression Vector

of correct sizes, while the other colonies showed only linearised DNA fragments, formed by single digestion. Therefore, screening was performed on pPICZ α A-IL-C through -H colonies using *Nco*I restriction enzymes. A gel electrophoresis analysis of this digestion is shown in Figure 4.5, showing correct insertion in pPICZ α A-IL-C and -F. The expression vectors from colonies pPICZ α A-IL-F and pPICZ α A-IL4-A were selected for transformation into *P. pastoris* X33 and SMD1168H strains.



Figure 4.3: A 2% agarose gel of product of PCR reaction using α -factor and 3'AOX primers on the plasmid DNA from the following colonies: **2+3**) pPICZ α A-IL-A, **4+5**) pPICZ α A-IL-B, **7+8**) pPICZ α A-IL4-A, **9+10**) pPICZ α A-IL4-B. Content of **1**), **6**) and **11**) is a 50 bp standard (Fermentas, Helsingborg, Sweden)

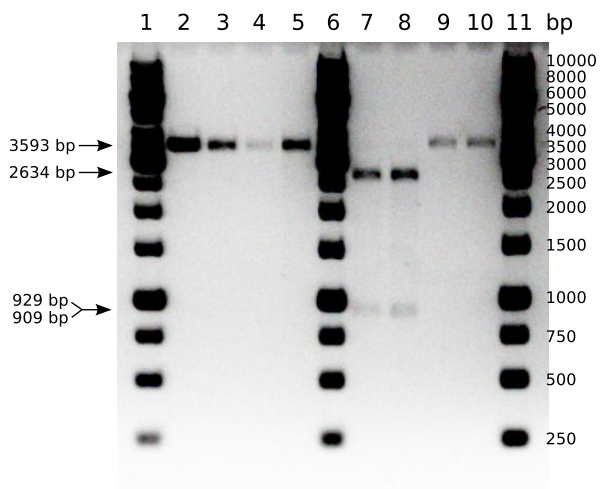


Figure 4.4: 1% agarose gel electrophoresis of *Nco*I-digested plasmid purified from pPICZ α A-IL colonies A (**2+3**) and B (**4+5**) and of pPICZ α A-IL4 colonies A (**7+8**) and B (**9+10**) against a 1kb standard ladder (Fermentas, Helsingborg, Sweden) in **1**), **6**) and **11**).

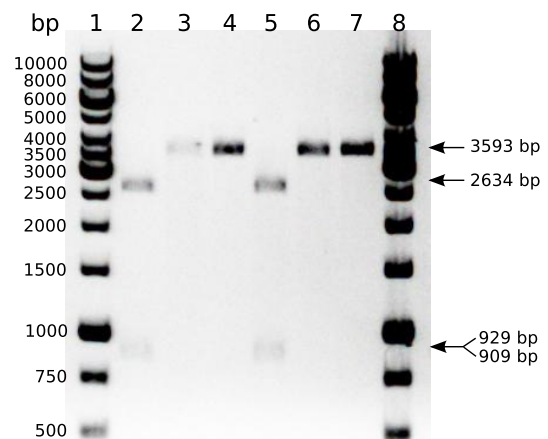


Figure 4.5: 1% agarose gel electrophoresis of *Nco*I-digested plasmid purified from pPICZ α A-IL colonies C-H in wells **2**) through **7**). Content of **1**) and **8**) is a 1kb standard ladder (Fermentas, Helsingborg, Sweden).

Very unfortunately the sequencing of the pPICZ α A-IL and -IL4 few weeks later in the project revealed mutations in the IL4 gene (see section B for sequence data). Therefore, new oligonucleotides were ordered and cloned into pPICZ α A using the same procedures as earlier. pPICZ α A-IL4_{new} plasmid was purified from eight *E. coli* transformants and digested with *Nco*I restriction enzymes for verification of correct insertion. Three out of eight colonies showed correct insertion (Figures 4.6 and 4.7) and pPICZ α A-IL4_{new}-A was selected for transformation into *P. pastoris* X33 and SMD1168H strains.

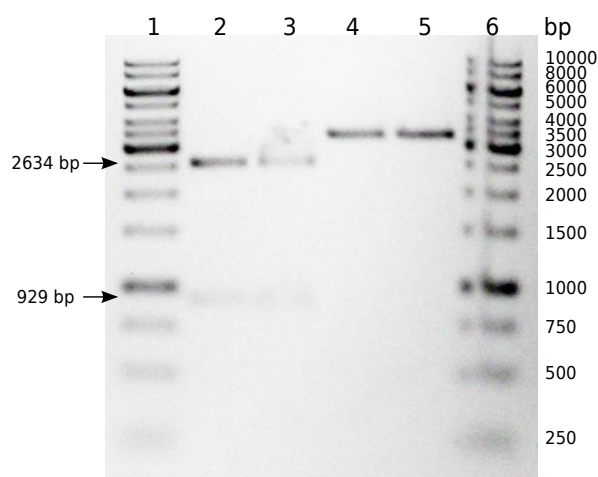


Figure 4.6: 1% agarose gel electrophoresis of *NcoI*-digested pPICZ α A-IL4_{new} colonies A-D in wells textbf2) through 5). Content of 1) and 6) is a 1kb standard ladder (Fermentas, Helsingborg, Sweden).

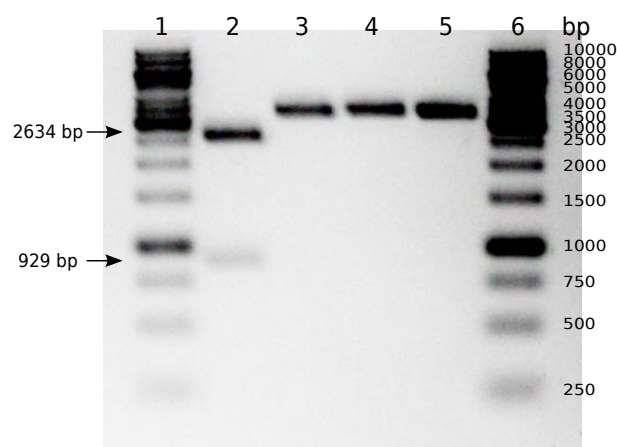


Figure 4.7: 1% agarose gel electrophoresis of *NcoI*-digested pPICZ α A-IL4_{new} colonies E-H in wells textbf2) through 5). Content of 1) and 6) is a 1kb standard ladder (Fermentas, Helsingborg, Sweden).

4.2 Transformation of *P. pastoris*

The expression vector from colony pPICZ α A-IL-F was purified and linearised with *SacI* restriction enzyme and transformed into *P. pastoris* X-33 and SMD1168H by electroporation yielding transformants labeled X33IL, X33IL4. Eight transformed colonies (A-H) were selected and replated on YPD-Zeocin plates and genomic DNA was isolated from cell material and screened by PCR using two sets of primers. Results from PCR screening of X-33 transformant DNA using 3'AOX and α -factor primers was analysed by gel electrophoresis and shown in Figure 4.8. The predicted fragment size of PCR product using the α -factor primers are 268 bp. All eight colonies screened shows a PCR product of similar size. The second PCR screening was made using *pre*AOX and 3'AOX primers. This was done to verify the integration of the entire shuttle vector. A single integration of the vector would yield a fragment of 1624 bp. Figure 4.9 shows gel analysis of extracted genomic DNA from X33IL colonies screened by PCR. 7 colonies shows successful single integration of the vector, while X33IL-I shows a PCR fragment of roughly 3,000 bp and no fragments of sizes around 1624 bp, indicating a different type of chromosomal integration than expected. Although an untransformed chromosome would yield a similar sized fragment after such PCR, this transformant would not survive the Zeocin selection pressure. Based on these screenings X33ILA was selected as candidates for expression studies. The difference in expression levels was to be investigated between the two types of chromosomal integrations (see section 4.4).

In general transformation into the protease deficient SMD1168H strain yielded similar amounts of colonies as the wild-type strain. Similar PCR screenings were made on chromosomal DNA isolated from SMDIL colonies A-H (Figure 4.10 and 4.11) using α -factor and 3'AOX primers. Six out of eight colonies shows a DNA fragment corresponding to the 268 bp. SMDIL-B and -H, however, showed two fragments slightly lower in size as well as one other fragment of 500-600 bp. Products from PCR screening, using *pre*AOX and 3'AOX primers on chromosomal DNA from these colonies did not reveal differences in SMDIL-B and -H compared to the six other colonies (Figure 4.12 and 4.13). As such, both PCR screenings are necessary for verifying correct transformations. The SMDIL-E transformant was selected for the *P. pastoris* SMD1168H candidate for the expression of IL.

After the second construction of the expression vector containing the IL4 gene, pPICZ α -IL4_{new}-A was transformed into both X33 and SMD1168H *P. pastoris* strains yielding colonies labelled X33IL4 and SMDIL4.

4.2 Transformation of *P. pastoris*

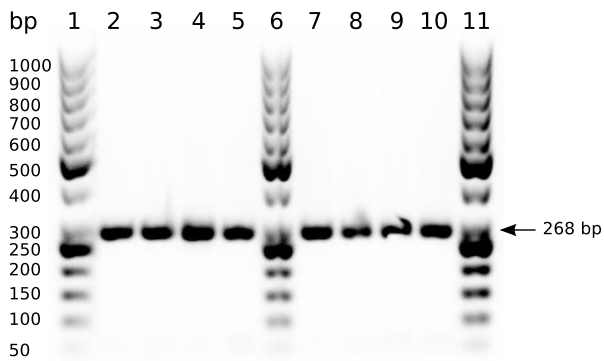


Figure 4.8: 2% agarose gel electrophoresis of PCR product of genomic DNA from X33IL colonies using α -factor and 3'AOX primers. Content of wells 2-5) are A, B, C, D and content of wells 7-10) are E, G, I, J colonies of X33IL. 1), 6) and 11) contains 50 bp standard (Fermentas, Helsingborg, Sweden).

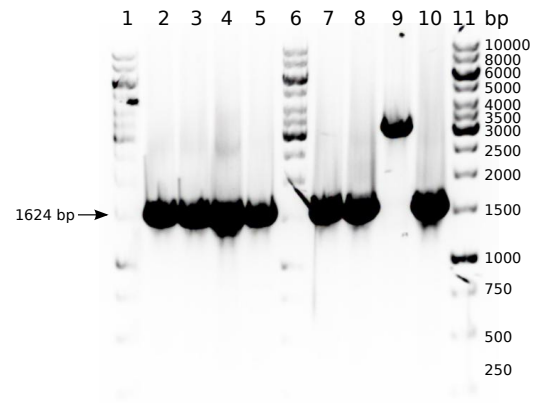


Figure 4.9: Integration analysis by PCR screening of genomic DNA of X33IL transformants using *pre*AOX and 3'AOX primers. Wells 2-5) contains colonies A, B, C, D and wells 7-10) contains colonies E, G, I, J, respectively. 1), 6) and 11) contains 1kb standard (Fermentas, Helsingborg, Sweden).

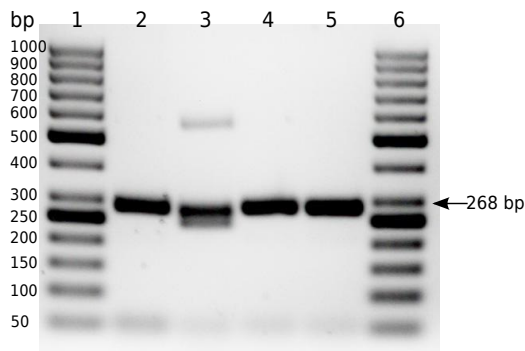


Figure 4.10: Integration analysis by PCR screening of genomic DNA of SMDIL transformants using α -factor and 3'AOX primers. Wells 2-5) contains colonies A, B, C, D. Wells 1), 6) contains 50 bp standard (Fermentas, Helsingborg, Sweden).

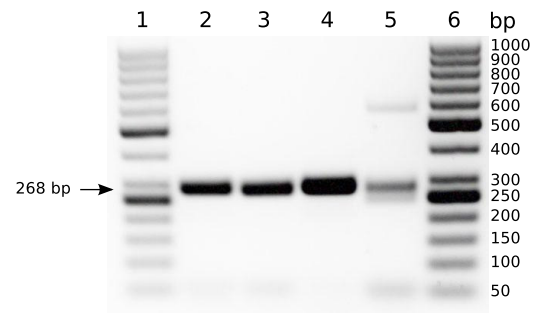


Figure 4.11: Integration analysis by PCR screening of genomic DNA of SMDIL transformants using α -factor and 3'AOX primers. Wells 2-5) contains colonies E, F, G, H. Wells 1), 6) contains 50 bp standard (Fermentas, Helsingborg, Sweden).

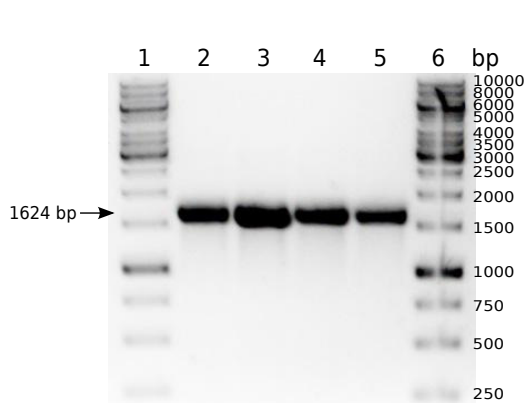


Figure 4.12: Integration analysis by PCR screening of genomic DNA of SMDIL transformants using *pre*AOX and 3'AOX primers. Wells 2-5) contains colonies A, B, C, D. Wells 1), 6) contains 1kb standard (Fermentas, Helsingborg, Sweden).

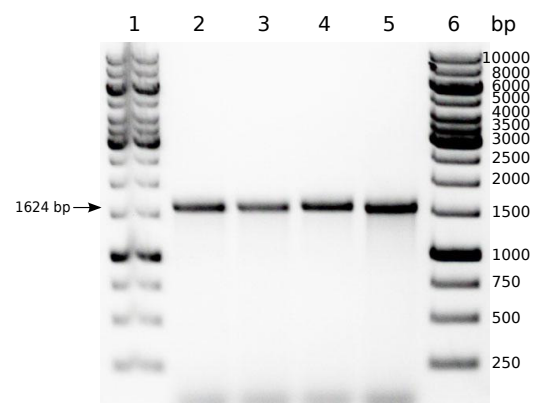


Figure 4.13: Integration analysis by PCR screening of genomic DNA of SMDIL transformants using *pre*AOX and 3'AOX primers. Wells 2-5) contains colonies E, F, G, H. Wells 1), 6) contains 1kb standard (Fermentas, Helsingborg, Sweden).

Four colonies were selected and replated on YPD-Zeocin plates. PCR screenings on isolated chromosomal DNA of X33IL4 was made using α -factor and 3'AOX primers and the product was analysed with gel electrophoresis against a 50 bp standard (Figure 4.14). The gel shows single DNA fragments of around 300 bp in all four samples, corresponding to the expected 268 bp fragment from the PCR. Additionally PCR was made using *pre*AOX and 3'AOX primers showing only single integrations in the genomic DNA (Figure 4.15). X33IL4-A was selected for further expression studies.

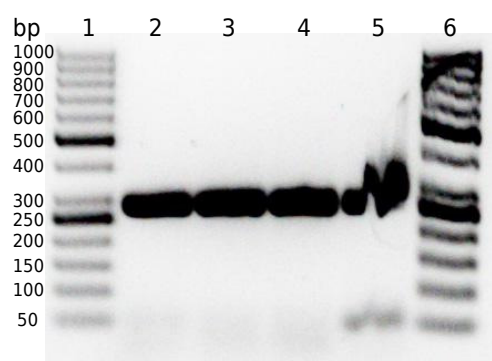


Figure 4.14: Integration analysis by PCR screening of genomic DNA of X33IL4 transformants using α -factor and 3'AOX primers. Wells 2-5) contains colonies A, B, C, D. Wells 1), 6) contains 50 bp standard (Fermentas, Helsingborg, Sweden).

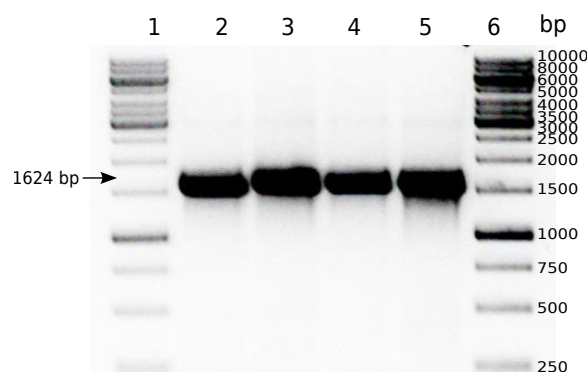


Figure 4.15: Integration analysis by PCR screening of genomic DNA of X33IL4 transformants using *pre*AOX and 3'AOX primers. Wells 2-5) contains colonies A, B, C, D. Wells 1), 6) contains 1kb standard (Fermentas, Helsingborg, Sweden).

Transforming pPICZ α -IL4_{new}-A into *P. pastoris* SMD1168H yielded similar amounts of colonies as X33. PCR products from four colonies using α -factor and 3'AOX primers showed successful transformation in all four colonies with amplified DNA of around 268 bp when analysed on gel electrophoresis, although one of the bands are slightly distorted (Figure 4.16). The PCR products using *pre*AOX and 3'AOX primers also revealed only single integration on the chromosomes (Figure 4.17) and SMDIL4-A was selected for subsequent expression studies.

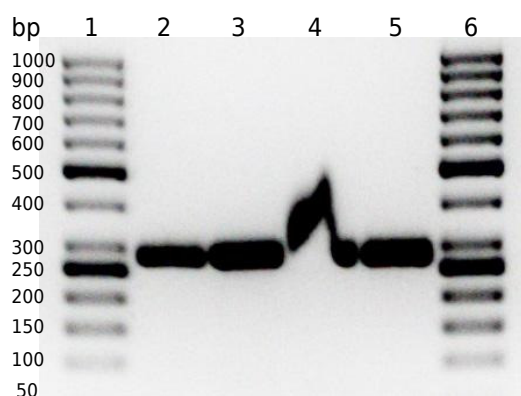


Figure 4.16: Integration analysis by PCR screening of genomic DNA of SMDIL4 transformants using α -factor and 3'AOX primers. Wells 2-5) contains colonies A, B, C, D. Wells 1), 6) contains 50 bp standard (Fermentas, Helsingborg, Sweden).

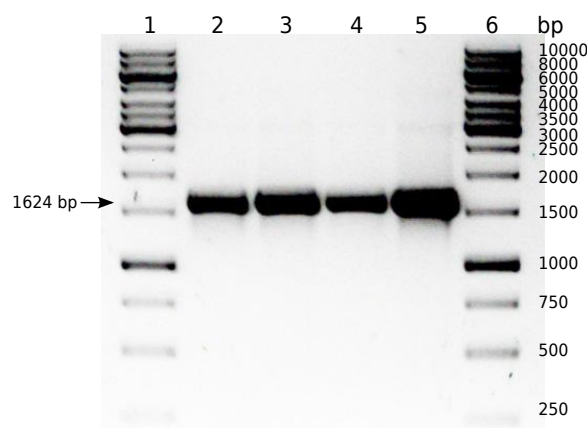


Figure 4.17: Integration analysis by PCR screening of genomic DNA of SMDIL4 transformants using *pre*AOX and 3'AOX primers. Wells 2-5) contains colonies A, B, C, D. Wells 1), 6) contains 1kb standard (Fermentas, Helsingborg, Sweden).

4.3 Sequencing of Construct

To verify ligation, insertion and transformation of the cloning process, a number of samples were sequenced. Figure 4.18 shows a DNA alignment of a part of the sequence data obtained from Sanger sequences performed by DNA Technology (Risskov, Denmark). The full data can be found in Appendix B. The sequencing was made on purified pPICZ α A-IL-F vector DNA (using 3'AOX primer only) and PCR product of extracted X33IL-A genomic DNA template (using *pre*AOX and 3'AOX primers). The alignment was made against the original pPICZ α A-IL sequence using ClustalW. The vector DNA shows high identity towards the original sequence, and no errors were found within the gene insert. A mutation was observed at position 1450, which was downstream the translational stop codon. The PCR product from the X33IL-A DNA shows 100% sequence identity with the original vector, and this mutation was not found in the recombinant genome. The sequencing of X33IL-A DNA using the reverse primer did not provide any signal in this area.

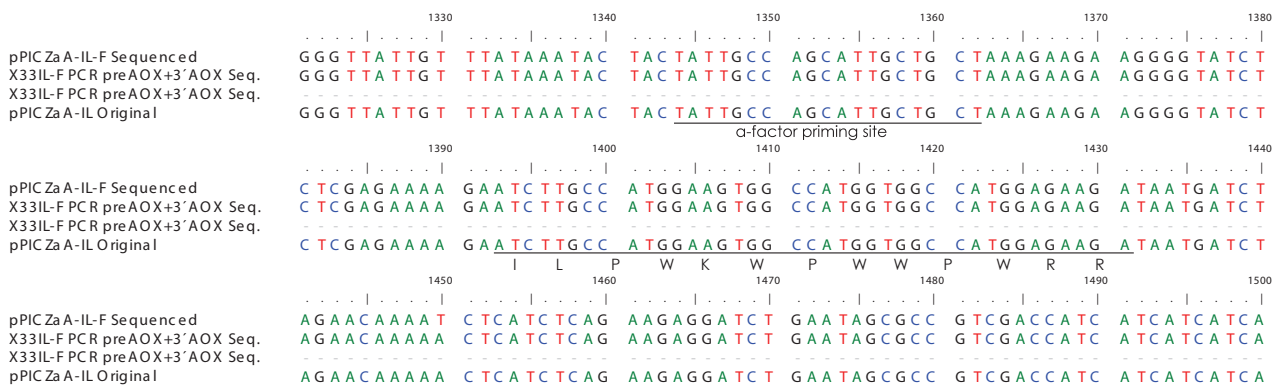


Figure 4.18: Segment of the alignment of sequence data of purified pPICZ α A-IL-F vector DNA (3'AOX primer only) and PCR product of extracted genomic DNA of X33IL-A colonies using *pre*AOX and 3'AOX primers. Sequencing was performed by DNA Technology (Risskov, Denmark) using mentioned primers. The alignment was made against the original pPICZ α A-IL sequence using ClustalW.

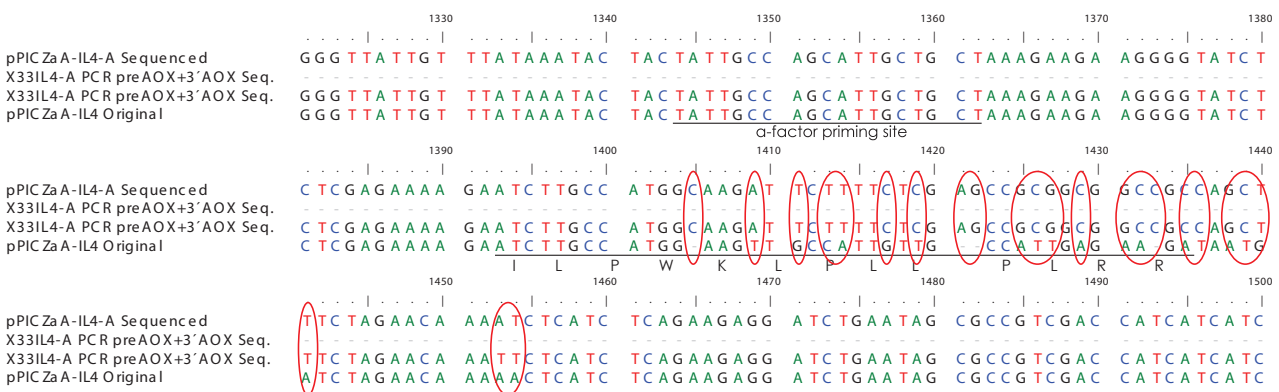


Figure 4.19: Segment of the alignment of sequence data of purified pPICZ α A-IL4-A vector DNA (3'AOX primer only) and PCR product of extracted genomic DNA of X33IL4-A colonies using *pre*AOX and 3'AOX primers. Sequencing was performed by DNA Technology (Risskov, Denmark) using mentioned primers. The alignment was made against the original pPICZ α A-IL4 sequence using ClustalW.

Sequencing data of the cloning process of IL4 were aligned similarly to IL, using original pPICZ α A-IL4 sequence as reference (Figure 4.19). Both purified vector DNA and PCR product of X33-IL4-A genomic DNA showed high error density within the IL4 insert region. Although no signal were obtained in this region with the PCR product sample using the forward primer, the mismatches are consistent between pPICZ α A-IL4-A

sequence data and PCR product sequence data using reverse primer. The signal from the vector sequencing chromatography was high in this area (Figure 4.20).

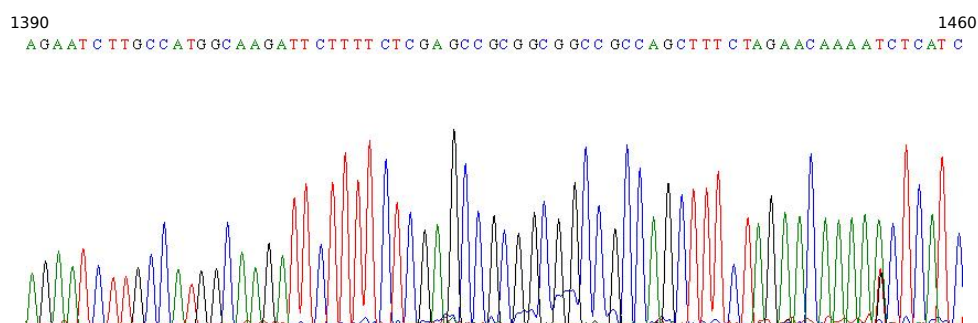


Figure 4.20: Segment of the sequence chromatogram of pPICZ α A-IL4-A vector samples.

4.4 Expression Study of Recombinant IL and IL4

The recombinant *P. pastoris* colonies X33IL-A, X33IL4-A, SMDIL-E and SMDIL4-A were selected for expression of IL and IL4 with X33 and SMD1168H *P. pastoris* strains as control. Cells were grown in BMGY (pH 6) overnight at 30°C and transferred to fresh BMMY medium for methanol induction. Three different pH (3, 4.5 and 6) were studied at 20°C and 30°C during induction making a total of six expressions per candidate. Samples were extracted and the OD₆₀₀ was measured every 24 hours. 0.5% methanol was added during sample extractions and the pH was adjusted. The cell growth of X33IL-A colonies are shown in Figure 4.21 under different conditions. No significant change in growth rate was observed when changing the induction temperature from 30°C to 20°C. Also, no tendency was observed of the influence of pH on growth rate during induction. The growth of X33IL-A on methanol is slightly lower under pH 4.5 and 20°C as well as pH 3 and 20°C.

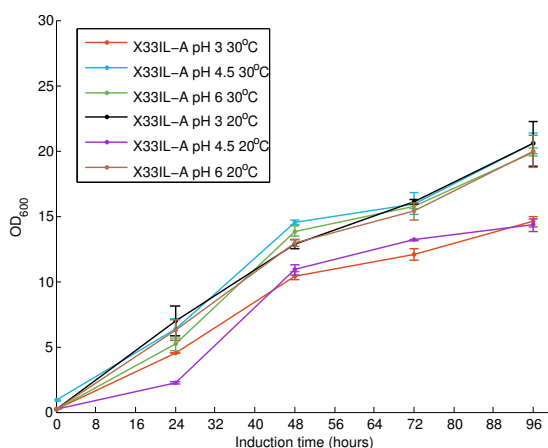


Figure 4.21: The measured OD₆₀₀ during methanol induction of *P. pastoris* X33IL-A colonies at time points 0, 24, 48, 72 and 96 hours. Error-bars represents standard deviation of the sample mean.

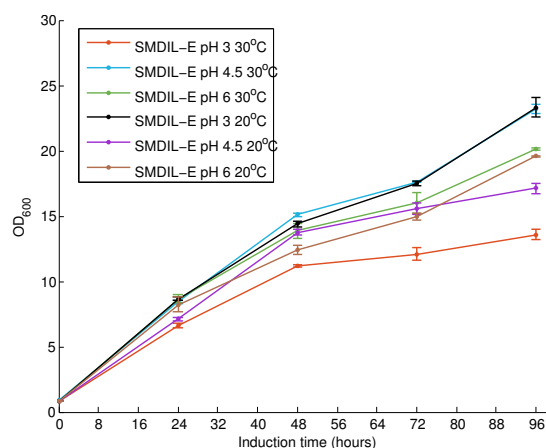


Figure 4.22: The measured OD₆₀₀ during methanol induction of *P. pastoris* SMDIL-E colonies at time points 0, 24, 48, 72 and 96 hours. Error-bars represents standard deviation of the sample mean.

When comparing growth profiles of recombinant X33 and SMD1168H strains expressing IL (Figure 4.21 and 4.22), high resemblance is observed. Like X33IL-A, the order of OD₆₀₀ measurements does not provide evidence that pH and temperature plays a role on cell growth, since it is seemingly random. However, the expression of IL under pH 3 and 30°C in both recombinant strains yields to lowest cell densities.

4.4 Expression Study of Recombinant IL and IL4

The measured optical density of shake-flask expressions of IL4 in *P. pastoris* X33 and SMD1168H strains are shown in Figure 4.23 and 4.24. The expressions show very similar growth profiles within the first 72 hours. Afterwards the density of the SMDIL4-A expressions climb to an average OD₆₀₀ of 30, where X33IL4-A expressions end with a optical density of average 20. A tendency is observed for the growth of cells at pH 3 and 30°C being the slowest while 20°C ends in the highest densities. This trend is to some extent inverse of what happens at pH 4.5, where optical density is highest at 30°C and lower at 20°C. As such, no general correlation was observed between pH or temperature and growth rate.

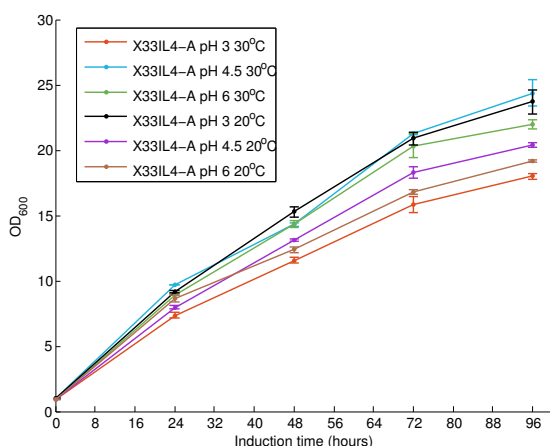


Figure 4.23: The measured OD₆₀₀ during methanol induction of *P. pastoris* X33IL4-A colonies at time points 0, 24, 48, 72 and 96 hours. Error-bars represents standard deviation of the sample mean.

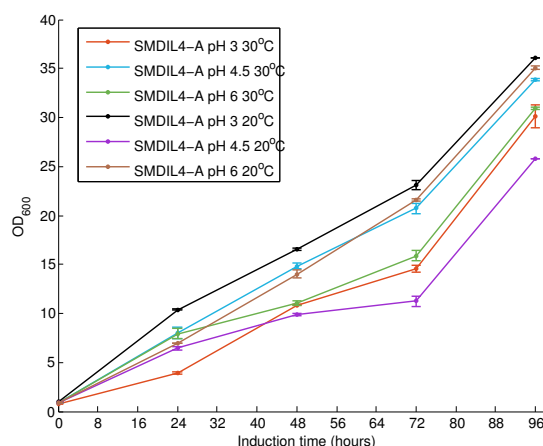


Figure 4.24: The measured OD₆₀₀ during methanol induction of *P. pastoris* SMDIL4-A colonies at time points 0, 24, 48, 72 and 96 hours. Error-bars represents standard deviation of the sample mean.

Finally, methanol induction were made on wild-type *P. pastoris* X33 and SMD1168H strains as references and the optical density was measured (Figure 4.25). The growth profiles are very similar to the previous expressions, but with greater variance at each time point. Also in the wild-type X33 and SMD1168H strains, the slower growth is found at pH 3 and 30°C compared to pH 3 and 20°C. In general, the wild-type X33 strain grows faster than the SMD1168H strain when compared under similar growth conditions, with the exception of pH 3 and 30°C.

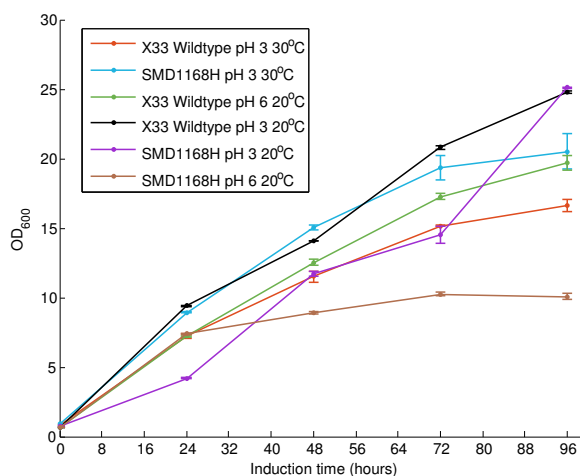


Figure 4.25: The measured OD₆₀₀ during methanol induction of *P. pastoris* X33 and SMD1168H strains at time points 0, 24, 48, 72 and 96 hours. Error-bars represents standard deviation of the sample mean.

4.4.1 Zone Inhibition Assay on Culture Supernatant

Before the analysis of antimicrobial activity of the culture supernatant of the shake-flask expressions, several bacterial strains were tested for inhibition by synthesized IL. *B. subtilis* showed the largest zones of inhibitions when subjected to 100 μ M non-amidated IL, compared to *P. putida*, *M. Luteus* and *E. coli* (data not shown). Therefore this bacteria was chosen for the zone inhibition assays and no further studies were made on the other bacterial strains. In all inhibition assays, ampicillin references were included as well as synthesized IL or IL4, depending on the respective expression.

Early *B. subtilis* zone inhibition assays of shake-flask supernatant of IL expressions in *P. pastoris* at pH 3 revealed a small zone of inhibition even though the samples were not freeze-dried (data not shown). Initial controls were made to investigate the antimicrobial activity of similar inductions of wild-type *P. pastoris* and no inhibition was observed (Figure 4.26). Additionally, 10X concentrated BMGY at different pH did not inhibit *B. subtilis*. Therefore, early assumptions were made, that the antimicrobial activity was only seen on recombinant expression supernatant. However, similar controls made much later in the project on concentrated supernatant from wild-type inductions, revealed antimicrobial activity against *B. subtilis*, which diminished the indications of the expression of IL by shake-flask expressions.

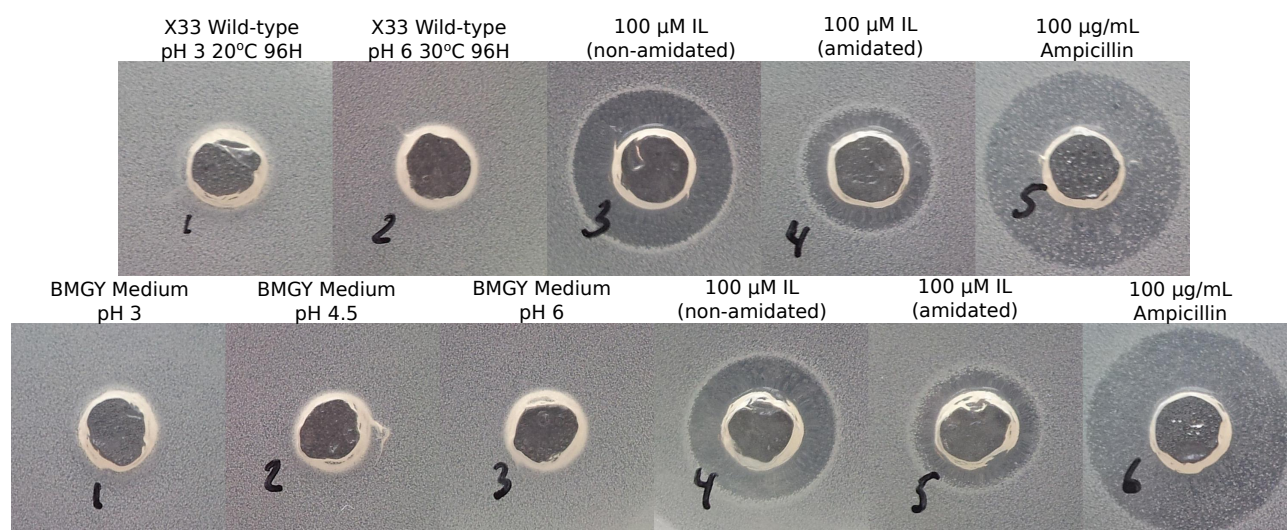


Figure 4.26: *B. subtilis* zone inhibition assays of controls consisting of X33 wild-type inductions (top) and 10X concentrated BMGY medium of pH 3, 4.5 and 6 (bottom). Each well is loaded with 20 μ L sample and the plates has been incubated for 24 hours.

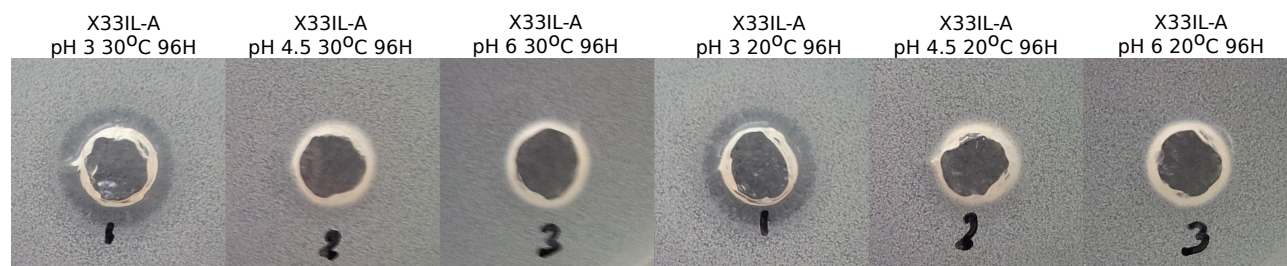


Figure 4.27: *B. subtilis* zone inhibition assays of culture supernatant from X33IL-A expressions under different conditions after 96 hours of methanol induction. Each well is loaded with 20 μ L 10X concentrated samples sample and the plates has been incubated for 24 hours.

4.4 Expression Study of Recombinant IL and IL4

5 mL of culture supernatant collected from the shake-flasks of X33IL-A expressions after 96 hours of induction was freeze-dried and resuspended in 500 μ L 10 mM Tris-HCl to a final concentration of 10:1. 20 μ L of concentrate was added to the wells of the prepared *B. subtilis* agarose-plates and incubated for 24 hours (Figure 4.27). Growth inhibition was observed for pH 3 at both 20°C and 30°C with very similar zone diameters, while expressions under pH 4.5 and 6 did not produce compounds with antimicrobial activity against *B. subtilis*.

Figure 4.28 shows *B. subtilis* zone inhibition assays of 10X concentrated culture supernatant from SMDIL-E expressions after 48 and 72 hours of induction. Antimicrobial activity is visible already after 48 hours of induction, larger in zone diameter than that of X33IL-A expressions after 96 hours. Again, this is only observed for expressions made at pH 3 with both temperatures. A considerably larger zone of inhibition was observed on SMDIL-E expressions made at 20°C compared to 30°C after 72 hours of induction.

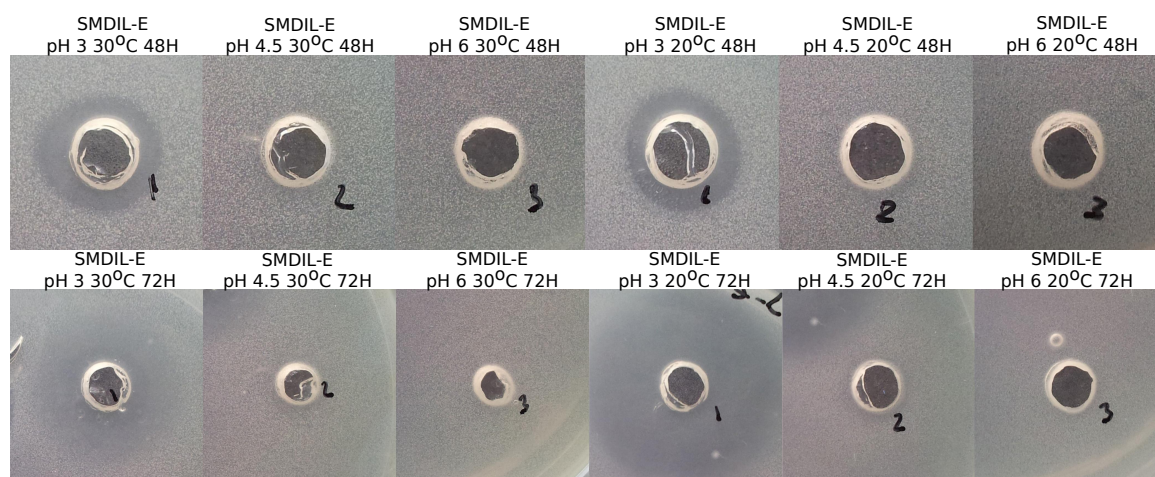


Figure 4.28: *B. subtilis* zone inhibition assays of culture supernatant from SMDIL-E expressions under different conditions after 48 hours (top) and 72 hours (bottom) of methanol induction. Each well is loaded with 20 μ L 10X concentrated sample and the plates has been incubated for 24 hours.

Also expressions of IL4 was analysed by zone inhibition assays. X33IL4-A expressions were measured for antimicrobial activity after 48 and 72 hours of methanol induction. 10X concentrated culture supernatant was analysed and the results is shown in Figure 4.29, after 48 and 72 hours of inductions. Similar to IL expressions, antimicrobial activity towards *B. subtilis* was observed at pH 3, but the zone of inhibition did not seem to increase at 72 hours of methanol induction, as in the case of the SMDIL-E expression study. The degree of inhibition was roughly the same with both 20°C and 30°C inductions at pH 3. Very small clear zones were observed by inductions at pH 4.5, which was not seen in IL expressions, as indicated by dark shadows.

Expressions of IL4 by SMDIL4-A colonies showed very similar results to X33IL4-A expression colonies. Again, inductions at pH 3 showed roughly the same degree of antimicrobial activity against *B. subtilis*, and no correlation was observed between temperature and zone of inhibition.

Late in the project, inductions of wild-type *P. pastoris* were re-made. This time, SMD1168H strain was included and three induction conditions were tested for both strains and the antimicrobial activity on *B. subtilis* was measured. Inductions at pH 3 and 6 were tested, and this time the culture supernatant was freeze-dried and resuspended in 500 μ L 10 mM Tris-HCl. The zone inhibition assays are shown in Figure 4.31. Surprisingly, this time inhibition was observed at pH 3 induction of both strains, in contrast to what was observed earlier (Figure 4.26) for X33 wild-type inductions. This time, however, the culture supernatant of the wild-type strains were freeze-dried and concentrated 10:1. Since these strains did not include either IL or IL4 genes, the inhibition of *B. subtilis* was not done by these antimicrobial peptides. Therefore, earlier results could not prove the production of IL or IL4 during induction.

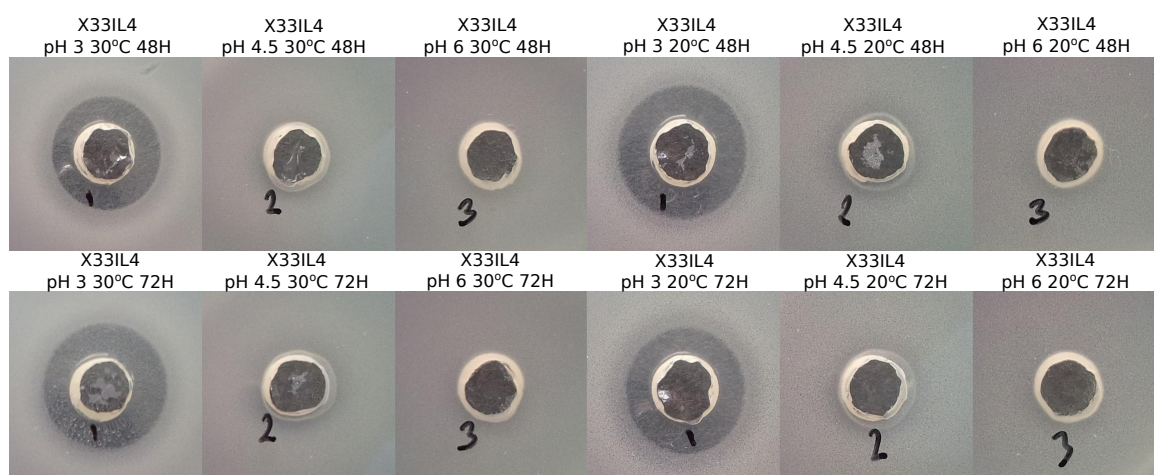


Figure 4.29: *B. subtilis* zone inhibition assays of culture supernatant from X33IL4-A expressions under different conditions after 48 hours (top) and 72 hours (bottom) of methanol induction. Each well is loaded with 20 μ L 10:1 concentrated sample and the plates has been incubated for 24 hours.

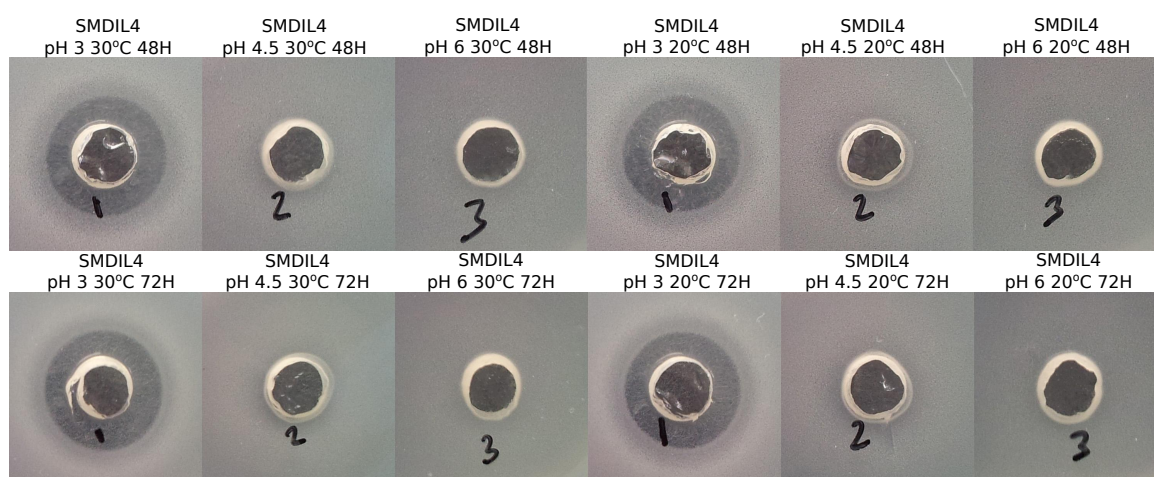


Figure 4.30: *B. subtilis* zone inhibition assays of culture supernatant from SMDIL4-A expressions under different conditions after 48 hours (top) and 72 hours (bottom) of methanol induction. Each well is loaded with 20 μ L 10:1 concentrated sample and the plates has been incubated for 24 hours.

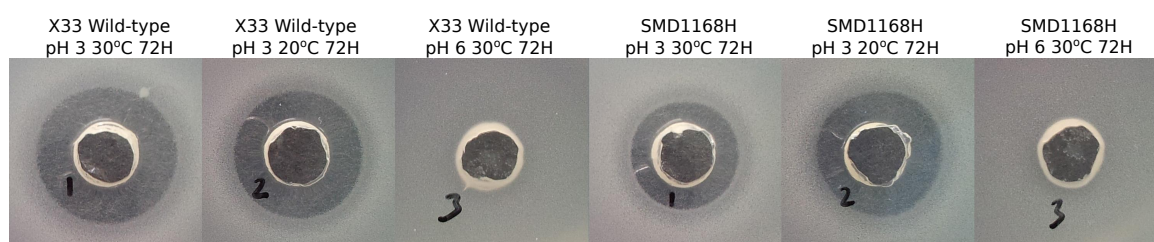


Figure 4.31: *B. subtilis* zone inhibition assays of culture supernatant from X33 wild-type (top) and SMD1168H strain (bottom) under different conditions after 72 hours of methanol induction. Each well is loaded with 20 μ L sample and the plates has been incubated for 24 hours.

4.4.2 Size-Analysis on Culture Supernatant by Tricine SDS-PAGE

In order to qualitatively measure the IL content of the shake flask expressions using the recombinant X33IL-A strain, supernatant was collected after 48 hours of methanol induction and loaded directly to a prepared tricine SDS-gel for size analysis. Therefore, this analysis was not made on concentrated supernatant. After electrophoresis the gel was stained by coomassie blue but no bands were visible near 2 kDa (data not shown). The coomassie stain was then removed by methanol and the gel was stained by silver nitrate. Figure 4.32 shows a picture taken after development of the silver stain. No bands were observed corresponding to the size of synthesized IL (wells 1 and 2). The smallest visible band is above the 3.4 kDa marker of the ladder, and as such above the weight of IL (1.9 kDa).

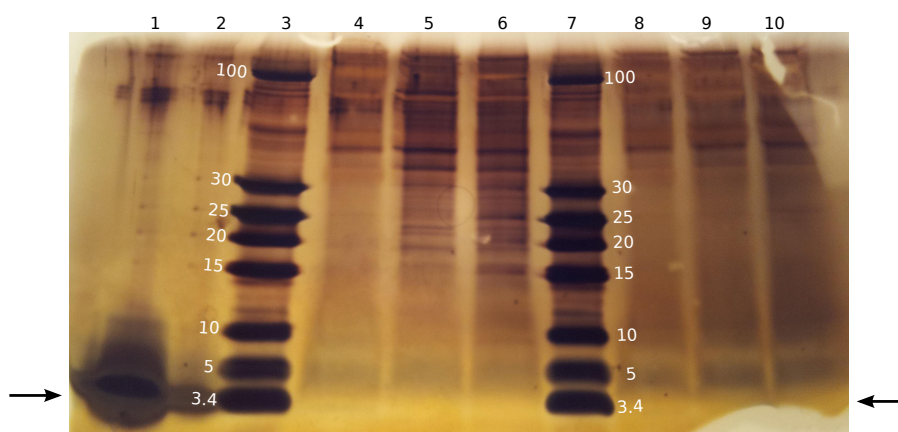


Figure 4.32: Size analysis by tricine SDS-PAGE of culture supernatant from shake flask expressions of IL using the recombinant X33IL-A strain. Samples were collected after 48 hours of methanol induction. Content of wells 1) and 2) is references of synthesized IL (100 and 10 μ M, respectively). 3+4) contain PageRuler™ Low Range Protein ladder (labels represents size in kDa). Wells 4-6) contains supernatant from expression made at 30°C and pH 3, 4.5 and 6, respectively. Wells 8-10) contains supernatant from expression made at 20°C and pH 3, 4.5 and 6, respectively. Gel was stained first with coomassie blue, then silver stained.

Similar size analysis was made on supernatant from shake flask expressions of IL using the recombinant SMDIL-E strain (Figure 4.33). Samples were collected after 96 hours of methanol induction and loaded directly to the SDS-gel. Similar to the previous size analysis, the gel was stained twice after electrophoresis since no band was observed after staining with coomassie blue. The silver-stained gel revealed a number of bands below the 10 kDa marker of the ladder. It was difficult to distinguish the bands below the 5 kDa marker but a single band in wells 5 and 6 appeared to have similar mass to the 3.4 kDa marker, according to the migration. These wells contained supernatant from expressions at 30°C and pH 4.5 and 6, respectively.

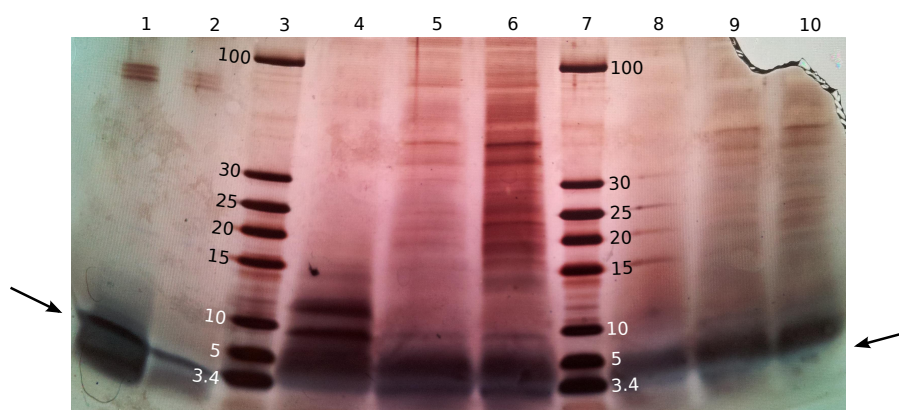


Figure 4.33: Size analysis by tricine SDS-PAGE of culture supernatant from shake flask expressions of IL using the recombinant SMDIL-E strain. Samples were collected after 96 hours of methanol induction. Content of wells **1**) and **2**) is references of synthesized IL (100 and 10 μ M, respectively). **3+4**) contain PageRuler™ Low Range Protein ladder (labels represents size in kDa). Wells **4-6**) contains supernatant from expression made at 30°C and pH 3, 4.5 and 6, respectively. Wells **8-10**) contains supernatant from expression made at 20°C and pH 3, 4.5 and 6, respectively. Gel was stained first with coomassie blue, then silver stained.

4.4.3 RP-HPLC Analysis of Culture Supernatant

The culture supernatant from shake-flask expressions of IL and IL4 was analysed by RP-HPLC and the chromatograms were compared to synthesized IL and IL4 to determine if either of the peptides had been expressed. Concentrated supernatant from X33IL-A expressions after 24 hours of induction was analysed by RP-HPLC (Figure 4.34, left). Large amount of compounds eluted at retention times between 6 and 8 minutes. Synthesized IL (non-amidated) eluted after 13.5 minutes when using optimized gradient, and only a very small peak was found at approximately this retention time (see zoomed view) from the culture supernatant. This peak was highest in supernatant from expressions made at pH 6 (green and brown lines) while non-existing at pH 3 (orange and black). The RP-HPLC analyses was made on very complex samples showing much of the compounds co-eluting early in the chromatogram (data not shown). In fact very low amount of material from the supernatant elutes at retention times greater than 10 minutes.

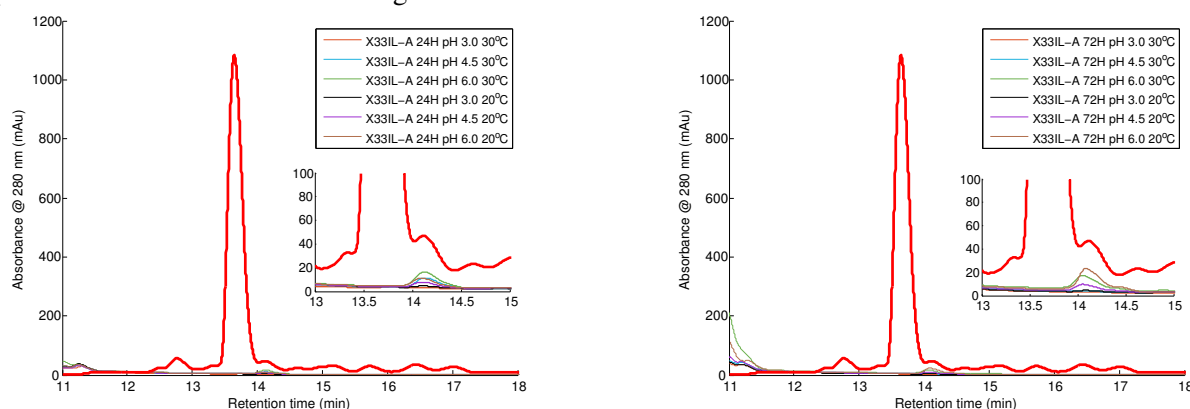


Figure 4.34: RP-HPLC analysis of 2X concentrated supernatant from shake-flask expressions of X33IL-A after 24 hours (left) and 72 hours (right) of methanol induction under various conditions. The chromatography was performed using an analytical C18 column equilibrated with 2% acetonitrile and 0.1% TFA. A reference containing 13 μ M synthesized IL (non-amidated) was also analysed (red line). Flow rate was 0.5 mL/min

Analysis were also made on X33IL-A culture supernatant after 72 hours of methanol induction to monitor the levels of material secreted to the supernatant, corresponding to the area underneath the peaks. The RP-HPLC chromatograms of supernatant after 72 hours of induction is shown in Figure 4.34 (right). There had

been only small increase in the area of the peak observed with similar retention time to synthesized IL (13.5 minutes), although not for supernatant from expressions at pH 3.

RP-HPLC was also made on culture supernatant from SMDIL-E shake-flask expressions. This time a newly acquired column was used and the flow rate was increased to 1 ml/min. As such, a new control was made with synthesized IL. The chromatography of supernatant after 48 hours of methanol induction is shown in Figure 4.35 (left). The reference IL now elutes after roughly 10 minutes. A zoomed view is presented from 9-11 minutes to search for compounds that resemble the hydrophobic nature of IL and match the retention time, but only a small peak at about 9 minutes is visible. This peak is mostly dominant in supernatant from expressions at pH 6 and greatest at 20°C induction temperatures. The supernatant after 72 hours of induction shows no new peaks formed at retention times matching that of synthesized IL (Figure 4.35, right) and the peak at 9 minute retention time has not increased significantly in area.

Analysis of the stability of synthesized IL injected to the supernatant was made by RP-HPLC. This was made using supernatant from expressions of SMDIL-E after 72 hours of methanol induction. A mixture of the supernatant and synthesized IL was prepared (resulting in 10 μ M IL) and incubated for 24 hours at room temperature. A control was also made with 10 μ M IL in buffer and the samples were analysed using the same gradient as above. The chromatogram is shown in Figure 4.36. The peptide could not be found at the retention times of the control sample, since the expected peak was completely diminished after incubation. This suggest the presence of proteases in the supernatant.

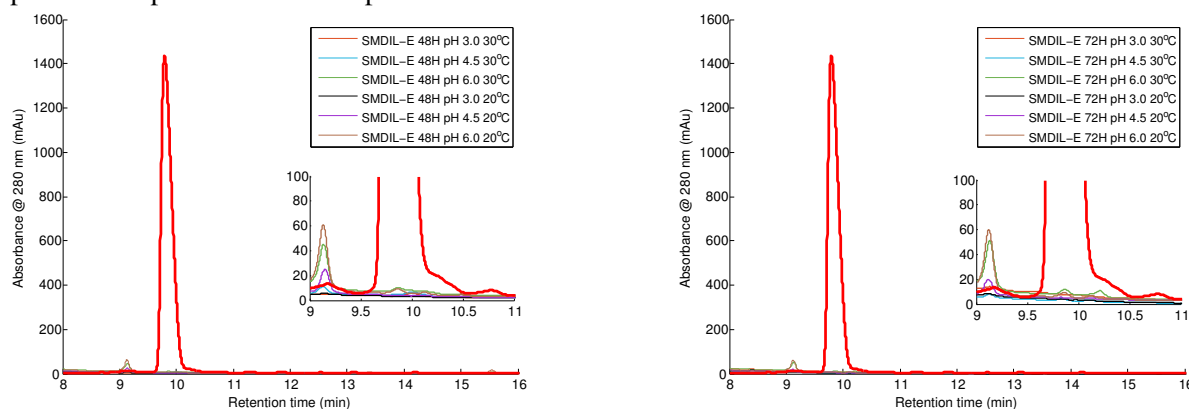


Figure 4.35: RP-HPLC analysis of 2X concentrated supernatant from shake-flask expressions of SMDIL-E after 48 hours (left) and 72 hours (right) of methanol induction under various conditions. The chromatography was performed using an analytical C18 column equilibrated with 2% acetonitrile and 0.1% TFA. A reference containing 13 μ M synthesized IL (non-amidated) was also analysed (red line). Flow rate was 1 mL/min

Since IL and IL4 has a high average charge per residue the affinity towards a SourceTM 15S cation-exchange column was also investigated. The system used was an Äkta Purifier 10 system and the peptides were eluted with 1M NaCl. However, the peptides (monitored by 280 nm absorption) showed no binding affinity towards the column material, even though several buffer systems were used. Therefore RP-HPLC was the only chromatography method used for purification of the supernatant.

4.5 Fermentation of recombinant *P. pastoris*

Scale-up expressions of IL was carried out by methanol-limited fed-batch fermentation using the recombinant *P. pastoris* X33IL-A expression strain. Data from the entire fermentation is shown in Figure 4.37. The fermentor was initially run in batch mode using glycerol as sole carbon source until a spike in pO₂ was observed after 20 hours. A glycerol feed was initiated at 35 μ L/min and increased to 82 μ L/min shortly after (red line). The glycerol fed-batch was run at growth limiting conditions, indicated by the steep increase in pO₂ at the 25

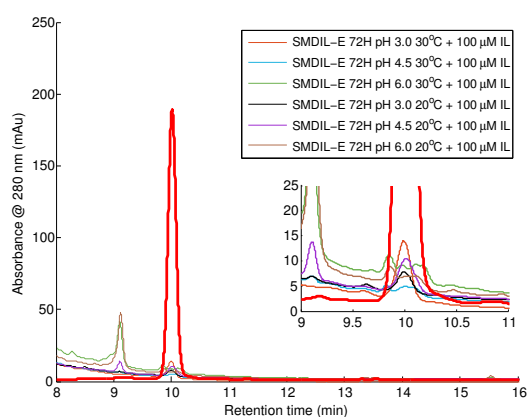


Figure 4.36: Degradation study of synthesized IL incubated in SMDIL-E supernatant at various expression conditions after 72 hours of methanol induction. The samples were incubated at room temperature for 24 hours. A control sample was made with 10 μM synthesized IL incubated in 10 mM Tris-HCl pH 6 for 24 hours (red line). The chromatography was performed using an analytical C18 column equilibrated with 2% acetonitrile and 0.1% TFA.

hour-mark when the substrate feeding pump was stopped briefly. The glycerol feed was slowed down to 35 $\mu\text{L}/\text{min}$ when methanol substrate feed was added to one of the feeding pump channels. Both substrates were fed simultaneously for 2.8 hours at which point the feed was stopped to inspect the pO_2 response (marked by \times symbol at 29 hours). No response was observed, indicating excess substrates, and the pump software was set to monitor the pO_2 and start the feed immediately after a spike was measured, which occurred roughly at the 30 hour mark.

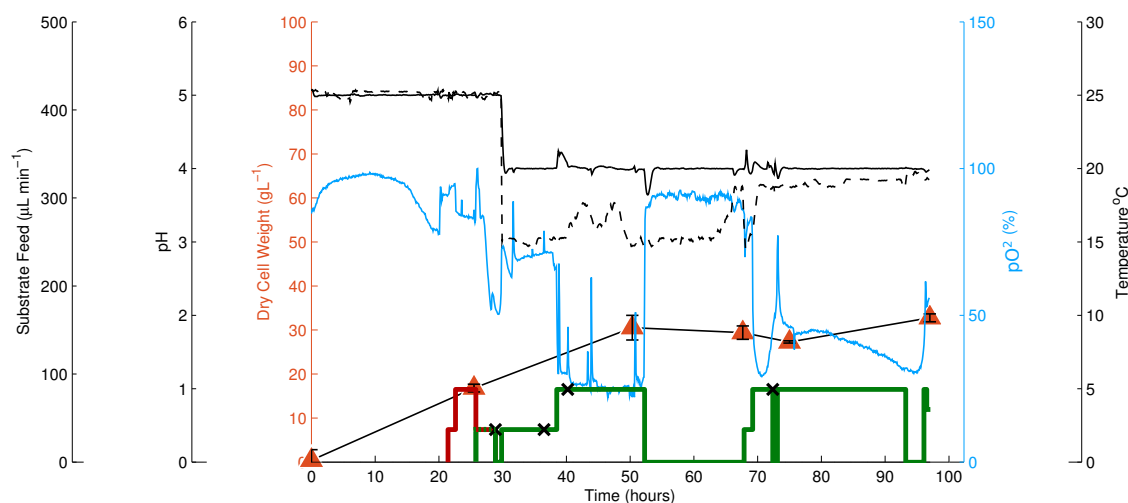


Figure 4.37: Methanol-limited fed-batch fermentation of X331L-A expression strain. Dry cell weight (\blacktriangle) was monitored off-line. pO_2 (—), temperature (—) and pH (---) was measured on-line. Feeding rate of glycerol (—) and methanol (—) are shown. Brief pauses in substrate feed are represented by \times symbols.

From here only methanol substrate was fed to the reactor (green line) according to the pO_2 levels. At 52.2 hours of fermentation, the methanol feeding stopped due to an error in the tubing pump that was not fixed until the next day, leaving a gap of 15 hours with no carbon source. No increase in cell density was observed during this period as expected from the starvation. After fixing the pump the methanol feed was re-enabled at 35 $\mu\text{L}/\text{min}$ and later increased to 82 $\mu\text{L}/\text{min}$. Methanol was oxidised immediately, as indicated by the sharp decrease in pO_2 after starting the methanol feed. An inspection of the pO_2 response pause in the methanol feed was made at the 72 hour-mark (as indicated by \times symbol). A delayed response of about 30 minutes

was observed at this time. This indicated that the feeding rate was higher than the methanol metabolism rate, and excess methanol was accumulated. The cell density during the fermentation did not reach significantly high values. A cell density of 30 g dry cell weight per liter was measured after 50 hours of fermentation and remained within ± 5 g/L for the rest of the fermentation.

Roughly 300 mL 2M ortho-phosphoric acid was consumed during the fermentation. The fermentor ran dry of acid after 65 hours when 200 mL had been consumed. The empty bottle was replaced by a bottle containing 50 mL 2M ortho-phosphoric acid which was all consumed within a short period of time. The pH setpoint was increased to 3.75 to overcome the large volume requirement of the acid supplied to keep the pH at 3 and another 200 mL 2M ortho-phosphoric acid was made accessible. A problem in the acid supply pump also caused fluctuations in the pH (at 40-50 hours of fermentation) but was fixed by adjusting the tubing pump. The final volume of this fermentation was roughly 1.8 L.

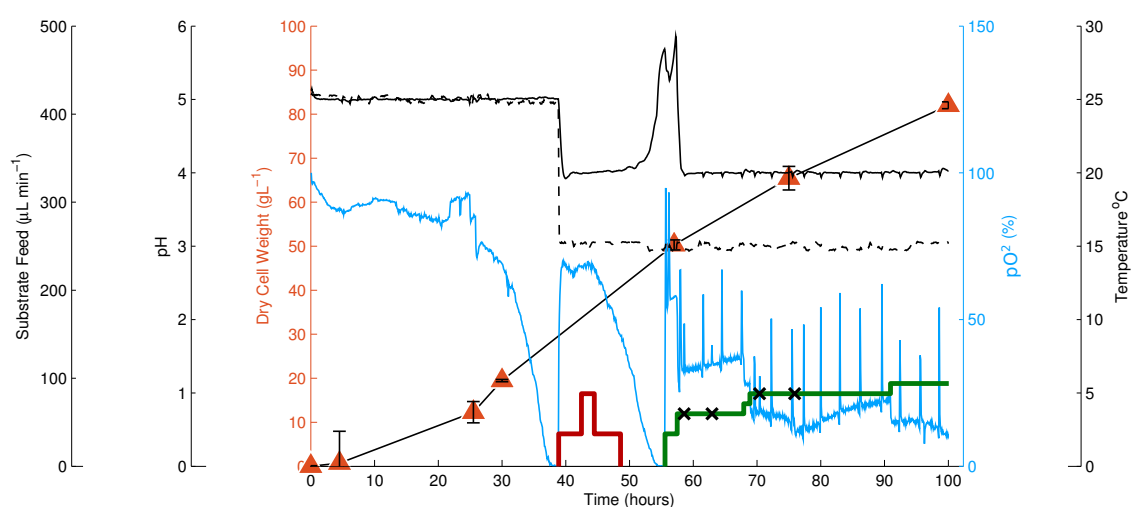


Figure 4.38: Methanol-limited fed-batch fermentation of SMDIL-E expression strain. Dry cell weight (\blacktriangle) was monitored off-line. pO_2 (—), temperature (—) and pH (---) was measured on-line. Feeding rate of glycerol (—) and methanol (—) are shown. Brief pauses in substrate feed are represented by \times symbols.

A new fermentation was made with the SMDIL-E expression strain and the data that was collected is shown in Figure 4.38. The glycerol batch lasted nearly twice as long as earlier and the pO_2 levels dropped to 0% before spiking to 70%. The glycerol feed was started at 35 $\mu\text{L min}^{-1}$ and increased to 82 $\mu\text{L min}^{-1}$ shortly after (red line). The dissolve oxygen levels did not respond immediately when increasing the glycerol feeding rate, but a steep decline in pO_2 was observed after a delay of three hours and the glycerol feed was decreased to 35 $\mu\text{L min}^{-1}$. When the pO_2 reached 45% the glycerol feed was stopped, and no subsequent increase in pO_2 was observed until after it reached 0%. Therefore, the glycerol substrate was presumably accumulated in the reactor during this period. A spike in pO_2 triggered the methanol feed at 35 $\mu\text{L min}^{-1}$ and the transition from glycerol to methanol substrate was instant. For the rest of the fermentation the methanol feeding rate was adjusted to lower the pO_2 . Short pauses in methanol feed caused the pO_2 levels to spike accordingly, indicating non-accumulation of methanol (marked by \times symbols).

The cell growth was significantly higher in this fermentation than earlier, reaching a final density of 82 g/L (dry cell weight). The cell density at the start of the induction phase was also more than double in this fermentation compared to previously. An increase in temperature from 20 $^{\circ}\text{C}$ to 28 $^{\circ}\text{C}$ can be seen from 53 to 58 hours, caused by drying-out of the cooling water bath.

Foam production was observed in this fermentation and 0.5 mL additional antifoam was added after 75

hours. Fluctuations in pO_2 and temperature was observed during induction, probably caused by pressure changes from foam being introduced to the exhaust condenser. The acid consumption of this fermentation was much lower than previous fermentation, consuming a final of 110 mL acid. The final volume of this fermentation was roughly 1.4 L.

4.5.1 Zone Inhibition Assay of Fermentation Supernatant

Culture supernatant from fed-batch fermentations of IL using the X33IL-A expression strain was analysed for antimicrobial activity by zone inhibition assay of *B. subtilis*. Six samples were analysed and the inhibition is showed in Figure 4.39. No inhibition is seen in the first two samples, collected from the fermentation prior to methanol induction. A large clear-zone was seen in samples collected after roughly 50 hours of fermentation (25 hours of induction). The inhibition zone diameter of *B. subtilis* is even larger after 67.7 hours, although 15 hours of starvation had occurred between these two samples. A significant decrease in inhibition is observed on samples collected after 75 hours and no antimicrobial activity is visible on supernatant from the end of the fermentation (97 hours).



Figure 4.39: *B. subtilis* zone inhibition assay of culture supernatant collected during fed-batch fermentation of IL using the *P. pastoris* X33IL-A expression strain. Each well is loaded with 20 μ L 10X concentrated supernatant and plates has been incubated for 24 hours.

Similar assays were made on supernatant collected during the fermentation of IL using the SMDIL-E expression strain, and the result is shown in Figure 4.40. No antimicrobial activity was observed within the first 57 hours of fermentation, as seen by the lack of clear zone around the sample wells containing supernatant from within this time period of fermentation. Inhibition of *B. subtilis* is observed by samples collected after 75 hours of fermentation and roughly 20 hours after the start of methanol induction. A small increase in clear-zone diameter by samples collected after 100 hours of fermentation indicated a small increase in antimicrobial activity.

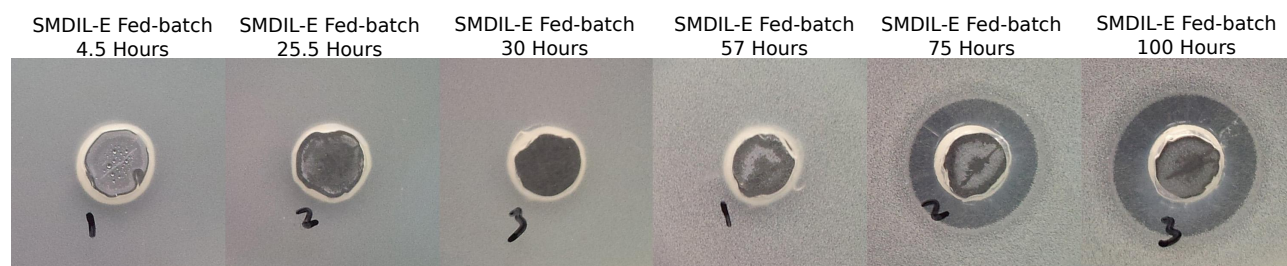


Figure 4.40: *B. subtilis* zone inhibition assay of culture supernatant collected during fed-batch fermentation of IL using the *P. pastoris* SMDIL-E expression strain. Each well is loaded with 20 μ L 10:1 concentrated supernatant and plates has been incubated for 24 hours.

To verify that the antimicrobial activity of the culture supernatant was caused by compounds produced by

4.5 Fermentation of recombinant *P. pastoris*

the expression strains, controls were made with basal salt medium concentrated 10:1. As such, the pH of the control samples were adjusted to 3, 4.5 and 6 prior to freeze-drying, to see the effect of pH on the inhibition of *B. subtilis*. The result is shown in Figure 4.41. A large area of crystallization was observed in these assays, which was not seen in fermentation supernatant samples. No clear zone was observed though, indicating that the concentrated fermentation medium did not inhibit growth of *B. subtilis*. It should be stressed that the pH of these samples were measured to be within 3.1 to 3.6.

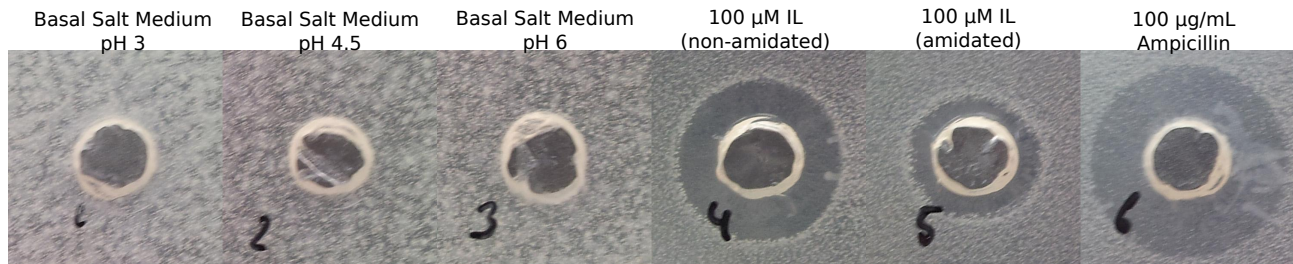


Figure 4.41: *B. subtilis* zone inhibition assay of control samples containing 10X concentrated basal salt medium and trace elements at pH 3, 4.5 and 6. Each well is loaded with 20 μ L concentrated medium and the plate has been incubated for 24 hours.

Finally, the supernatant collected from shake-flask and fermentation cultures were tested for antimicrobial activity towards *E. coli* and *M. luteus*. Supernatant from shake flasks (wells 1-6) showed inhibition of *E. coli* only for cultures induced at pH 3. Like *B. subtilis* samples from SMDIL-E show higher antimicrobial activity towards the bacteria than from X33IL-A expressions. However, significantly lower activity was observed against the gram positive *M. luteus* bacteria by the shake-flask expression supernatant. Supernatant from 67.6 hours of X33IL-A fermentation showed similar activity towards *E. coli* and *M. luteus* to that of *B. subtilis*. Synthesized IL did not show activity against *E. coli* and *M. luteus*, which was unexpected. Only *E. coli* is inhibited by IL4 at 165 μ M.

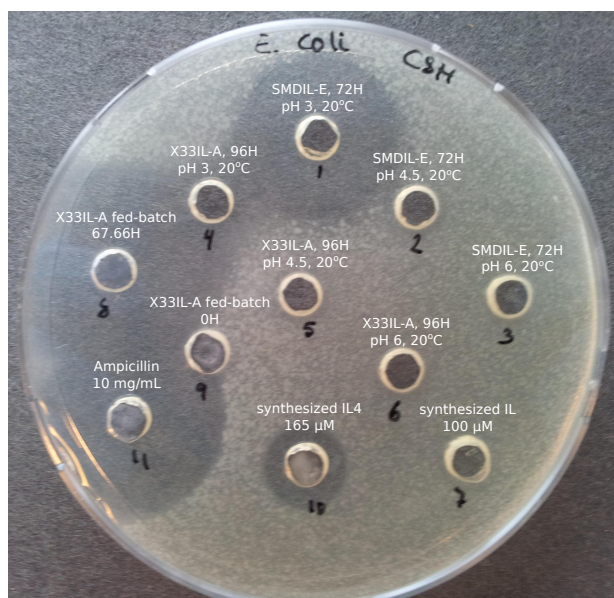


Figure 4.42: *E. coli* zone inhibition assay of shake-flask and fermentation supernatant. Each well is loaded with 20 μ L concentrated medium and the plate has been incubated for 24 hours.

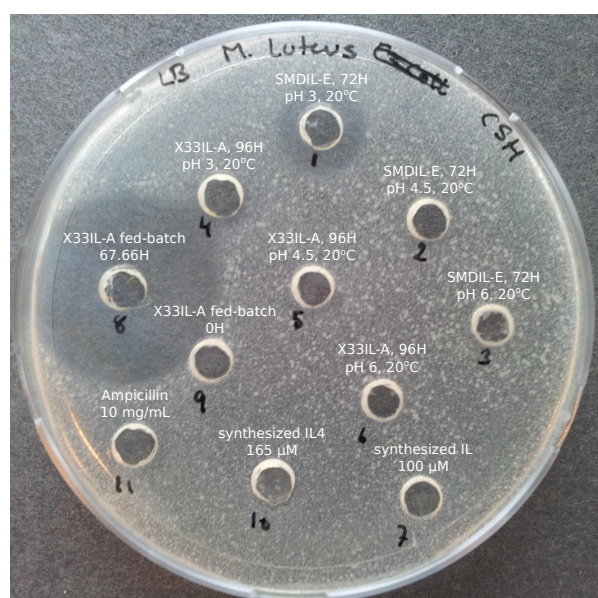


Figure 4.43: *M. luteus* zone inhibition assay of shake-flask and fermentation supernatant. Each well is loaded with 20 μ L concentrated medium and the plate has been incubated for 24 hours.

4.5.2 RP-HPLC Analysis of Fermentation Supernatant

Reverse phase-HPLC analyses was made on culture supernatant from the two fed-batch fermentations. The analysis was done to investigate the production of peptides with similar elution-properties to IL. 2X concentrated supernatant was filtered and loaded to the HPLC injection loop, and chromatography was performed, using a 60 minute gradient. The chromatograms of samples from IL expression using X33IL-A strains are shown in Figure 4.44. Only a very small peak is observed at retention times corresponding to that of synthesized IL (red line). However, the signal is too low to conclude that expressions of IL has been performed by the recombinant X33IL-A strain. Rather, the peak is most likely a contamination from previous analyses, since the same blunt-ended injection needle was washed and reused.

The chromatograms reveal a large variety of substances eluted within the first 20 minutes of retention, indicating large amount of relatively hydrophilic compounds in the supernatant. However, the sample is considerably less complex than those collected from shake-flask expressions (results not shown). Some peaks were observed to vanish during methanol induction, while others were formed as indicated by the difference between the analysed samples. Samples collected at 50.33 hours of fermentation (prior to the starvation period) showed considerably different chromatograms than the remaining samples. However, no further investigation was made on these products.

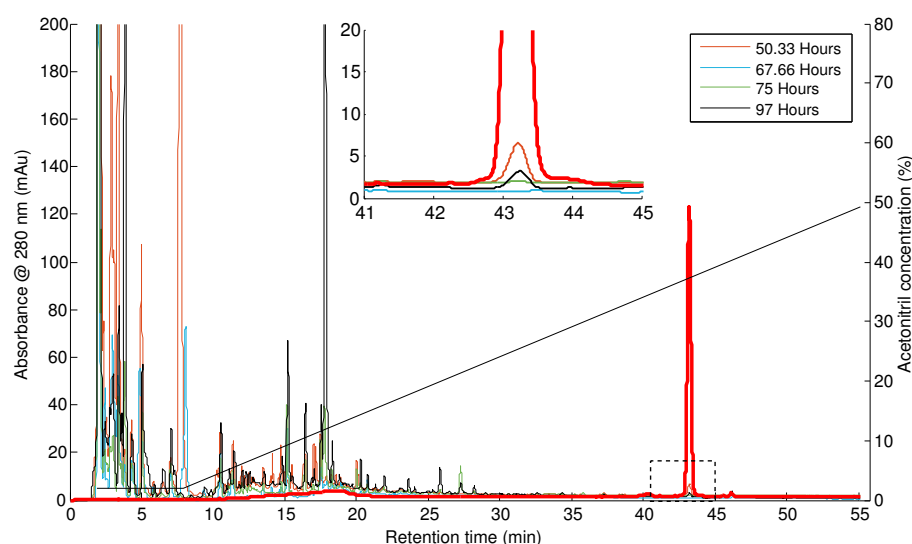


Figure 4.44: Reverse phase-HPLC analysis of supernatant collected during fermentation of IL using the X33IL-A expression strain. The chromatography was performed using an analytical C18 column equilibrated with 2% acetonitrile and 0.1% TFA. A reference containing 13 μ M synthesized IL (non-amidated) was also analysed (red line). The gradient has been shifted by the void time to depict the acetonitrile concentration at the site of the UV detector upon absorbance measurements. The flow rate in this run was 1 mL/min

The analysis of the supernatant from the expression of IL using SMDIL-E expression strains showed much lower signal when compared to similar collection times of X33IL-A expressions (Figure 4.45). Chromatograms of samples collected after 57 hours of fermentation showed only few peaks of significant absorbance, which was increased in subsequently collected samples (75 and 100 hours of fermentation). No peak was observed correlating to the retention times of synthesized IL, indicating the absence of the peptide in the culture supernatant.

Degradation studies were made to investigate the stability of IL when incubated in the fermentation supernatant for 24 hours. X33IL-A fermentation supernatant showed generally much lower proteolytic activity towards the synthetic peptide. The area of these peaks corresponded to 39.4% and 30.4% of IL remained after incubation. This was compared to SMDIL-E fermentation supernatant, of which 19.8% and 10.8% of the peptides remained after incubation in the supernatant.

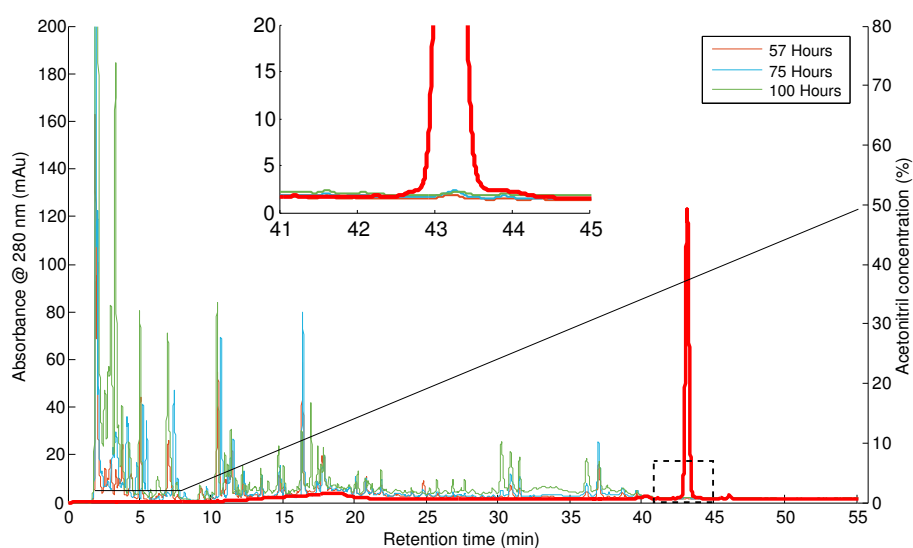


Figure 4.45: Reverse phase-HPLC analysis of supernatant collected during fermentation of IL using the SMDIL-E expression strain. The chromatography was performed using an analytical C18 column equilibrated with 2% acetonitrile and 0.1% TFA. A reference containing 13 μM synthesized IL (non-amidated) was also analysed (red line). The gradient has been shifted by the void time to depict the acetonitrile concentration at the site of the UV detector upon absorbance measurements. The flow rate in this run was 1 mL/min

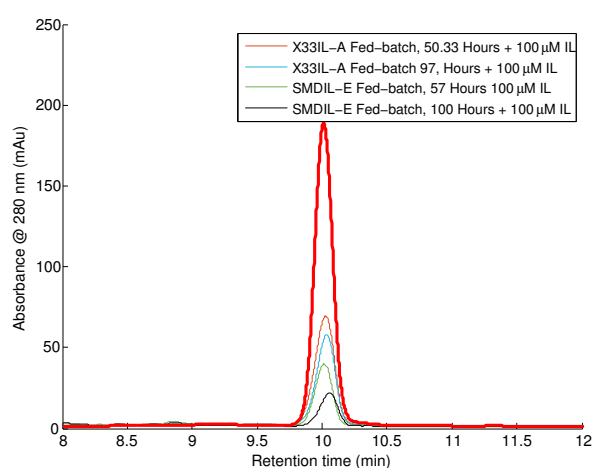


Figure 4.46: Reverse phase-HPLC analysis of supernatant collected during fermentation of IL incubated 24 hours with 100 μM synthesized IL. The chromatography was performed using an analytical C18 column equilibrated with 2% acetonitrile and 0.1% TFA. A reference were made with synthesized IL incubated in 10 mM Tris-HCl buffer (red line). The gradient has been shifted by the void time to depict the acetonitrile concentration at the site of the UV detector upon absorbance measurements. The flow rate in this run was 1 mL/min

Recombinant expression of small antimicrobial peptide is no easy task. Choosing the expression system and technology is linked to a number of consequences, involving low expression yield, downstream purification and activation challenges and self-toxic effects. Most attempts of recombinant expression of antimicrobial peptides have been performed in *E. coli* using fusion strategies to disable self-toxicity and reduce the affinity towards proteases. However, these strategies require extensive purification processes and activation of the peptide using cleavage reagents such as cyanogen bromide, which is unfit for pharmaceutical applications.

In this study the recombinant production of the antimicrobial peptide indolicidin (IL) and its single-tryptophan derivative indolicidin-4 (IL4) has been attempted in *P. pastoris*. IL shows a broad spectrum of antibacterial and antifungal activity and possesses immunomodulatory functions that can be used for anti-infectious therapy. The strategy of expression in *P. pastoris* is based on homologous recombination of the *AOX1* gene, utilizing the strong *AOX1* promoter inducible by methanol. In order to facilitate secretion of active IL and IL4, the genes were both cloned in-frame with a reduced α -MF pre-pro leader sequence, retaining the native N-terminus of the recombinant peptides.

5.1 Expression of IL and IL4

No evidence of IL or IL4 being produced in shake-flask expressions were found by RP-HPLC and SDS-PAGE analyses. Expression of IL concatamers has previously been reported in *E. coli* expression host with a 12 kDa thioredoxin fusion protein but with very low yield (150 μ g/L purified peptide)^[27]. The fusion protein was thought to disable the toxicity of IL towards the expression host.

Secretion of active IL4 in *P. pastoris* X33 has been reported earlier in-house, but generally with very low yield (μ g/L range)^[82]. The expression was performed in shake-flask cultures using similar strategy as this study. The author concluded that in order to increase expression levels, other induction conditions, such as pH, must be studied and scale-up experiments by fed-batch fermentations should be investigated^[82].

Generally, only few studies of the expression of small (<35 amino acid) antimicrobial peptides in *P. pastoris* have been reported^[41,42]. 15 mg/L pure ABP-CM4 peptide has been expressed in shake-flask expressions^[41] and 22 mg/L pure CA-MA peptide has been produced in fed-batch fermentations^[42]. These peptides both share linear α -helical structure upon interactions with amphiphathic environment, while IL and IL4 show extended structure. This structural property could make IL and IL4 more susceptible to proteases or intracellular targets than the α -helical peptides.

5.1.1 Intracellular Processing of IL and IL4

Early inhibition assays were performed on wild-type *P. pastoris* using synthesized IL and IL4 (non-amidated) to study the activity towards the expression host. No inhibition was observed using the highest concentrations available (results not shown). The peptides may, however, posses antimicrobial activity towards *P. pastoris* through intracellular targets, which could not be concluded from this assay.

The reason no trace of IL and IL4 was found in the expression studies may have been due to ineffective intracellular trafficking. A number of reasons for inaccurate secretion has been reported^[56], but only those of relevant probability are being discussed. Since the recombinant peptides do not have a defined structure the quality control system may recognize them as being misfolded when being processed in the ER. Therefore the peptide may not reach the Golgi apparatus for secretion.

The same physicochemical properties of the peptides that are responsible for their antimicrobial activity may also be limiting expression. Boettner *et al.* reported a significant association between a relatively high isoelectric point and non-detectable intracellular expression of large proteins in *P. pastoris*^[65]. The reason for the low-yield correlation to the high pI was, however, not concluded. Both IL and IL4 have a pI of 12.4 in their non-amidated form. This may have prevented the peptides from being expressed. Also the size (13 a.a.) of the peptides may affect the secretory expression.

Since the peptides were secreted using a reduced α -MF leader sequence, lacking the Glu-Ala dipeptide repeat normally cleaved by STE13 protease, the signal sequence may have been inefficiently processed. Although expressions of antimicrobial peptides in *P. pastoris* using this strategy has been reported with success^[42], it is unknown if the folding of the leader sequence is depending on the fusion partner. The dipeptide repeats also prevents steric hindrance of the Kex2 cleavage site^[55]. The cleavage efficiency of Kex2 proteases can also be influenced by close proximity of proline residues in the in-frame heterologous gene^[57]. Since IL and IL4 contains a proline residue at position three, it may be argued that the Kex2 cleavage is prevented during expression. If the Kex2 cleavage is inhibited, it has been reported to result in the secretion of intact pro-protein into the medium by *S. cerevisiae*^[83]. This would yield high-mass extension of the recombinant protein much greater than the expected 1.5-2 kDa.

Therefore, the addition of the Glu-Ala repeat may provide extra free space for the cleavage site and assist correct processing. However, the inclusion of the Glu-Ala dipeptide junction has been reported to permit the addition of extra amino acids to the N-terminal region of recombinant antimicrobial peptide, which may disable antimicrobial activity^[44].

Truncation of basic residues on the C-terminal of recombinant proteins in *P. pastoris* has been reported^[71]. The cleavage of C-terminal arginine and lysine is performed by Kex1 carboxypeptidase. Since IL and IL4 both contains two arginine residues at the C-terminal position, it is possible that these peptides has been reduced. This would cause the peptides to become less basic and more hydrophobic. Self-aggregation of native IL and IL4 happens at concentrations above 30 μ M and 5 mM, respectively^[84,82]. Since aggregation of IL and IL4 has been reported to be correlated to the hydrophobicity of the peptides, a reduction of the positive charge would only induce the aggregation further. These aggregations may serve as a bottle-neck for the secretion of the antimicrobial peptides. Although Kex2 protease recognizes Arg-Arg sequences, which is present in both IL and IL4, no reduction in the recombinant peptides is expected from this protease since the cleavage occur on the carboxyl end of the recognition sequence.

5.1.2 Proteolytic Digestion of IL and IL4

One of the main challenges in secreted expression of peptides is the activity of proteases in the culture supernatant. Therefore, the reason that no IL could be detected may be proteolytic digestion of the active peptide. A number of efforts were made to prevent proteolytic digestion of the active peptide expressed recombinantly. First and foremost, the expression was made under different pH and temperatures to analyse the effect on protease activity. Several studies have reported success in lowering pH and temperature to overcome the otherwise prohibited production by proteases^[75,76]. Secondly, the protease-deficient *P. pastoris* strain, SMD1168H, was used as expression host in addition to the wild-type strain. This was done to prevent digestion from some vacuolar peptidases that may be leaked to the supernatant during high-density cultivation. The presence of phosphoric acid and ammonia in the medium has also been reported to prevent the production of proteases during fermentation^[85]. Therefore ortho-phosphoric acid and ammonium hydroxide was used for controlling the pH during fermentation.

The assumption that proteolytic activity was one of the reasons for the lack of IL in the supernatant, is

supported by the degradation studies by RP-HPLC of synthesized IL incubated in culture supernatant, showing no sign of IL after 24 hours of incubation (Figure 4.36). This study was made on shake-flask supernatant from expressions using the protease-deficient *P. pastoris* strain collected after 72 hours of methanol induction. The analysis indicates that some important peptidases are still active in this strain.

It was speculated that such proteases may have been released due to the environmental stress caused by the accumulation of methanol during induction^[73]. Since 0.5% methanol was added every 24 hours, the culture experiences a burst in concentrations of methanol, presumably after a period of starvation since the last induction. The claim of methanol-induced stress is supported by the fact that degradation studies on fermentation supernatant showed much lower proteolytic activity (Figure 4.46). In the fermentation, the methanol consumption was more constant than the the shake-flask environment. However, since the methanol consumption is higher in fermentation, more oxygen peroxide is processed in the cell to form molecular oxygen. If this by-product accumulates, the cell may respond to the high oxidative stress with increase in protease production.

One of the main differences between the two fed-batch fermentations made, was the transition from glycerol to methanol substrate. A zoom of the substrate transitions are presented in Figure 5.1 and 5.2 below. In the first fermentation of IL, by the recombinant X33IL-A strain, the transition to methanol, made over a period of three hours, may have been less stressful for the cells. Degradation studies showed that 30% of the synthetic peptide remained after a 24 hour incubation in supernatant from the end of this fermentation (Figure 4.46). This should be compared to 11% in supernatant from the fermentation using the recombinant SMDIL-E strain, where an abrupt transition was made. The highest proteolytic activity was therefore found in the fermentation of IL where an abrupt transition was made from glycerol to methanol, even though in this fermentation a protease-deficient host was used.

In general, many of these issues can be solved in bioreactors equipped with a methanol substrate detector, enabling direct feedback to the methanol feed. This way the methanol concentration can be monitored while the focus may be put on the growth of the cells and production of recombinant peptides. Increasing methanol feeding rates and oxygen transfer rates will not necessarily cause increase in specific production when working with peptides highly susceptible to protease and other inhibiting processes. Although the growth would still be methanol-limited, the rate of methanol consumption would increase, causing unwanted by-products that induces cell stress. Rather, the aim in fed-batch fermentation would be to keep the cell stress to a minimum.

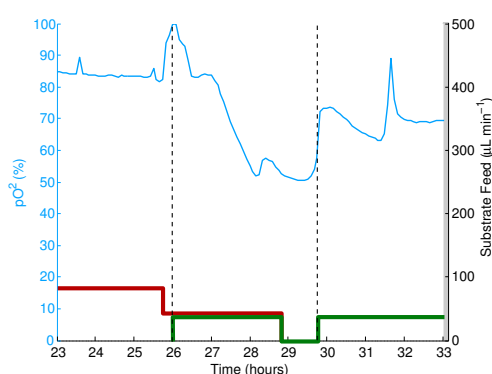


Figure 5.1: The substrate transition in fed-batch fermentations of X33IL-A expression strain. Feeding rate of glycerol (—) and methanol (—) are shown. Area between dashed lines shows the transition phase.

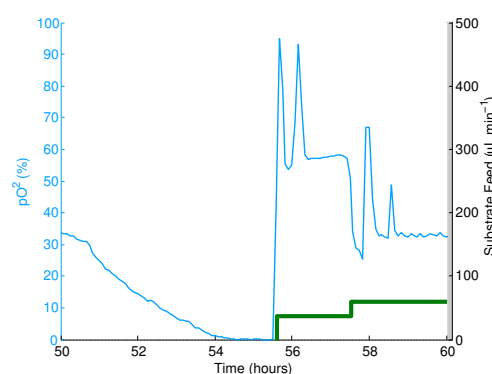


Figure 5.2: The abrupt substrate transition in fed-batch fermentations of SMDIL-E expression strain. Feeding rate of methanol (—) is shown.

Since no methanol detector was available, the methanol substrate concentration could not be monitored directly during fermentation. Therefore, it is suggested that the abrupt transition from glycerol to methanol

caused accumulation of methanol, since no AOX enzymes had been expressed to catalyse the oxidation. This is supported by the slight increase in pO_2 for 2 hours after the start of methanol induction (Figure 5.2). This means that oxygen consumption is lower than the oxygen-transfer rate in this period of induction, where an abrupt substrate transition is made. In contrast, in the fermentation where a three hour transition phase was applied, the pO_2 is decreasing after the glycerol substrate feed has stopped and only methanol is fed (Figure 5.1). Here, enough AOX enzymes have been produced to oxidise the methanol.

There was no evidence that starvation caused elevated proteolytic activity in the fermentation supernatant. This was also concluded from the degradation studies, in which the supernatant with lowest proteolytic activity originated from the X33IL-A fermentation undergoing a large period of starvation (Figure 4.37). However these degradation studies should be taken lightly, since the cell density is not the same in the two fermentations at the time of sample collection. Therefore, the high cell density in fermentations of SMDIL-E compared to X33IL-A may naturally contribute to the increase in protease activity.

It should be noted that the scale-up from shake-flask expressions to fed-batch fermentation involved a number of changes to the environment. In shake-flask environments the medium used was a complex peptone rich medium while the fermentation was made in basal salt medium containing trace elements and vitamin H. The yeast extract and peptone medium, containing numerous small peptides, could serve as antagonists to the proteases and limit the activity towards the recombinant peptide^[86,87]. The peptone medium in the shake-flasks may also induce the expression of extracellular proteases, which attributes to the increased activity. However, further investigations are needed to support this theory. Additionally, the control of oxygen was also significantly different between the two expression technologies. In shake-flask expressions increased aeration was attempted by the use of cheese cloth, instead of cotton plug. However, in the bioreactor, the direct supply of air provides considerably more oxygen to the medium. Since *P. pastoris* is an obligate aerobe when growing on methanol, reduce in oxygen transfer in shake-flask cultures may effect the core metabolism by causing energy deprivation^[88]. This influences cellular redox reactions and protein folding and as such causes oxidative stress on the organism. Therefore, an increased amount of extracellular proteases may be leaked to the medium during such stress. However, the effect on recombinant expression of larger proteins in *P. pastoris*, have been reported to increase under hypoxic conditions^[88]. This may be due to the less susceptible nature of larger proteins towards protease activities during such conditions, and may not be the case for small peptides.

5.2 Causes of Bacterial Inhibition

Only supernatant samples from methanol inductions of *P. pastoris* under low pH caused inhibition of *B. subtilis*. Since the pH of all the 10:1 concentrated supernatant samples was measured to be above 3, the low pH itself did not cause the inhibition of *B. subtilis*. This conclusion was based on the control experiments made on culture medium at pH 3, 4.5 and 6, showing no inhibition. The large diameter of the zone of inhibition from samples collected after 67 hours of X33ILA fermentations suggest that it is caused by a small molecule, due to relatively fast radial diffusion (Figure 4.39). It was not considered to be caused by methanol itself, since this sample was collected after a long period of starvation, as indicated by the pO_2 (Figure 4.37). High traces of salt is also a candidate for growth inhibition due to osmotic shock. However, control experiments with 10X concentrated basal salt medium reveals no such inhibition, but only crystallisation (Figure 4.41). Therefore, high levels of salt was not considered the cause of the inhibition.

The reason for the antimicrobial activity against *B. subtilis* observed only in samples of pH 3, may be due to acidic toxins secreted by the yeast, that are only active at low pH. A number of toxins has been identified among yeasts^[89,90], but none so far in *P. pastoris*^[91]. Some of these toxins have also been found to exhibit bactericidal

activity^[92]. Since similar degree of inhibition was observed on gram-negative *E. coli* and gram-positive *M. luteus* it suggest a broad range of activity. It is assumed that the bacteriocidal compound was secreted or leaked into the supernatant due to the environmental stress caused by methanol. This was based on the fact that no inhibition was observed prior to methanol induction in the fermentation of SMDIL-E when the cell density was 50 g/L, but considerable activity was observed during methanol induction of fermentations of X33IL-A, even though the cell density was only 30 g/L. Therefore the degree of inhibition was not correlated to the cell density and no inhibition has been observed during growth on glycerol. However, since the sample showing highest antimicrobial activity was collected after a long period of starvation, methanol is not the only cause for the leakage or secretion of the toxin.

If the unidentified antimicrobial compound was a protein it should be detectable on the silver-stained SDS-PAGE made on shake-flask supernatant. Therefore the SDS-PAGE analyses was inspected for compounds only existing in supernatant collected from shake-flask expressions made at pH 3, where bacterial inhibition was observed. However, there was no unique protein observed (Figure 4.32 and 4.33). Therefore, no detectable proteins was correlated to the compound showing antimicrobial activity on *B. subtilis*, and the compound remain unknown.

Conclusion

6

The antimicrobial peptides indolicidin and its single-tryptophan derivative indolicidin-4 can only be expressed in *E. coli* by the use of fusion proteins. However purification of active recombinant peptides is difficult and the yield generally low. In the present study, IL and IL4 were produced in the active form by secreted expression in *P. pastoris*. The productions were made in shake-flasks and fed-batch fermentations. However, the presence of recombinant peptides could not be detected in the supernatant of these productions. It was suggested that the expression was blocked by intracellular interactions or by digestion from proteolytic activity. Synthetic non-amidated IL and IL4 was found to be highly susceptible to proteases found in the supernatant. A number of attempts were made to control proteolysis, such as lowering temperature and pH and utilizing protease-deficient host organisms but without success.

The antimicrobial activity of compounds produced natively by *P. pastoris* during methanol inductions at pH 3 has been reported in the current study. The compounds very effectively inhibited the growth of *E. coli*, *B. subtilis* and *M. luteus*. Supernatant containing antimicrobial activity was analysed in tricine SDS-PAGE and RP-HPLC but the compounds could not be identified.

References

- [1] M. Zucca, S. Scutera, and D. Savoia, “Antimicrobial peptides: New frontiers in the therapy of infections,”
- [2] R. Emes, L. Goodstadt, E. Winter, and C. Ponting, “Comparison of the genomes of human and mouse lays the foundation of genome zoology,” *Human molecular genetics*, vol. 12, no. 7, pp. 701–709, 2003.
- [3] A. Maxwell, G. Morrison, and J. Dorin, “Rapid sequence divergence in mammalian [beta]-defensins by adaptive evolution,” *Molecular immunology*, vol. 40, no. 7, pp. 413–421, 2003.
- [4] M. Zasloff *et al.*, “Antimicrobial peptides of multicellular organisms,” *Nature*, vol. 415, no. 6870, pp. 389–395, 2002.
- [5] T. Ganz *et al.*, “Defensins: antimicrobial peptides of innate immunity,” *Nature Reviews Immunology*, vol. 3, no. 9, pp. 710–720, 2003.
- [6] M. Selsted, M. Novotny, W. Morris, Y. Tang, W. Smith, and J. Cullor, “Indolicidin, a novel bactericidal tridecapeptide amide from neutrophils,” *Journal of Biological Chemistry*, vol. 267, no. 7, p. 4292, 1992.
- [7] A. Ladokhin, M. Selsted, and S. White, “Cd spectra of indolicidin antimicrobial peptides suggest turns, not polyproline helix,” *Biochemistry*, vol. 38, no. 38, pp. 12313–12319, 1999.
- [8] I. Ahmad, W. Perkins, D. Lupan, M. Selsted, and A. Janoff, “Liposomal entrapment of the neutrophil-derived peptide indolicidin endows it with in vivo antifungal activity,” *Biochimica et Biophysica Acta (BBA)-Biomembranes*, vol. 1237, no. 2, pp. 109–114, 1995.
- [9] D. Lee, H. Kim, S. Kim, Y. Park, S. Park, S. Jang, and K. Hahm, “Fungicidal effect of indolicidin and its interaction with phospholipid membranes,” *Biochemical and biophysical research communications*, vol. 305, no. 2, pp. 305–310, 2003.
- [10] C. Subbalakshmi, V. Krishnakumari, R. Nagaraj, and N. Sitaram, “Requirements for antibacterial and hemolytic activities in the bovine neutrophil derived 13-residue peptide indolicidin,” *FEBS letters*, vol. 395, no. 1, pp. 48–52, 1996.
- [11] W. Robinson, B. McDougall, D. Tran, and M. Selsted, “Anti-HIV-1 activity of indolicidin, an antimicrobial peptide from neutrophils,” *Journal of leukocyte biology*, vol. 63, no. 1, p. 94, 1998.
- [12] C. Subbalakshmi, E. Bikshapathy, N. Sitaram, and R. Nagaraj, “Antibacterial and hemolytic activities of single tryptophan analogs of indolicidin,” *Biochemical and biophysical research communications*, vol. 274, no. 3, pp. 714–716, 2000.
- [13] C. Subbalakshmi and N. Sitaram, “Mechanism of antimicrobial action of indolicidin,” *FEMS microbiology letters*, vol. 160, no. 1, pp. 91–96, 1998.
- [14] R. Hancock and H. Sahl, “Antimicrobial and host-defense peptides as new anti-infective therapeutic strategies,” *Nature biotechnology*, vol. 24, no. 12, pp. 1551–1557, 2006.
- [15] D. Bowdish, D. Davidson, M. Scott, and R. Hancock, “Immunomodulatory activities of small host defense peptides,” *Antimicrobial agents and chemotherapy*, vol. 49, no. 5, pp. 1727–1732, 2005.
- [16] K. Brogden, “Antimicrobial peptides: pore formers or metabolic inhibitors in bacteria?,” *Nature Reviews Microbiology*, vol. 3, no. 3, pp. 238–250, 2005.
- [17] J. Shaw, J. Alattia, J. Verity, G. Privé, and C. Yip, “Mechanisms of antimicrobial peptide action: studies of indolicidin assembly at model membrane interfaces by in situ atomic force microscopy,” *Journal of*

- structural biology*, vol. 154, no. 1, pp. 42–58, 2006.
- [18] T. Falla, D. Karunaratne, and R. Hancock, “Mode of action of the antimicrobial peptide indolicidin,” *Journal of Biological Chemistry*, vol. 271, no. 32, p. 19298, 1996.
- [19] Y. Nan, K. Park, Y. Park, Y. Jeon, Y. Kim, I. Park, K. Hahm, and S. Shin, “Investigating the effects of positive charge and hydrophobicity on the cell selectivity, mechanism of action and anti-inflammatory activity of a trp-rich antimicrobial peptide indolicidin,” *FEMS microbiology letters*, vol. 292, no. 1, pp. 134–140, 2009.
- [20] Y. Nan, J. Bang, and S. Shin, “Design of novel indolicidin-derived antimicrobial peptides with enhanced cell specificity and potent anti-inflammatory activity,” *Peptides*, vol. 30, no. 5, pp. 832–838, 2009.
- [21] A. Yeung, S. Gellatly, and R. Hancock, “Multifunctional cationic host defence peptides and their clinical applications,” *Cellular and Molecular Life Sciences*, pp. 1–16, 2011.
- [22] L. Zhang and T. Falla, “Antimicrobial peptides: therapeutic potential,” 2006.
- [23] A. Ingham and R. Moore, “Recombinant production of antimicrobial peptides in heterologous microbial systems,” *Biotechnology and applied biochemistry*, vol. 47, no. 1, pp. 1–9, 2007.
- [24] A. Peschel and H. Sahl, “The co-evolution of host cationic antimicrobial peptides and microbial resistance,” *Nature Reviews Microbiology*, vol. 4, no. 7, pp. 529–536, 2006.
- [25] J. Lee, J. Kim, S. Hwang, W. Lee, H. Yoon, H. Lee, and S. Hong, “High-level expression of antimicrobial peptide mediated by a fusion partner reinforcing formation of inclusion bodies,” *Biochemical and Biophysical Research Communications*, vol. 277, no. 3, pp. 575–580, 2000.
- [26] Q. Wei, Y. Kim, J. Seo, W. Jang, I. Lee, and H. Cha, “Facilitation of expression and purification of an antimicrobial peptide by fusion with baculoviral polyhedrin in escherichia coli,” *Applied and environmental microbiology*, vol. 71, no. 9, p. 5038, 2005.
- [27] K. Morin, S. Arcidiacono, R. Beckwitt, and C. Mello, “Recombinant expression of indolicidin concatamers in escherichia coli,” *Applied microbiology and biotechnology*, vol. 70, no. 6, pp. 698–704, 2006.
- [28] Y. Li, “Recombinant production of antimicrobial peptides in escherichia coli: A review,” *Protein Expression and Purification*, 2011.
- [29] X. Chen, F. Zhu, Y. Cao, and S. Qiao, “Novel expression vector for secretion of cecropin ad in bacillus subtilis with enhanced antimicrobial activity,” *Antimicrobial agents and chemotherapy*, vol. 53, no. 9, pp. 3683–3689, 2009.
- [30] X. Xu, F. Jin, X. Yu, S. Ren, J. Hu, and W. Zhang, “High-level expression of the recombinant hybrid peptide cecropina (1-8)-magainin2 (1-12) with an ubiquitin fusion partner in escherichia coli,” *Protein expression and purification*, vol. 55, no. 1, pp. 175–182, 2007.
- [31] L. Metlitskaia, J. Cabralda, D. Suleman, C. Kerry, J. Brinkman, D. Bartfeld, and M. Guarna, “Recombinant antimicrobial peptides efficiently produced using novel cloning and purification processes,” *Biotechnology and applied biochemistry*, vol. 39, no. 3, pp. 339–345, 2004.
- [32] J. Lee, I. Minn, C. Park, and S. Kim, “Acidic peptide-mediated expression of the antimicrobial peptide buforin ii as tandem repeats in escherichia coli,” *Protein expression and purification*, vol. 12, no. 1, pp. 53–60, 1998.
- [33] H. Peng, M. Yang, W. Huang, J. Ding, H. Qu, J. Cai, N. Zhang, and K. Wang, “Soluble expression and purification of a crab antimicrobial peptide scygonadin in different expression plasmids and analysis of its antimicrobial activity,” *Protein expression and purification*, vol. 70, no. 1, pp. 109–115, 2010.
- [34] S. Harrison, A. McManus, J. Marcus, K. Goulter, J. Green, K. Nielsen, D. Craik, D. Maclean, and J. Manners, “Purification and characterization of a plant antimicrobial peptide expressed in escherichia coli,” *Protein expression and purification*, vol. 15, no. 2, pp. 171–177, 1999.
- [35] P. Supungul, S. Tang, C. Maneeruttanarungroj, V. Rimphanitchayakit, I. Hirono, T. Aoki, and A. Tas-

- sanakajon, "Cloning, expression and antimicrobial activity of crustinpm1, a major isoform of crustin, from the black tiger shrimp *penaeus monodon*," *Developmental & Comparative Immunology*, vol. 32, no. 1, pp. 61–70, 2008.
- [36] J. Shao, Y. Wang, X. Wu, R. Jiang, R. Zhang, C. Wu, and J. Zhang, "Cloning, expression, and pharmacological activity of bmk as, an active peptide from scorpion *buthus martensii karsch*," *Biotechnology letters*, vol. 30, no. 1, pp. 23–29, 2008.
- [37] B. Srinivasulu, R. Syvitski, J. Seo, N. Mattatall, L. Knickle, and S. Douglas, "Expression, purification and structural characterization of recombinant hepcidin, an antimicrobial peptide identified in japanese flounder, *paralichthys olivaceus*," *Protein expression and purification*, vol. 61, no. 1, pp. 36–44, 2008.
- [38] J. Dai, H. Xie, G. Jin, W. Wang, Y. Zhang, and Y. Guo, "Preliminary study on high-level expression of tandem-arranged tachyplesin-encoding gene in *bacillus subtilis* wb800 and its antibacterial activity," *Marine biotechnology*, vol. 11, no. 1, pp. 109–117, 2009.
- [39] S. Sooriyaarachchi, E. Jaber, A. Covarrubias, W. Ubhayasekera, F. Asiegbu, and S. Mowbray, "Expression and β -glucan binding properties of scots pine (*pinus sylvestris* l.) antimicrobial protein (sp-amp)," *Plant molecular biology*, pp. 1–13, 2011.
- [40] L. Li, J. Wang, X. Zhao, C. Kang, N. Liu, J. Xiang, F. Li, S. Sueda, and H. Kondo, "High level expression, purification, and characterization of the shrimp antimicrobial peptide, ch-penaedin, in *Pichia pastoris*," *Protein expression and purification*, vol. 39, no. 2, pp. 144–151, 2005.
- [41] J. Zhang, X. Wu, *et al.*, "Expression and characterization of antimicrobial peptide abp-cm4 in methylotrophic yeast *Pichia pastoris*," *Process Biochemistry*, vol. 41, no. 2, pp. 251–256, 2006.
- [42] F. Jin, X. Xu, L. Wang, W. Zhang, and D. Gu, "Expression of recombinant hybrid peptide cecropina (1-8)-magainin2 (1-12) in *Pichia pastoris*: Purification and characterization," *Protein expression and purification*, vol. 50, no. 2, pp. 147–156, 2006.
- [43] H. Peng, H. Liu, B. Chen, H. Hao, and K. Wang, "Optimized production of scygonadin in *Pichia pastoris* and analysis of its antimicrobial and antiviral activities," *Protein Expression and Purification*, 2011.
- [44] Z. Chen, D. Wang, Y. Cong, J. Wang, J. Zhu, J. Yang, Z. Hu, X. Hu, Y. Tan, F. Hu, *et al.*, "Recombinant antimicrobial peptide hpab- β expressed in *Pichia pastoris*, a potential agent active against methicillin-resistant *staphylococcus aureus*," *Applied microbiology and biotechnology*, vol. 89, no. 2, pp. 281–291, 2011.
- [45] M. Egel-Mitani, A. Andersen, I. Diers, M. Hach, L. Thim, S. Hastrup, and K. Vad, "Yield improvement of heterologous peptides expressed in *yps1*-disrupted *saccharomyces cerevisiae* strains," *Enzyme and microbial technology*, vol. 26, no. 9-10, pp. 671–677, 2000.
- [46] M. Jahic, J. Rotticci-Mulder, M. Martinelle, K. Hult, and S. Enfors, "Modeling of growth and energy metabolism of *Pichia pastoris* producing a fusion protein," *Bioprocess and Biosystems Engineering*, vol. 24, no. 6, pp. 385–393, 2002.
- [47] T. Charoenrat, M. Ketudat-Cairns, H. Stendahl-Andersen, M. Jahic, and S. Enfors, "Oxygen-limited fed-batch process: an alternative control for *Pichia pastoris* recombinant protein processes," *Bioprocess and biosystems engineering*, vol. 27, no. 6, pp. 399–406, 2005.
- [48] M. Jahic, A. Veide, T. Charoenrat, T. Teeri, and S. Enfors, "Process technology for production and recovery of heterologous proteins with *Pichia pastoris*," *Biotechnology progress*, vol. 22, no. 6, pp. 1465–1473, 2006.
- [49] F. Hong, N. Meinander, and L. Jansson, "Fermentation strategies for improved heterologous expression of laccase in *Pichia pastoris*," *Biotechnology and bioengineering*, vol. 79, no. 4, pp. 438–449, 2002.
- [50] A. Xiao, X. Zhou, L. Zhou, and Y. Zhang, "Improvement of cell viability and hirudin production by ascorbic acid in *Pichia pastoris* fermentation," *Applied microbiology and biotechnology*, vol. 72, no. 4,

- pp. 837–844.
- [51] M. Jahic, *Process techniques for production of recombinant proteins with Pichia pastoris*. Royal Institute of technology, Stockholm, 2003.
- [52] J. Berg, J. Tymoczko, and L. Stryer, “Biochemistry: International version,” 2002.
- [53] H. Lodish, A. Berk, S. Zipursky, P. Matsudaira, D. Baltimore, and J. Darnell, “Molecular cell biology,” *New York*, 1995.
- [54] G. Gellissen, “Heterologous protein production in methylotrophic yeasts,” *Applied microbiology and biotechnology*, vol. 54, no. 6, pp. 741–750, 2000.
- [55] R. Daly and M. Hearn, “Expression of heterologous proteins in *Pichia pastoris*: a useful experimental tool in protein engineering and production,” *Journal of Molecular Recognition*, vol. 18, no. 2, pp. 119–138, 2005.
- [56] K. Sreeriksha, R. Brankamp, K. Kropp, D. Blankenship, J. Tsay, P. Smith, J. Wierschke, A. Subramaniam, and L. Birkenberger, “Strategies for optimal synthesis and secretion of heterologous proteins in the methylotrophic yeast *Pichia pastoris*,” *Gene*, vol. 190, no. 1, pp. 55–62, 1997.
- [57] J. Cereghino and J. Cregg, “Heterologous protein expression in the methylotrophic yeast *Pichia pastoris*,” *FEMS microbiology reviews*, vol. 24, no. 1, pp. 45–66, 2000.
- [58] D. Higgins and J. Cregg, *Pichia protocols*, vol. 103. Humana Pr Inc, 1998.
- [59] Y. Chen, J. Cino, G. Hart, D. Freedman, C. White, and E. Komives, “High protein expression in fermentation of recombinant *Pichia pastoris* by a fed-batch process,” *Process Biochemistry*, vol. 32, no. 2, pp. 107–111, 1997.
- [60] M. van der Heide, C. Hollenberg, I. van der Klei, and M. Veenhuis, “Overproduction of BiP negatively affects the secretion of *Aspergillus niger* glucose oxidase by the yeast *Hansenula polymorpha*,” *Applied microbiology and biotechnology*, vol. 58, no. 4, pp. 487–494, 2002.
- [61] J. Ahn, E. Choi, H. Lee, S. Hwang, C. Kim, H. Jang, S. Haam, and J. Jung, “Enhanced secretion of *Bacillus stearothermophilus* L1 lipase in *Saccharomyces cerevisiae* by translational fusion to cellulose-binding domain,” *Applied microbiology and biotechnology*, vol. 64, no. 6, pp. 833–839, 2004.
- [62] G. Gellissen, *Production of recombinant proteins: Novel microbial and eukaryotic expression systems*. Vch Verlagsgesellschaft Mbh, 2005.
- [63] A. Idiris, H. Tohda, H. Kumagai, and K. Takegawa, “Engineering of protein secretion in yeast: strategies and impact on protein production,” *Applied microbiology and biotechnology*, vol. 86, no. 2, pp. 403–417, 2010.
- [64] M. Harmsen, M. Bruyne, H. Raue, and J. Maat, “Overexpression of binding protein and disruption of the PMR1 gene synergistically stimulate secretion of bovine prochymosin but not plant thaumatin in yeast,” *Applied microbiology and biotechnology*, vol. 46, no. 4, pp. 365–370, 1996.
- [65] M. Boettner, C. Steffens, C. von Mering, P. Bork, U. Stahl, and C. Lang, “Sequence-based factors influencing the expression of heterologous genes in the yeast *Pichia pastoris*: A comparative view on 79 human genes,” *Journal of biotechnology*, vol. 130, no. 1, pp. 1–10, 2007.
- [66] Y. Zhang, R. Liu, and X. Wu, “The proteolytic systems and heterologous proteins degradation in the methylotrophic yeast *Pichia pastoris*,” *Annals of microbiology*, vol. 57, no. 4, pp. 553–560, 2007.
- [67] A. Koller, W. Snyder, K. Faber, T. Wenzel, L. Rangell, G. Keller, and S. Subramani, “Pex22p of *Pichia pastoris*, essential for peroxisomal matrix protein import, anchors the ubiquitin-conjugating enzyme, pex4p, on the peroxisomal membrane,” *The Journal of cell biology*, vol. 146, no. 1, pp. 99–112, 1999.
- [68] D. Tuttle and W. Dunn, “Divergent modes of autophagy in the methylotrophic yeast *Pichia pastoris*,” *Journal of cell science*, vol. 108, no. 1, pp. 25–35, 1995.
- [69] J. Rothman, C. Hunter, L. Valls, and T. Stevens, “Overproduction-induced mislocalization of a yeast

- vacuolar protein allows isolation of its structural gene,” *Proceedings of the National Academy of Sciences*, vol. 83, no. 10, p. 3248, 1986.
- [70] A. Dmochowska, D. Dignard, D. Henning, D. Thomas, H. Bussey, *et al.*, “Yeast *kex1* gene encodes a putative protease with a carboxypeptidase b-like function involved in killer toxin and alpha-factor precursor processing.,” *Cell*, vol. 50, no. 4, p. 573, 1987.
- [71] T. Boehm, S. Pirie-Shepherd, L. Trinh, J. Shiloach, and J. Folkman, “Disruption of the *kex1* gene in *Pichia pastoris* allows expression of full-length murine and human endostatin,” *Yeast*, vol. 15, no. 7, pp. 563–572, 1999.
- [72] R. Hansen, R. Switzer, H. Hinze, and H. Holzer, “Effects of glucose and nitrogen source on the levels of proteinases, peptidases, and proteinase inhibitors in yeast,” *Biochimica et Biophysica Acta (BBA)-General Subjects*, vol. 496, no. 1, pp. 103–114, 1977.
- [73] J. Sinha, B. Plantz, M. Inan, and M. Meagher, “Causes of proteolytic degradation of secreted recombinant proteins produced in methylotrophic yeast *Pichia pastoris*: Case study with recombinant ovine interferon- τ ,” *Biotechnology and bioengineering*, vol. 89, no. 1, pp. 102–112, 2005.
- [74] M. Inan, V. Chiruvolu, K. Eskridge, G. Vlasuk, K. Dickerson, S. Brown, and M. Meagher, “Optimization of temperature-glycerol-ph conditions for a fed-batch fermentation process for recombinant hookworm (*ancylostoma caninum*) anticoagulant peptide (acap-5) production by *Pichia pastoris*,” *Enzyme and microbial technology*, vol. 24, no. 7, pp. 438–445, 1999.
- [75] N. Koganesawa, T. Aizawa, H. Shimojo, K. Miura, A. Ohnishi, M. Demura, Y. Hayakawa, K. Nitta, and K. Kawano, “Expression and purification of a small cytokine growth-blocking peptide from army-worm *pseudaletia separata* by an optimized fermentation method using the methylotrophic yeast *Pichia pastoris*,” *Protein expression and purification*, vol. 25, no. 3, pp. 416–425, 2002.
- [76] Z. Li, F. Xiong, Q. Lin, M. d’Anjou, A. Daugulis, D. Yang, and C. Hew, “Low-temperature increases the yield of biologically active herring antifreeze protein in *Pichia pastoris*,” *Protein expression and purification*, vol. 21, no. 3, pp. 438–445, 2001.
- [77] S. Macauley-Patrick, M. Fazenda, B. McNeil, and L. Harvey, “Heterologous protein production using the *Pichia pastoris* expression system,” *Yeast*, vol. 22, no. 4, pp. 249–270, 2005.
- [78] R. Bretthauer and F. Castellino, “Glycosylation of *Pichia pastoris*-derived proteins,” *Biotechnology and applied biochemistry*, vol. 30, no. 3, pp. 193–200, 1999.
- [79] W. Tanner, L. Lehle, *et al.*, “Protein glycosylation in yeast.,” *Biochimica et biophysica acta*, vol. 906, no. 1, p. 81, 1987.
- [80] T. Vincze, J. Posfai, and R. Roberts, “Nebcutter: a program to cleave dna with restriction enzymes,” *Nucleic acids research*, vol. 31, no. 13, pp. 3688–3691, 2003.
- [81] A. Maghsoudi, S. Hosseini, S. Shojaosadati, E. Vasheghani-Farahani, M. Nosrati, and A. Bahrami, “A new methanol-feeding strategy for the improved production of β -galactosidase in high cell-density fed-batch cultures of *Pichia pastoris* mut+ strains,” *Biotechnology and Bioprocess Engineering*, vol. 17, no. 1, pp. 76–83, 2012.
- [82] B. Justesen, “Recombinant production of an indolicidin analogue in *Pichia pastoris*,” Master’s thesis, Department of Physics and Nanotechnology, Aalborg University, 2008.
- [83] D. Julius, A. Brake, L. Blair, R. Kunisawa, J. Thorner, *et al.*, “Isolation of the putative structural gene for the lysine-arginine-cleaving endopeptidase required for processing of yeast prepro-alpha-factor.,” *Cell*, vol. 37, no. 3, p. 1075, 1984.
- [84] A. Ladokhin, M. Selsted, and S. White, “Bilayer interactions of indolicidin, a small antimicrobial peptide rich in tryptophan, proline, and basic amino acids,” *Biophysical journal*, vol. 72, no. 2, pp. 794–805, 1997.
- [85] K. Kobayashi, S. Kuwae, T. Ohya, T. Ohda, M. Ohyama, H. Ohi, K. Tomomitsu, and T. Ohmura, “High-

- level expression of recombinant human serum albumin from the methylotrophic yeast *Pichia pastoris* with minimal protease production and activation,” *Journal of bioscience and bioengineering*, vol. 89, no. 1, pp. 55–61, 2000.
- [86] D. Wu, Y. Hao, J. Chu, Y. Zhuang, and S. Zhang, “Inhibition of degradation and aggregation of recombinant human consensus interferon- α mutant expressed in *Pichia pastoris* with complex medium in bioreactor,” *Applied microbiology and biotechnology*, vol. 80, no. 6, pp. 1063–1071, 2008.
- [87] R. Vad, E. Nafstad, L. Dahl, and O. Gabrielsen, “Engineering of a *Pichia pastoris* expression system for secretion of high amounts of intact human parathyroid hormone,” *Journal of biotechnology*, vol. 116, no. 3, pp. 251–260, 2005.
- [88] B. Kristin, C. Marc, D. Martin, G. Alexandra, J. Paula, M. Hannu, G. Brigitte, A. Joan, M. Diethard, and F. Pau, “A multi-level study of recombinant *Pichia pastoris* in different oxygen conditions,” *BMC Systems Biology*, vol. 4.
- [89] W. Magliani, S. Conti, M. Gerloni, D. Bertolotti, and L. Polonelli, “Yeast killer systems.,” *Clinical microbiology reviews*, vol. 10, no. 3, pp. 369–400, 1997.
- [90] D. Marquina, A. Santos, and J. Peinado, “Biology of killer yeasts,” *International Microbiology*, vol. 5, no. 2, pp. 65–71, 2002.
- [91] M. Verma *et al.*, “Search for a novel killer toxin in yeast *Pichia pastoris*,” *Plasmid*, vol. 43, no. 2, pp. 181–183, 2000.
- [92] F. İzgü, D. Altınbay, and T. Acun, “Killer toxin of *Pichia anomala* ncyc 432; purification, characterization and its *exo*- β -1, 3-glucanase activity,” *Enzyme and microbial technology*, vol. 39, no. 4, pp. 669–676, 2006.

Shuttle vectors

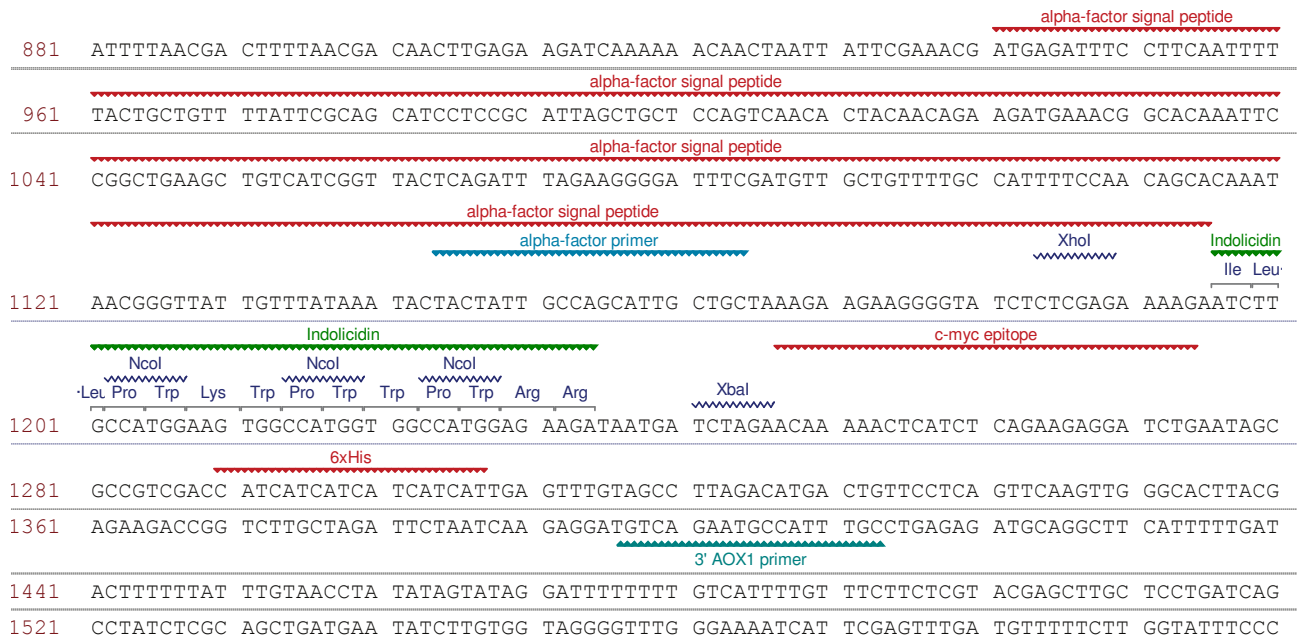


Figure A.1: The 881-1601 bp part of the pPICZ α A-IL shuttle vector used for the recombinant integration of *IL* gene into *P. pastoris*. Important restriction and primer sites are highlighted above the DNA sequence. The three-letter amino acid sequence of IL is shown.

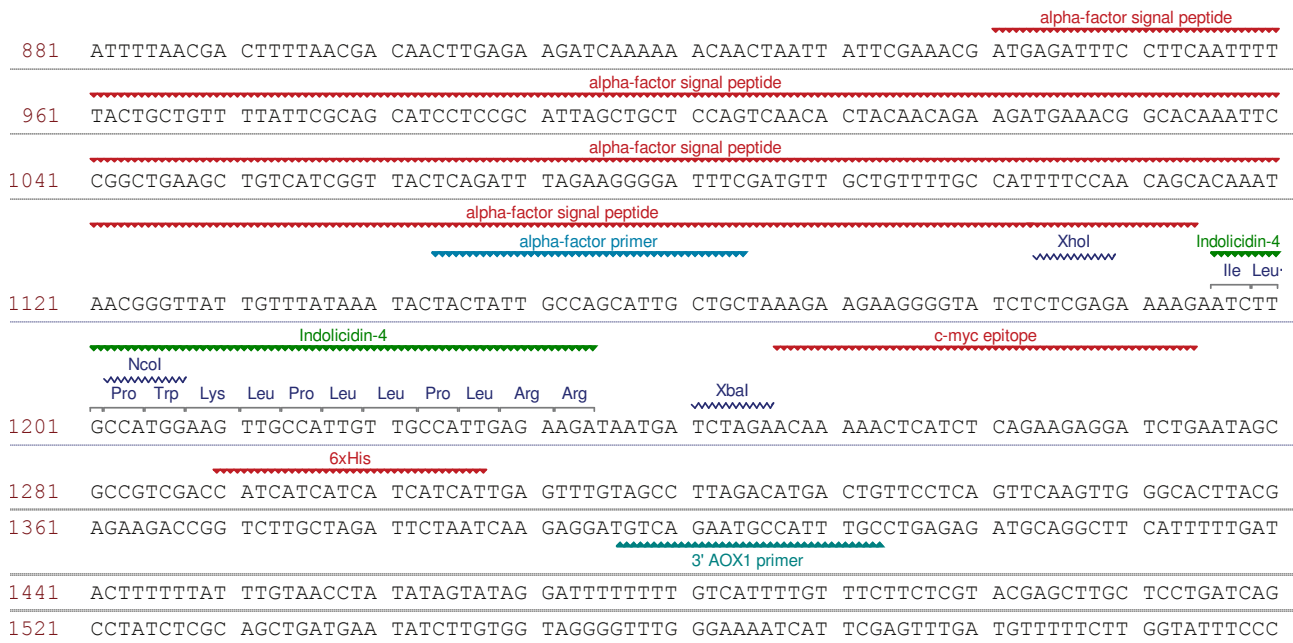


Figure A.2: The 881-1601 bp part of the pPICZ α A-IL4 shuttle vector used for the recombinant integration of *IL4* gene into *P. pastoris*. Important restriction and primer sites are highlighted above the DNA sequence. The three-letter amino acid sequence of IL4 is shown.

Sequencing of Insert

B

The following pages shows the alignment of the sequence data of the expression vectors made early in this project against the expected sequences. Sequence data of chromosomal DNA extracted from recombinant *P. pastoris* colonies were also aligned.

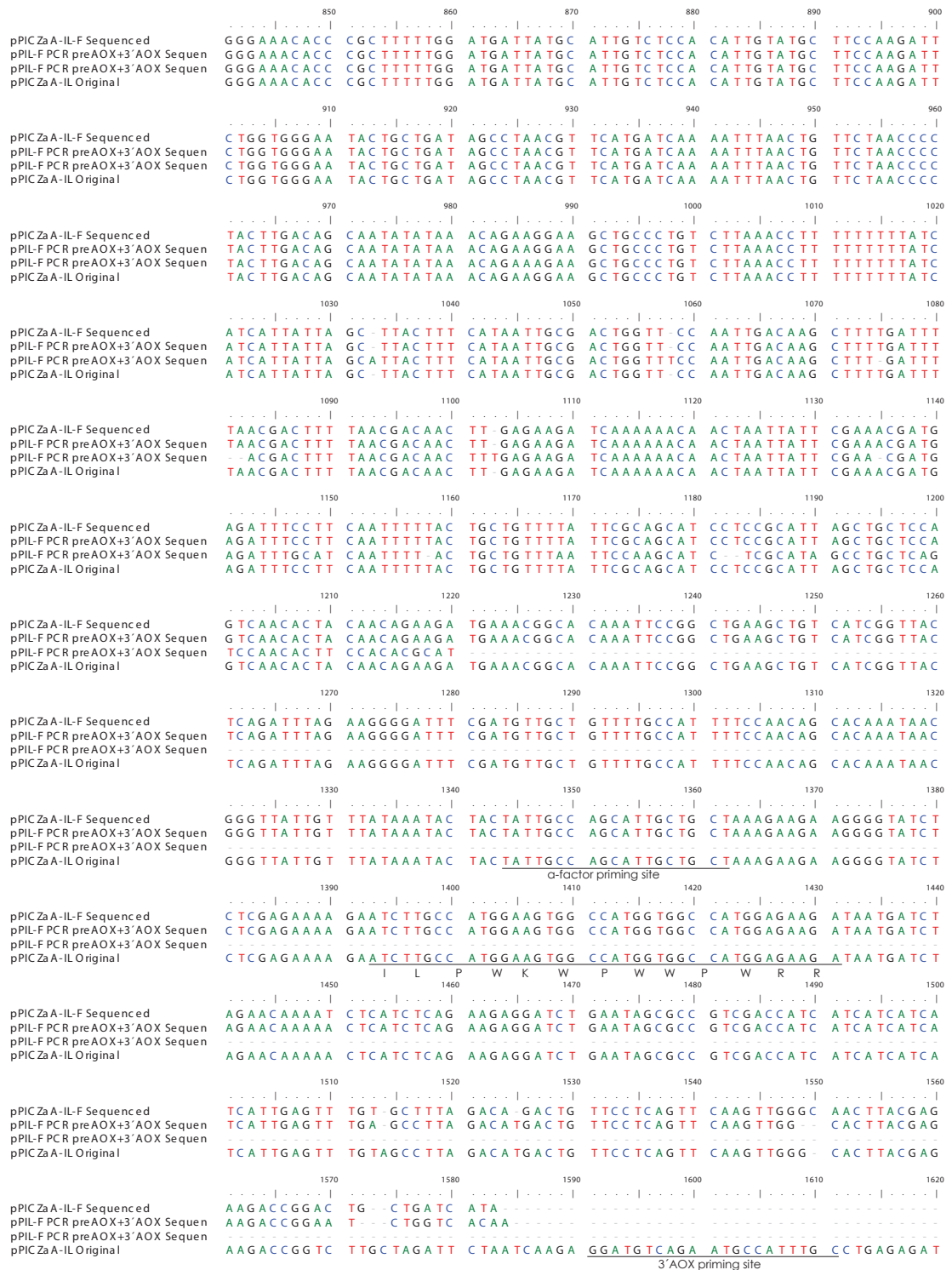


Figure B.1: Alignment of sequence data of purified pPICZ α A-IL-F vector DNA (3'AOX primer only) and PCR product of extracted genomic DNA of X33IL-A colonies using *pre*AOX and 3'AOX primers. Sequencing was performed by DNA Technology (Risskov, Denmark) using mentioned primers. The alignment was made against the original pPICZ α A-IL sequence using ClustalW. Ending part of the vector is not shown.

	10	20	30	40	50	60
pPICZaA-IL4-A Sequenced						
pIL4-A PCR preAOX+3 'AOX Seque	GCGTTCC	GGTTTGC	ACTCTAA	AACGCAT	CGCCTTT	TTTGGAG
pIL4-A PCR preAOX+3 'AOX Seque
pPICZaA-IL4 Original
	70	80	90	100	110	120
pPICZaA-IL4-A Sequenced						
pIL4-A PCR preAOX+3 'AOX Seque	ACTGTCAG	TGATGCC	AAATCCCA	CCATACAA	TGACATTT	ATTTGGTT
pIL4-A PCR preAOX+3 'AOX Seque
pPICZaA-IL4 Original
	130	140	150	160	170	180
pPICZaA-IL4-A Sequenced						
pIL4-A PCR preAOX+3 'AOX Seque	CTCATGTT	TATTTGT	TAGACGC	TCCGGAA	TGAAAAA	CAGTTATT
pIL4-A PCR preAOX+3 'AOX Seque
pPICZaA-IL4 Original	AGA	TCTAACAT
	190	200	210	220	230	240
pPICZaA-IL4-A Sequenced						
pIL4-A PCR preAOX+3 'AOX Seque	TCGAGAT	ACATCCA	ACGAAAG	GAAATGA	TTTTTGC	CCGACAT
pIL4-A PCR preAOX+3 'AOX Seque
pPICZaA-IL4 Original	AAAGACG	GGTTGA	AACCTTT	CCATCCG	TCCACAG	CATTTCT
	250	260	270	280	290	300
pPICZaA-IL4-A Sequenced						
pIL4-A PCR preAOX+3 'AOX Seque	CAGGTCAT	CTCACAC	AGTGCCAA	GCAACAG	GGGATAC	AGCAGCAG
pIL4-A PCR preAOX+3 'AOX Seque
pPICZaA-IL4 Original	CATAAGT	AAACGCA	GGAGGGG	CACTAGC	AGACCGT	AAACGCAG
	310	320	330	340	350	360
pPICZaA-IL4-A Sequenced						
pIL4-A PCR preAOX+3 'AOX Seque	CGTTGCAA	GCAGGAC	CCTCCTCT	CTCCTCAA	CCCACITT	TCCGTAT
pIL4-A PCR preAOX+3 'AOX Seque
pPICZaA-IL4 Original	CCCTCCAC	TCTTCTC	AACCCCA	TTTGCCAT	AAAAACC	C-CAGTAT
	370	380	390	400	410	420
pPICZaA-IL4-A Sequenced						
pIL4-A PCR preAOX+3 'AOX Seque	AGTAATGA	TCTGCGC	CATATAAC	TCCTTTAT	TAGGCTAC	CGCCATGT
pIL4-A PCR preAOX+3 'AOX Seque
pPICZaA-IL4 Original	GGGCTTGA	GGAGCTC	CATTCCA	TCCTTCT	TAGGCTAC	ACACCATG
	430	440	450	460	470	480
pPICZaA-IL4-A Sequenced						
pIL4-A PCR preAOX+3 'AOX Seque	CTTTTAAT	AGCCTGT	TAA-TGCG	CCCCCCCC	TGGGCGAG	GTCAITGTT
pIL4-A PCR preAOX+3 'AOX Seque
pPICZaA-IL4 Original	ACTAACAC	TGACTTAT	AGCCTGT	TCCTGGCC	CCTGGCAG	TTCAITGTT
	490	500	510	520	530	540
pPICZaA-IL4-A Sequenced						
pIL4-A PCR preAOX+3 'AOX Seque	GTTTTATT	CCGGA	AACAAGC	CGCAATA	ACCAGAA	TCACTCC
pIL4-A PCR preAOX+3 'AOX Seque
pPICZaA-IL4 Original	GTTTTATT	CCGGA	AACAAGC	CGCAATA	ACCAGAA	TCACTCC
	550	560	570	580	590	600
pPICZaA-IL4-A Sequenced						
pIL4-A PCR preAOX+3 'AOX Seque	ATGAGGGC	CTGAGTG	GGGGTCAA	AGTTTCA	TCCC-AA	GCCCCAA
pIL4-A PCR preAOX+3 'AOX Seque
pPICZaA-IL4 Original	ATGAGGGC	CTGAGTG	GGG-TCAA	AGTTTCA	TCCCCAA	GCCCCAA
	610	620	630	640	650	660
pPICZaA-IL4-A Sequenced						
pIL4-A PCR preAOX+3 'AOX Seque	GACAGTTT	ACGCTGT	GGAAACT	ATGACAAA	CGTGATCT	TCCAAGAT
pIL4-A PCR preAOX+3 'AOX Seque
pPICZaA-IL4 Original	GACAGTTT	ACGCTGT	GGAAACT	ATGACAAA	CGTGATCT	TCCAAGAT
	670	680	690	700	710	720
pPICZaA-IL4-A Sequenced						
pIL4-A PCR preAOX+3 'AOX Seque	ACTAAGTT	GGTTCGT	AAATGCT	GCCAGTTG	CAAAAAG	CTTCCAAA
pIL4-A PCR preAOX+3 'AOX Seque
pPICZaA-IL4 Original	ACTAAGTT	GGTTCGT	AAATGCT	GCCAGTTG	CAAAAAG	CTTCCAAA
	730	740	750	760	770	780
pPICZaA-IL4-A Sequenced						
pIL4-A PCR preAOX+3 'AOX Seque	TCGGCAT	GTTTGTCT	TTTGGTAT	ATTGACGA	GCTCAAAA	AAATCTCA
pIL4-A PCR preAOX+3 'AOX Seque
pPICZaA-IL4 Original	TCGGCAT	GTTTGTCT	TTTGGTAT	ATTGACGA	GCTCAAAA	AAATCTCA
	790	800	810	820	830	840
pPICZaA-IL4-A Sequenced						
pIL4-A PCR preAOX+3 'AOX Seque	ATGCTTAG	CAGTCTCT	ATCGTCT	AACCCGG	CACCTGT	GAAACGCA
pIL4-A PCR preAOX+3 'AOX Seque
pPICZaA-IL4 Original	ATGCTTAG	CAGTCTCT	ATCGTCT	AACCCGG	CACCTGT	GAAACGCA

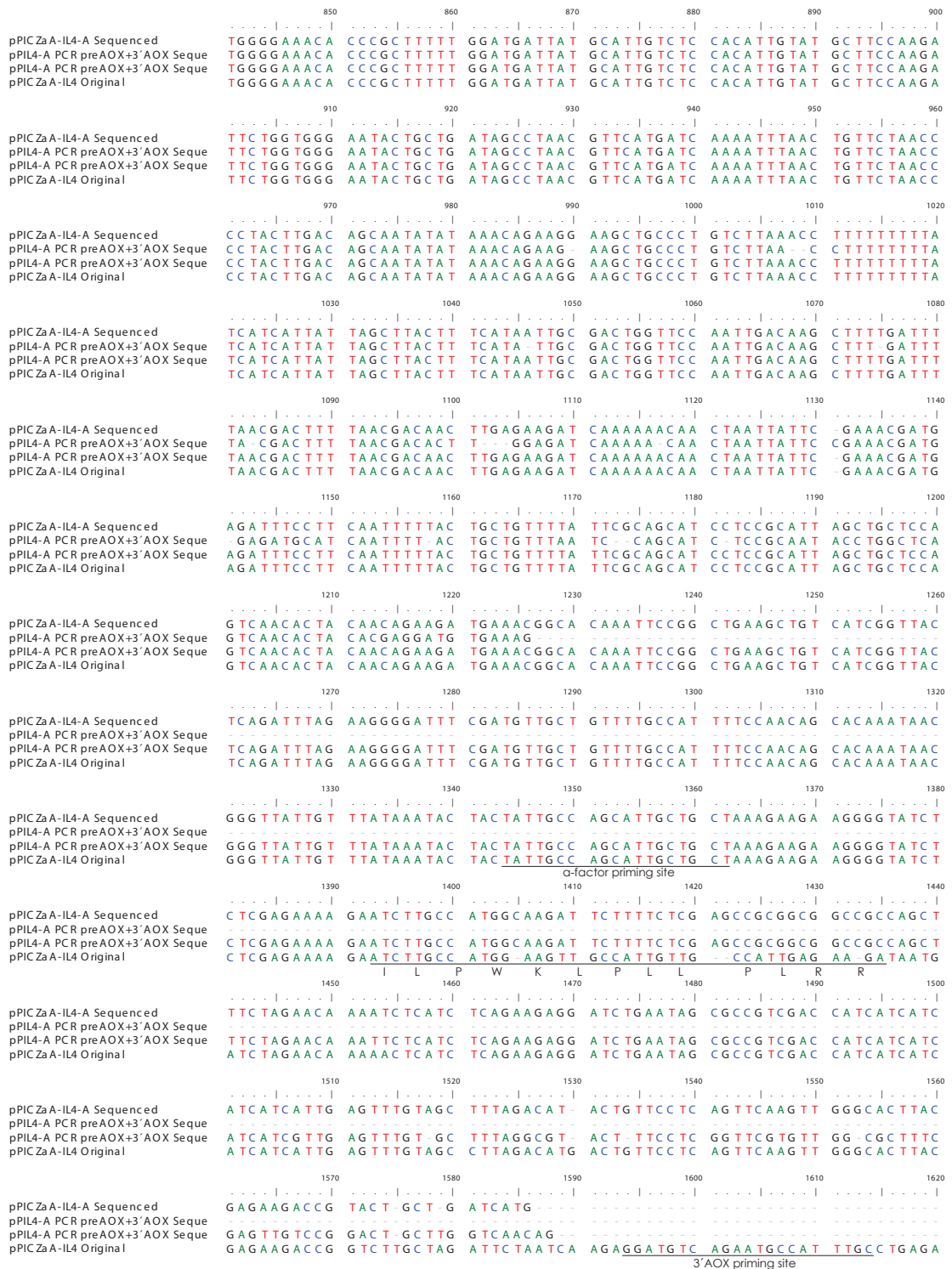


Figure B.2: Alignment of sequence data of purified pPICZα-IL4-A vector DNA (3'AOX primer only) and PCR product of extracted genomic DNA of X33IL4-A colonies using *pre*AOX and 3'AOX primers. Sequencing was performed by DNA Technology (Risskov, Denmark) using mentioned primers. The alignment was made against the original pPICZα-IL4 sequence using ClustalW. Ending part of the vector is not shown.